

**HOST TARGET AND FUNCTION OF THE TYPE III SECRETED EFFECTORS NleB
AND EspL OF ATTACHING AND EFFACING BACTERIAL PATHOGENS**

by

Robyn Jamie Law

B.Sc., The University of Manitoba, 2005

M.Sc., The University of Manitoba, 2009

A THESIS SUBMITTED IN PARTIAL FULFILLMENT OF
THE REQUIREMENTS FOR THE DEGREE OF

DOCTOR OF PHILOSOPHY

in

THE FACULTY OF GRADUATE AND POSTDOCTORAL STUDIES
(Microbiology and Immunology)

THE UNIVERSITY OF BRITISH COLUMBIA
(Vancouver)

May 2015

© Robyn Jamie Law, 2015

Abstract

Enteropathogenic *Escherichia coli* (EPEC) and enterohemorrhagic *E. coli* (EHEC) cause enteric diseases resulting in significant morbidity and mortality worldwide. EPEC is a leading cause of potentially fatal watery diarrhea associated with vomiting, fever and dehydration in young children in developing countries, while EHEC causes severe gastroenteritis in both developing and industrialized nations. The success of these pathogens relies on their ability to inject secreted effectors directly into host cells that manipulate a variety of host cell signaling pathways while the pathogen remains extracellular. Much work has been done to identify EPEC/EHEC secreted effectors but the molecular mechanisms of action of many effectors and their contribution to virulence remain poorly understood.

To identify novel host targets for EPEC/EHEC-secreted effectors we performed a global mass spectrometry screen using the SILAC (stable isotope labeling with amino acids in cell culture)-labeling method. Using this technology, we were able to identify host binding partners for a number of EPEC/EHEC effectors. Among them, two conserved effectors, NleB and EspL, were found to interact with the same host factor, ensconsin. Ensconsin is a microtubule associated protein that has been identified as an essential cofactor of kinesin-1.

This thesis describes the identification and characterization of the interaction between NleB/EspL and ensconsin and identifies a role for these effectors during infection. We use fluorescent time-lapse imaging to demonstrate the significant effect EPEC have on the kinetics of host receptor trafficking during on-going infections and use the *Citrobacter rodentium*-mouse model of infection to further characterize how these effectors impact virulence during infection.

We hypothesize that NleB and EspL play critical roles during A/E pathogen infections and contribute to pathogenesis through alteration of ensconsin function. Information gathered from this study provides insight into our current understanding of the virulence mechanisms of these pathogens as well as the role of secreted effectors during host cell interactions. A more detailed understanding of how pathogenic bacteria alter host cellular functions as part of the disease process could ultimately lead to development of new therapeutics to help control these significant enteric pathogens.

Preface

Work in this dissertation was produced in part through collaborative efforts with members of the Finlay laboratory, the Foster laboratory and the Coombs laboratory at UBC, as well as the external laboratory of Dr. Julian Guttman at Simon Fraser University. Formal contributions of the authors are as follows:

Chapter 1: Parts of Chapter 1 have been published as “Recent advances in understanding enteric pathogenic *Escherichia coli*” in *Clinical Microbiology Reviews*; 2013, 26(4):822 and as “*In vitro* and *in vivo* model systems for studying enteropathogenic *Escherichia coli* infections” in *Cold Spring Harbor Perspectives in Medicine*; 2013, 3(3):a009977. I wrote the section, “Enteropathogenic *E. coli*”, in “Recent advances in understanding enteric pathogenic *Escherichia coli*”. Other review sections for this manuscript were written by Drs. M. Croxen, R. Scholz, K. Keeney and M. Wlodarska. All authors contributed to editing and figure preparation for this manuscript. L. Gur-Arie wrote the section “*in vitro* infection models” in “*In vitro* and *in vivo* model systems for studying enteropathogenic *Escherichia coli* infections”. I wrote all other sections of this manuscript and designed Figures 1, 3 and 4. Drs. I. Rosenshine and B.B. Finlay provided important input and contributed to the editing of these manuscripts.

Chapter 2: A version of Chapter 2 (along with Chapter 3) is currently being prepared for submission. Co-authors for this manuscript contributed as follows: C. de Hoog and Y. Li performed SILAC experiments and Dr. L.J. Foster performed SILAC data analysis. Dr. R. Scholz assisted with protein purification. Drs. S.R. Shames and M.A. Croxen created pGEX-6P-

3-HA₃::*nleB1* and pGEX-6P-3-HA₃::*espL2*, respectively. J. van der Heijden provided purified SseK1. All remaining experiments and data collection were my own work. I was primarily responsible for writing of the manuscript and figure preparation with intellectual input from co-authors Drs. J.A. Guttman and B.B. Finlay.

Chapter 3: A version of Chapter 3 (along with Chapter 2) is currently being prepared for submission. Co-authors for this manuscript contributed as follows: Dr. W. Deng created the EPEC $\Delta nleB2$ strain. H.T. Law performed all live cell imaging and J. Scurll assisted with particle tracking analysis. All remaining experiments and data collection were my own work. I was primarily responsible for writing of the manuscript and figure preparation with intellectual input from co-authors Drs. J.A. Guttman and B.B. Finlay.

Chapter 4: I was responsible for generation of *C. rodentium* mutants and figure preparation for this chapter. I performed tissue RNA extractions and real-time polymerase chain reaction (PCR) analysis. Dr. M. Wlodarska and I contributed equally to experimental design and data analysis. Dr. M. Wlodarska performed infections, tissue staining and pathology scoring for this chapter.

Chapter 5: Parts of Chapter 5 have been published as “*In vitro* and *in vivo* model systems for studying enteropathogenic *Escherichia coli* infections” in *Cold Spring Harbor Perspectives in Medicine*; 2013, 3(3):a009977. Author contributions are described as above for Chapter 1.

Publications arising from graduate work

Law, R.J., Law, HT, Scurll, J.M., Scholz, R., Shames, S.R., Deng, W., Croxen, M.A., Li, Y., de Hoog, C.L., van der Heijden, J., Foster, L.J., Guttman, J.A., and Finlay, B.B. (2015). Quantitative proteomics screen identifies novel host binding partner for the pathogenic *Escherichia coli* type III secretion system effectors, NleB and EspL. (*Manuscript in preparation*)

Besides the studies presented in this dissertation, a list of additional publications arising during graduate work but not directly related to the research presented in this dissertation can be found in Appendix A.

The mouse work presented in this dissertation was approved by the UBC Animal Care Committee, certificate number: A10-0089.

Table of Contents

| | |
|---|-------------|
| Abstract..... | ii |
| Preface..... | iv |
| Table of Contents | vii |
| List of Tables | xii |
| List of Figures..... | xiii |
| List of Abbreviations | xv |
| Acknowledgements | xix |
| Dedication | xx |
| Chapter 1: Introduction | 1 |
| 1.1 Pathogenic <i>Escherichia coli</i> | 1 |
| 1.1.1 Enteropathogenic <i>E. coli</i> (EPEC) classification | 2 |
| 1.1.2 Enterohemorrhagic <i>E. coli</i> (EHEC) classification | 3 |
| 1.2 Epidemiology of EPEC and EHEC: incidence, transmission and symptoms..... | 3 |
| 1.2.1 Incidence of infection | 4 |
| 1.2.2 Transmission and reservoirs | 6 |
| 1.2.3 Symptoms and onset of disease | 7 |
| 1.3 Pathogenesis of A/E pathogens..... | 8 |
| 1.3.1 Formation of A/E lesions | 10 |
| 1.3.2 Type III secretion systems and A/E pathogen infection | 11 |
| 1.3.3 Effector proteins of EPEC and EHEC | 11 |
| 1.3.3.1 LEE-encoded effectors..... | 13 |
| 1.3.3.2 Non-LEE-encoded effectors | 14 |

vii

| | | |
|--|--|-----------|
| 1.3.3.3 | T3SS effectors and diarrhea production | 16 |
| 1.4 | Model systems for studying A/E pathogens | 17 |
| 1.4.1 | <i>In vitro</i> models for studying A/E pathogens | 17 |
| 1.4.2 | <i>In vivo</i> models for studying A/E pathogens | 19 |
| 1.4.2.1 | The REPEC model of infection | 19 |
| 1.4.2.2 | The <i>C. rodentium</i> -mouse model of infection | 20 |
| 1.5 | A/E pathogen infection and the host cytoskeleton..... | 22 |
| 1.6 | Microtubule associated proteins (MAPs)..... | 23 |
| 1.6.1 | Ensconsin (MAP7 / EMAP-115) | 24 |
| 1.7 | Summary of thesis..... | 25 |
| Chapter 2: The type III secretion system effectors, NleB and EspL, interact with host ensconsin | | 27 |
| 2.1 | Introduction..... | 27 |
| 2.2 | Materials and methods | 30 |
| 2.2.1 | Tissue culture, bacterial strains and plasmids | 30 |
| 2.2.2 | Cloning of effector gene sequences into pGEX-6P-3::HA ₃ | 32 |
| 2.2.3 | Generation of MAP7-FLAG fusion | 32 |
| 2.2.4 | Generation of MAP7-FLAG truncations | 32 |
| 2.2.5 | Cloning of <i>Salmonella sseK1</i> into pET28a..... | 34 |
| 2.2.6 | Recombinant protein expression and purification | 34 |
| 2.2.7 | SILAC labeling and analysis | 35 |
| 2.2.8 | Co-immunoprecipitation | 38 |
| 2.2.9 | Western blotting..... | 38 |

| | | |
|--|--|-----------|
| 2.3 | Results..... | 39 |
| 2.3.1 | The EHEC T3SS effectors, NleB1 and EspL2, interact with host ensconsin..... | 39 |
| 2.3.2 | The EPEC T3SS effectors, NleB1, NleB2 and EspL, interact with host ensconsin . | 42 |
| 2.3.3 | The NleB homolog, SseK1, does not interact with host ensconsin | 44 |
| 2.3.4 | The effector-ensconsin interaction is specific and mediated by the MTB region of ensconsin..... | 45 |
| 2.4 | Discussion | 49 |
| Chapter 3: EPEC disrupts host transferrin receptor trafficking using NleB/EspL..... | | 53 |
| 3.1 | Introduction..... | 53 |
| 3.2 | Materials and methods | 55 |
| 3.2.1 | Tissue culture, bacterial strains and plasmids..... | 55 |
| 3.2.2 | Generation of <i>pnleB1</i> and <i>pespL</i> | 56 |
| 3.2.3 | Green fluorescent protein (GFP) fusion to NleB1 and EspL..... | 56 |
| 3.2.4 | Generation of EPEC effector deletion mutants..... | 58 |
| 3.2.5 | Generation of <i>nleB1mut</i> | 59 |
| 3.2.6 | Co-immunoprecipitation | 59 |
| 3.2.7 | Western blotting..... | 60 |
| 3.2.8 | RNA extraction | 60 |
| 3.2.9 | Real-time PCR | 61 |
| 3.2.10 | Transfection of HeLa cells with pEGFP- <i>nleB1</i> or pEGFP- <i>espL</i> | 61 |
| 3.2.11 | Confocal microscopy | 61 |
| 3.2.12 | Live cell imaging and analysis..... | 62 |
| 3.2.13 | Statistical analyses | 63 |

| | | |
|--------|--|----|
| 3.3 | Results..... | 63 |
| 3.3.1 | EPEC blocks transferrin receptor transport in a T3SS-dependent manner..... | 63 |
| 3.3.2 | NleB1 and EspL inhibit TfR vesicle trafficking in EPEC-infected cells..... | 65 |
| 3.3.3 | Trans-complementation of the EPEC $\Delta nleB1$ and $\Delta espL$ mutants | 67 |
| 3.3.4 | Effector overexpression does not affect TfR vesicle trafficking | 69 |
| 3.3.5 | EPEC targets kinesin-1-based vesicle motility in Ptk2 cells | 70 |
| 3.3.6 | NleB and EspL do not affect Kif5b binding to ensconsin in EPEC-infected cells... | 71 |
| 3.3.7 | Ensconsin expression is not affected by infection with EPEC | 73 |
| 3.3.8 | Localization of ensconsin is unaffected by EPEC infection..... | 74 |
| 3.3.9 | Microtubule structure is unaffected by NleB and EspL during EPEC infection | 76 |
| 3.3.10 | Overexpression of NleB1 and EspL does not affect microtubule structure..... | 77 |
| 3.3.11 | Separate roles for NleB1 during infection with EPEC | 79 |
| 3.4 | Discussion | 81 |

Chapter 4: Distinct virulence-associated phenotypes of the type III secretion system

| | | |
|--|--|-----------|
| effectors, NleB and EspL, in the cecum of <i>C. rodentium</i>-infected mice | | 85 |
| 4.1 | Introduction..... | 85 |
| 4.2 | Materials and methods | 87 |
| 4.2.1 | Generation of <i>C. rodentium</i> deletion mutants..... | 87 |
| 4.2.2 | Infection of mice with <i>C. rodentium</i> and effector mutants..... | 88 |
| 4.2.3 | <i>C. rodentium</i> CFU and cytokine determination..... | 89 |
| 4.2.4 | RNA isolation and cDNA synthesis | 90 |
| 4.2.5 | Real-time PCR | 90 |
| 4.2.6 | Immunohistochemistry | 90 |

| | | |
|--|--|------------|
| 4.2.7 | Pathology scoring..... | 91 |
| 4.3 | Results..... | 91 |
| 4.3.1 | Infection analysis of a <i>C. rodentium</i> $\Delta nleB\Delta espL$ mutant in C3H/HeJ mice | 91 |
| 4.3.2 | Tir-adherent <i>C. rodentium</i> is reduced in the cecum during infection with the $\Delta nleB\Delta espL$ mutant..... | 94 |
| 4.3.3 | NleB, but not EspL, is essential for pathological changes in the cecum of <i>C. rodentium</i> -infected mice | 95 |
| 4.3.4 | Infection with <i>C. rodentium</i> $\Delta nleB\Delta espL$ does not result in weight differences of the cecum or spleen compared to wild type controls..... | 97 |
| 4.3.5 | Reduced inflammation in the spleen and cecum correlates with attenuated colonization of the $\Delta nleB\Delta espL$ mutant..... | 98 |
| 4.3.6 | <i>C. rodentium</i> infection does not affect ensconsin relative expression..... | 100 |
| 4.4 | Discussion..... | 101 |
| Chapter 5: Conclusions | | 106 |
| 5.1 | Relevance and contributions to the field..... | 106 |
| 5.2 | Future research directions | 108 |
| 5.3 | Challenges facing A/E pathogens research..... | 110 |
| 5.4 | The future of A/E pathogens research | 112 |
| Bibliography | | 113 |
| Appendix A – Additional publications..... | | 132 |
| Appendix B – Particle tracking of TfR-mCherry containing vesicles in EPEC-infected Ptk2 cells (stringent track linking parameters)..... | | 133 |

List of Tables

| | |
|--|----|
| Table 2.1 Bacterial strains used in this study..... | 31 |
| Table 2.2 Plasmids used in this study | 31 |
| Table 2.3 Oligonucleotide primers used in this study..... | 33 |
| Table 2.4 Summary of host targets identified by LC-MS/MS as specifically immunoprecipitated with tagged effectors in SILAC experiments..... | 40 |
| Table 3.1 Bacterial strains used in this study..... | 55 |
| Table 3.2 Oligonucleotide primers used in this study..... | 57 |
| Table 3.3 Plasmids used in this study | 58 |
| Table 3.4 Movement of TfR-mCherry particles is unaffected by NleB1 overexpression | 70 |
| Table 4.1 Bacterial strains used in this study..... | 88 |
| Table 4.2 Primers used in this study | 88 |

List of Figures

| | |
|---|----|
| Figure 1.1 Major T3SS effector proteins of EPEC/EHEC and their targets within host cells. | 13 |
| Figure 2.1 Schematic representation of SILAC methodology..... | 37 |
| Figure 2.2 Ensconsin (MAP7) interacts with type III secreted effectors, NleB1 and EspL2. | 41 |
| Figure 2.3 The EPEC effectors, NleB1 and EspL, interact with host ensconsin (MAP7)..... | 43 |
| Figure 2.4 The EPEC T3SS effector, NleB2, interacts with host ensconsin (MAP7)..... | 43 |
| Figure 2.5 The <i>Salmonella</i> T3SS effector, SseK1, does not interact with host ensconsin. | 45 |
| Figure 2.6 Protein expression levels of ensconsin truncations in HEK293T cells. | 46 |
| Figure 2.7 NleB1 and EspL interact with the microtubule binding (MTB) region of ensconsin. | 48 |
| Figure 2.8 Protein expression of the ensconsin truncation mutant, MAP7 Δ N. | 48 |
| Figure 2.9 NleB1 and EspL do not interact with the C-terminal “activity” region of ensconsin. | 49 |
| Figure 3.1 Enteropathogenic <i>E. coli</i> (EPEC) infection halts TfR-mCherry transport in a type III secretion system-dependent manner. | 64 |
| Figure 3.2 Enteropathogenic <i>E. coli</i> (EPEC) infection halts TfR-mCherry transport in an NleB1/EspL-dependent manner..... | 66 |
| Figure 3.3 Mean squared displacements of TfR-mCherry particles in EPEC-infected cells..... | 67 |
| Figure 3.4 Trans complementation of <i>nleB1</i> and <i>espL</i> restores trafficking inhibition during EPEC infection. | 68 |
| Figure 3.5 EPEC specifically inhibits kinesin-1-based vesicle motility..... | 71 |
| Figure 3.6 Enteropathogenic <i>E. coli</i> (EPEC) infection does not affect ensconsin (MAP7)-kinesin (Kif5b) interaction. | 72 |
| Figure 3.7 EPEC infection does not affect ensconsin expression..... | 74 |
| Figure 3.8 Localization of ensconsin during EPEC infection..... | 75 |

| | |
|--|-----|
| Figure 3.9 EPEC infection does not affect microtubule stability. | 77 |
| Figure 3.10 Overexpression of NleB1 or EspL does not affect microtubule structure..... | 78 |
| Figure 3.11 NleB1 GlcNAcylation activity does not affect TfR-mCherry vesicle trafficking.... | 80 |
| Figure 3.12 Schematic model of proposed NleB1/EspL function during infection with EPEC.. | 83 |
| Figure 4.1 A <i>C. rodentium</i> $\Delta nleB\Delta espL$ mutant is attenuated in its ability to colonize the spleens, but not the ceca of C3H/HeJ mice. | 93 |
| Figure 4.2 Fecal shedding of wild type <i>C. rodentium</i> or effector mutant derivatives from C3H/HeJ mice. | 93 |
| Figure 4.3 The <i>C. rodentium</i> $\Delta nleB\Delta espL$ mutant is attenuated in its ability to attach to and infect the mouse intestine..... | 95 |
| Figure 4.4 The <i>C. rodentium</i> $\Delta nleB\Delta espL$ mutant causes reduced histological damage in the cecal tissues of C3H/HeJ mice..... | 97 |
| Figure 4.5 Organ weights of C3H/HeJ mice infected with wild type <i>C. rodentium</i> or effector mutant strains. | 98 |
| Figure 4.6 Cecum cytokine production in <i>C. rodentium</i> infected C3H/HeJ mice..... | 99 |
| Figure 4.7 Spleen cytokine production in <i>C. rodentium</i> infected C3H/HeJ mice. | 100 |
| Figure 4.8 Real-time analysis of ensconsin relative gene expression in mice infected with <i>C.</i> <i>rodentium</i> or effector mutant derivatives..... | 101 |
| Figure B.1 EPEC disrupts TfR trafficking in an NleB1/EspL dependent manner..... | 133 |
| Figure B.2 Complementation of <i>nleB1/espL</i> restores trafficking inhibition..... | 134 |
| Figure B.3 EPEC specifically disrupts kinesin-1-based vesicle movement..... | 134 |
| Figure B.4 NleB1 GlcNAcylation activity does not affect TfR-mCherry trafficking..... | 135 |

List of Abbreviations

| | |
|--------|---|
| A/E | Attaching and effacing |
| aEPEC | Atypical enteropathogenic <i>Escherichia coli</i> |
| Arp2/3 | Actin related protein 2/3 |
| BFP | Bundle forming pilus |
| BSA | Bovine serum albumin |
| CBA | Cytometric bead array |
| CFU | Colony forming units |
| CI | Confidence interval |
| COPI | Coat protein complex-1 |
| COPII | Coat protein complex-2 |
| DAEC | Diffusely adherent <i>Escherichia coli</i> |
| DAPI | 4',6-diamidino-2-phenylindole |
| DEPEC | Dog enteropathogenic <i>Escherichia coli</i> |
| DMEM | Dulbecco's modified eagle medium |
| DNA | Deoxyribonucleic acid |
| DPI | Days post-infection |
| EAEC | Enteraggregative <i>Escherichia coli</i> |
| EAF | Enteropathogenic <i>Escherichia coli</i> adherence factor |
| ECL | Enhanced chemiluminescence |
| EGFP | Enhanced green fluorescent protein |
| EHEC | Enterohemorrhagic <i>Escherichia coli</i> |

| | |
|--------------|--|
| EIEC | Enteroinvasive <i>Escherichia coli</i> |
| EPEC | Enteropathogenic <i>Escherichia coli</i> |
| ER | Endoplasmic reticulum |
| ETEC | Enterotoxigenic <i>Escherichia coli</i> |
| ExPEC | Extraintestinal pathogenic <i>Escherichia coli</i> |
| GEMS | Global Enteric Multicentre Study |
| HC | Hemorrhagic colitis |
| HCP | Hemorrhagic coli pilus |
| HEK | Human embryonic kidney |
| HUS | Hemolytic uremic syndrome |
| I κ B | Inhibitor of kappa B |
| IEC | Intestinal epithelial cell |
| IL-8 | Interleukin-8 |
| IPTG | isopropyl β -D-1-thiogalactopyranoside |
| IVOC | <i>In vitro</i> organ culture |
| kb | Kilobase |
| kDa | Kilodalton |
| LA | Localized adherence |
| LC-MS/MS | Liquid chromatography-tandem mass spectrometry |
| LEE | Locus of enterocyte effacement |
| Lfp | Long polar fimbriae |
| m/z | Mass to charge ratio |

| | |
|----------------|---|
| MAP | Microtubule associated protein |
| min | Minute |
| MLST | Multi-locus sequence typing |
| m.o.i. | Multiplicity of infection |
| MSD | Mean squared displacement |
| MT | Microtubule |
| MTB | Microtubule binding |
| N-WASP | Neuronal Wiskott-Aldrich syndrome protein |
| NF- κ B | Nuclear factor-kappa B |
| NHERF2 | Sodium hydrogen exchange regulatory factor 2 |
| Nle | Non-LEE encoded |
| NMEC | Neonatal meningitis <i>Escherichia coli</i> |
| NP40 | Nonidet P40 |
| GlcNAc | N-acetyl-D-glucosamine |
| PAGE | Polyacrylamide electrophoresis |
| PAI | Pathogenicity island |
| PBS | Phosphate-buffered saline |
| PBST/BSA | Phosphate-buffered saline Tween-20 / bovine serum albumin |
| PEPEC | Pig enteropathogenic <i>Escherichia coli</i> |
| RDEC | Rabbit diarrheagenic <i>Escherichia coli</i> |
| REPEC | Rabbit enteropathogenic <i>Escherichia coli</i> |
| SERT | Serotonin transporter |

| | |
|---------------|--|
| SGLT1 | Sodium glucose co-transporter 1 |
| SNX9 | Sorting nexin 9 |
| SILAC | Stable isotope labeling with amino acids in cell culture |
| STEC | Shiga toxin-producing <i>Escherichia coli</i> |
| Stx | Shiga toxin |
| T3SS | Type III secretion system |
| TBS | Tris-buffered saline |
| TBST | Tris-buffered saline Tween-20 |
| tEPEC | Typical enteropathogenic <i>Escherichia coli</i> |
| Tf | Transferrin |
| TfR | Transferrin receptor |
| Tir | Translocated intimin receptor |
| TNF- α | Tumor necrosis factor alpha |
| Un | Uninfected |
| UPEC | Uropathogenic <i>Escherichia coli</i> |
| VTEC | Verocytotoxin-producing <i>Escherichia coli</i> |
| Wt | Wild type |

Acknowledgements

The road to completion of this dissertation and PhD has been long and difficult and would not have been possible without the help of many.

First and foremost, I would like to thank my graduate supervisor, Dr. B. Brett Finlay, whose guidance has been invaluable throughout my development. Thank you for providing me with the tools to do great science and the freedom to follow my own path.

I would like to express my gratitude to the members of my supervisory committee, Drs. Julian Guttman, Leonard Foster and Erin Gaynor, for their insightful advice and for always challenging me to think more deeply about my research.

I would also like to thank my amazing collaborators for sharing their expertise and enthusiasm for the project. It has been an honor working with you all.

Thank you to Drs. Stephanie Shames, Marta Wlodarska, Roland Scholz, Joris van der Heijden, Matthew Croxen and other members of the Finlay lab for their friendship and support. You will never know how much it has meant... I would not have made it through this without you.

Finally, I would like to thank my close friends and family for their constant love and encouragement throughout this process and for understanding that my path in life will take me far from home.

Thank you.

To all those who encouraged me to continue....

Chapter 1: Introduction

1.1 Pathogenic *Escherichia coli*

Escherichia coli is a Gram-negative rod normally found as a harmless commensal of the intestinal microflora. Some strains, however, have acquired the ability to cause disease in animals and in humans ranging from meningitis to urinary tract infections and diarrhea with hundreds of millions of people affected annually (Croxen and Finlay, 2010). The size of the *E. coli* genome varies significantly between commensal and pathogenic variants (Croxen et al., 2013) with the gain and loss of genetic material having contributed largely to the evolution of these pathogens (Touchon et al., 2009). The placement of *E. coli* strains into various pathovars is based on genotypic and phenotypic properties. Of the eight well studied *E. coli* pathovars, uropathogenic *E. coli* (UPEC) and neonatal meningitis *E. coli* (NMEC) are classified as extraintestinal pathogenic *E. coli* (ExPEC), while the remaining six are classified as diarrheagenic (Croxen and Finlay, 2010). The six diarrheagenic pathovars include enteropathogenic *E. coli* (EPEC), enterohemorrhagic *E. coli* (EHEC), enterotoxigenic *E. coli* (ETEC), enteroinvasive *E. coli* (EIEC), enteroaggregative *E. coli* (EAEC) and diffusely adherent *E. coli* (DAEC).

The work completed in this thesis focuses primarily on two *E. coli* pathovars, EPEC and EHEC, which are grouped, along with certain animal pathogens, into a set of bacterial strains collectively known as the attaching and effacing (A/E) pathogens.

1.1.1 Enteropathogenic *E. coli* (EPEC) classification

The term ‘EPEC’ was first used in 1955 (Neter et al., 1955) to describe a number of *E. coli* strains epidemiologically related to a series of outbreaks of infantile diarrhea in the 1940’s and 1950’s (Bray, 1945; Robins-Browne, 1987). Most EPEC isolates correspond to conventional O serogroups (Reid et al., 2000; Wirth et al., 2006) but advances in molecular and cellular detection of EPEC have expanded the known repertoire of EPEC lineages to include strains that would not have been considered “EPEC” based on serotypes alone (Scaletsky et al., 2010). EPEC is distinguished from EHEC by the inability to produce Shiga toxin (Stx), and from other diarrheagenic *E. coli* by the ability to form A/E lesions in the small intestine, a phenotype afforded to it by genes of the locus of enterocyte effacement (LEE) (Kaper et al., 2004). EPEC is further classified into ‘typical’ and ‘atypical’ subtypes based on the presence or absence of the *E. coli* adherence factor plasmid (EAF) (Trabulsi et al., 2002). Based on multilocus sequence typing (MLST), strains of EPEC fall into 4 clonal lineages, designated EPEC1-EPEC4, that seem to have evolved through independent acquisition of the LEE and pEAF (Lacher et al., 2007). Despite their formal designation as EPEC, typical and atypical isolates constitute two distinct groups of organisms with some atypical EPEC (aEPEC) strains being even more closely related to EHEC in serotypes, genetic characteristics, virulence properties and reservoirs (Trabulsi et al., 2002). In contrast to tEPEC, aEPEC is a highly heterogenous group, and despite its relatively high prevalence in children without diarrhea, aEPEC is now thought to be important in endemic diarrhea in children as well as in outbreaks (Ochoa and Contreras, 2011).

1.1.2 Enterohemorrhagic *E. coli* (EHEC) classification

The presence of Stx-encoding genes (*stx₁* or *stx₂*) qualifies an *E. coli* isolate as Stx-producing *E. coli* (STEC) or verocytotoxin-producing *E. coli* (VTEC) but only a subset of these strains have been linked to illness in humans (Blanco et al., 2004). EHEC are a subset of STEC that cause more serious diarrhea than EPEC. EHEC provoke a variety of symptoms that range in severity from acute gastroenteritis to hemorrhagic colitis (HC) and in the most severe cases, hemolytic uremic syndrome (HUS) (Goosney et al., 2000), with progression to HUS occurring in 15% of childhood cases (Tarr et al., 2005). In general, EHEC are LEE-positive and form A/E lesions similar to EPEC. The most prevalent serotype causing outbreaks in North America is O157:H7 which has been the subject of many studies on EHEC pathogenesis (Croxen et al., 2013). EHEC O157:H7 falls into the EHEC 1 lineage of STEC and is further subdivided into lineages I and II based on lineage-specific polymorphisms (Whittam et al., 1993; Yang et al., 2004). Cattle often serve as the primary reservoir for this highly infectious organism, thus making EHEC contamination a major issue in food and water safety (Croxen and Finlay, 2010). Due to its ability to colonize animals and infect humans, EHEC has important implications for diverse fields of study such as veterinary microbiology, food microbiology, environmental microbiology and clinical microbiology (Croxen et al., 2013).

1.2 Epidemiology of EPEC and EHEC: incidence, transmission and symptoms

Diarrheal illnesses are the cause of much morbidity and mortality worldwide and while many etiological agents are responsible for diarrhea, EPEC and EHEC remain major contributors. Great strides have been made in understanding the microbiology, pathogenesis and interactions of A/E pathogens with their hosts and while both EPEC and EHEC cause diarrhea, the incidence

rates, clinical symptoms and outcomes of disease, as well as the sites and mechanism of colonization, can differ significantly (Croxen et al., 2013).

1.2.1 Incidence of infection

The epidemiology of EPEC infection has shifted since these strains were first identified in the 1940's and 1950's. Infection occurs in the small bowel and initially, EPEC was thought to be an important cause of infantile diarrhea in the developed world but over the years has become much more prevalent in developing countries (Nataro and Kaper, 1998). The prevalence of EPEC infection varies between epidemiological studies based on differences in study populations, age distributions and methods used for detection and diagnosis (Ochoa et al., 2008). In addition, geographic region and socioeconomic class may also contribute to the epidemiology of EPEC-induced diarrheal disease (Maranhão et al., 2008). In order to understand these issues, large case studies like the Global Enteric Multicenter Study (GEMS) are needed to more accurately assess the etiology and population-based burden of EPEC-induced diarrheal disease. Based on recent GEMS data, tEPEC was significantly associated with moderate-to-severe diarrhea in children under 2 years of age in Kenya whereas aEPEC was not associated with this type of diarrhea at any of the GEMS sites (Kotloff et al., 2013). Overall, tEPEC was not strongly associated with cases of moderate-to-severe diarrhea, but when present, was associated with an increased risk of death in patients aged 0-11 months (Kotloff et al., 2013).

For many years, infections with aEPEC were thought to predominate in industrialized nations while being relatively rare in the developing world (Afset et al., 2004; Trabulsi et al., 2002); however, recent data indicate that infections with aEPEC exceed those with tEPEC in both

developing and developed countries (Hernandes et al., 2009; Ochoa et al., 2008). However, this notion cannot be generalized as other studies still report tEPEC being more prevalent than aEPEC as a cause of diarrhea (Alikhani et al., 2006). Although many countries no longer consider tEPEC strains to be an important cause of acute diarrhea, the occurrence of severe disease outcomes associated with these infections has re-emerged and this pathogen continues to be regarded as a serious threat to children under the age of two.

Unlike infections with EPEC, EHEC infection occurs in the large intestine and the incidence of disease are not influenced by socioeconomic factors. Infections with EHEC occur worldwide with incidences in Europe, Asia, Australia, and North America (Croxen et al., 2013). According to the National Enteric Surveillance Program, the incidence rate of EHEC O157:H7 cases in Canada has improved from 3/100,000 cases in 2006 to 1.18/100,000 cases in 2010 (NESP, 2010). In the United States, the annual hospitalization rate for laboratory-confirmed EHEC O157 infections is 46.2% compared to that of non-O157 Stx-producing *E. coli* infections with a rate of only 12.8% (Scallan et al., 2011). Similarly, the case-fatality rate for EHEC O157 infections was 2 fold higher than for non-O157 strains in 2011 (CDC, 2012). EHEC is also found in developing countries, such as Argentina, which is reported to have one of the highest incidence rates for children with HUS worldwide (Rivero et al., 2010). These data may reflect an increase in exposure to risk factors like high meat consumption, contact with contaminated recreational water sources and poor hygiene (Bentancor et al., 2012).

1.2.2 Transmission and reservoirs

As with other diarrheagenic *E. coli*, transmission of EPEC and EHEC occurs via the fecal-oral route. EPEC is transmitted from host to host through contaminated surfaces, weaning fluids and human carriers (Levine and Edelman, 1984). Although rare, outbreaks among adults seem to occur through ingestion of contaminated food and water but no specific environmental reservoir has been identified as the most likely source of infection (Nataro and Kaper, 1998). The infectious dose in adult volunteers is quite high, at $10^8 - 10^{10}$ organisms (Bieber et al., 1998; Levine et al., 1978), while the actual dose required to cause disease during natural infection is unknown. EPEC outbreaks have been reported to show a seasonal distribution with peaks during the warm months (Afset et al., 2003, 2004; Behiry et al., 2011; Levine et al., 1993). Humans are the only known reservoir for tEPEC with symptomatic and asymptomatic children and asymptomatic adults being the most likely source (Levine and Edelman, 1984). On the other hand, atypical strains have been isolated from human and animal sources including dogs, rabbits, monkeys and sheep (Moura et al., 2009; Sekse et al., 2011). Many human and animal EPEC species are clonally related (Moura et al., 2009), sharing many virulence properties. A recent survey of laboratory rabbits found a disease-associated human strain of aEPEC in animal stools and a significant association between diarrheic animals and the presence of EPEC (Swennes et al., 2012). These data suggest inter-species transmission as a means for human infection with aEPEC and rabbits as a possible animal reservoir. Strategies to prevent transmission and spread of EPEC include proper hand washing and improvements in sanitary conditions and freshwater supplies, as well as instruction on food, domestic and personal hygiene (Maranhão et al., 2008).

In contrast to EPEC, the infectious dose of EHEC is thought to be quite low with reports suggesting an infectious dose of less than 675 organisms per contaminated patty of beef (Tuttle et al., 1999). Cattle are a major reservoir for EHEC O157:H7 but these strains have also been isolated from other animals including sheep, pigs, rabbits, dogs, birds, rodents and insects (Ferens and Hovde, 2011; Gyles, 2007). Exposure to EHEC mainly occurs from contact with contaminated fecal matter or from direct contact with contaminated animals or animal products. EHEC O157:H7 can survive in water sources for up to 2 years (Avery et al., 2008) and 68 % of infections in the United States are estimated to be the result of food related contamination (Scallan et al., 2011); however, person-to-person transmission of EHEC has been reported during outbreaks (Snedeker et al., 2009) and could occur through contact with asymptomatic shedders, especially when highly susceptible individuals are involved.

1.2.3 Symptoms and onset of disease

Although EPEC and EHEC share a similar route of transmission and pathogenic strategy during human infection, the symptoms and onset of disease caused by these pathogens are quite different. EPEC is a significant cause of infectious diarrhea that is often accompanied by fever, vomiting and dehydration in children under 2 years of age (Goosney et al., 2000; Kaper et al., 2004; Nataro and Kaper, 1998). In human volunteers, the onset of diarrhea due to EPEC is fairly rapid, occurring as early as 2.9 hours post ingestion of wild type bacteria (Donnenberg et al., 1993). Acute diarrhea is the most likely result of EPEC infection but persistent cases, lasting more than 2 weeks, have also been reported (Levine and Edelman, 1984; Nataro and Kaper, 1998). In comparison to other diarrheal pathogens such as Adenovirus, Rotavirus, *Campylobacter* and *Salmonella*, infection with EPEC is more likely to lead to development of

persistent diarrhea and hospitalization (Nguyen et al., 2006). Other clinical features associated with EPEC-induced diarrhea include intolerance to cow's milk and an increase in failure to respond to oral rehydration therapy (Ochoa et al., 2008).

The clinical presentation of EHEC infections can range in severity from mild watery diarrhea to HC with a risk of development to HUS. The incubation period is short, lasting approximately 3 days before the first appearance of symptoms (Bell et al., 1994). Diarrhea is usually accompanied by fever, abdominal cramping or vomiting (Tarr et al., 2005) with progression to HC in the days following initial onset of diarrhea. It is generally believed that EHEC O157:H7 infection leads to higher rates of HC compared to non-O157 strains (Croxen et al., 2013). In general, EHEC-induced diarrhea resolves in about 1 week but the association of EHEC with HUS is a major health concern worldwide. Additionally, serious long term complications can develop in 20-40% of HUS patients including cardiac and gastrointestinal complications, hypertension and chronic renal disease (Rosales et al., 2012).

1.3 Pathogenesis of A/E pathogens

In general, EPEC and EHEC are non-invasive organisms that share a similar pathogenic strategy with a few exceptions. EPEC do not produce heat-labile or heat-stable enterotoxins while EHEC produce at least one type of Stx, a key virulence factor in strains causing HUS. EHEC are likely to have evolved from an EPEC ancestor strain through acquisition of lysogenic bacteriophage carrying Stx-encoding genes (O'Brien et al., 1984). Another distinguishing feature between EPEC and EHEC involves initial adherence to epithelial cells. Attachment of EPEC to the surface of the host intestinal epithelium is mediated by the bundle forming pilus (BFP) (Girón et

al., 1991). BFP are type IV pili that tether individual bacteria to one another, producing a localized adherence (LA) pattern in the form of compact three-dimensional microcolonies that can be seen on HeLa cells within 3 hours of infection (Scaletsky et al., 1984). The LA phenotype correlates with EPEC1 and EPEC2 clonal lineage strains carrying large *E. coli* EAF plasmids (Baldini et al., 1983). In contrast, EHEC do not harbor pEAF and thus do not express BFP. However, EHEC do encode a number of adhesins that likely contribute to colonization. Two operons encoding long polar fimbriae (Lfp) have been found in EHEC O157:H7 that have been shown to contribute to colonization and tissue tropism (Farfan and Torres, 2012; Fitzhenry et al., 2006). EHEC also encodes a type IV pilus known as the hemorrhagic coli pilus (HCP) that forms long bundled fibres capable of attaching to the surface of the epithelium (Xicohtencatl-Cortes et al., 2007, 2009). Interestingly, both EPEC and EHEC express LifA (lymphocyte inhibitory factor), a large surface protein that contributes to cell adherence *in vitro* (Badea et al., 2003) and is required for intestinal colonization of mice by the related A/E pathogen *C. rodentium* (Klapproth et al., 2005). LifA has recently been identified as the largest secreted effector for any pathogen possessing a type III secretion system (T3SS) (Deng et al., 2012) but unlike LifA_{EPEC}, LifA_{EHEC} does not possess lymphostatin activity (Abu-Median et al., 2006).

Following initial attachment, EPEC and EHEC utilize a bacterial receptor to intimately attach to intestinal epithelial cell (IEC) surfaces concomitant with reorganization of filamentous actin to produce the characteristic A/E lesion. EPEC is the prototype organism for strains causing A/E histopathology, however, EHEC and other human pathogens such as *E. albertii*, as well as

several animal pathogens such as REPEC/RDEC-1 (rabbit), PEPEC (pig), DEPEC (dog) and *C. rodentium* (mouse) are also members of the A/E pathogens group (Goosney et al., 2000).

1.3.1 Formation of A/E lesions

Inclusion of EPEC and EHEC in the A/E pathogens group is based on their ability to form distinctive pedestal-like structures on the surfaces of IECs. This distinctive lesion is a hallmark of A/E pathogenesis characterized by effacement of brush border microvilli at the site of bacterial attachment (Moon et al., 1983). The dissolution of the intestinal brush border is accompanied by formation of actin pedestals that extend from the surface of the epithelium into the lumen (Rosenshine et al., 1996). Formation of the A/E lesion occurs by subversion of actin dynamics within host cells and is mediated by the interaction between intimin and the bacterial translocated intimin receptor, Tir (Gruenheid et al., 2001; Kalman et al., 1999; Kenny et al., 1997). Intimin is a 94 kilodalton (kDa) protein encoded by the *eae* gene which is found in all strains capable of inducing A/E histopathology (Nataro and Kaper, 1998). The N-terminus of intimin is highly conserved among A/E pathogens, whereas the C-terminus shows much less homology (Frankel et al., 1994) and for EPEC, differences in the C-terminal region of intimin have been used as a basis for classification into distinct subtypes (Tardelli Gomes and Gonzalez-Pedrajo, 2010). Intimate attachment of EPEC to intestinal cells induces diverse signal transduction pathways within the host, leading to subversion of many cellular processes for the benefit of the pathogen. Formation of A/E lesions is contingent on the secretion of bacterial virulence proteins via a type III secretion system (T3SS) that is absolutely required for EPEC/EHEC pathogenesis (Kenny, 2002).

1.3.2 Type III secretion systems and A/E pathogen infection

EPEC and EHEC are normally non-invasive pathogens requiring a T3SS for intimate attachment and initiation of disease. The EPEC/EHEC T3SS is encoded on a conserved 35 kilobase pathogenicity island (PAI) found in all A/E pathogens, known as the locus of enterocyte effacement (LEE) (McDaniel et al., 1995). The core LEE encodes a T3SS, the main function of which is to secrete protein components of the translocon (EspA, EspB, and EspD) and to drive effectors directly into host cells. The LEE T3SS is absent in non-pathogenic strains of *E. coli* and the EPEC LEE has been shown to induce actin rearrangement and pedestal formation in infected cells when transformed into avirulent *E. coli* K-12 strains (McDaniel and Kaper, 1997). In some EPEC and EHEC strains the presence of additional genes in the LEE flanking regions can extend the LEE up to 110 kb (Müller et al., 2009), although the role of these additional genes in pathogenesis is variable or unknown. In addition to the T3SS apparatus, the LEE encodes regulatory proteins, secreted effectors and their related chaperones (Deng et al., 2004; Frankel et al., 1998; Iguchi et al., 2009). The T3SS is required for the translocation of an assortment of effector proteins into host cells, which subvert cellular processes in order to promote A/E pathogen infection (Dean et al., 2005; Kenny, 2002). To date, several LEE-encoded effectors, as well as a number of non-LEE (Nle)-encoded effectors (Deng et al., 2004), have been identified in pathogenic *E. coli* strains (Coburn et al., 2007; Iguchi et al., 2009), all of which exploit the LEE T3SS for delivery into host cells.

1.3.3 Effector proteins of EPEC and EHEC

Effector proteins perform pivotal roles during T3SS-mediated disease by subverting host defenses and cellular trafficking and by manipulating the host cytoskeleton (Coburn et al., 2007).

There are seven LEE-encoded T3SS effectors that are well conserved across A/E pathogenic species while the number and type of Nle-encoded effectors vary significantly (Dean and Kenny, 2009). The prototypic EPEC strain E2348/69 encodes at least 23 effectors (Deng et al., 2012; Iguchi et al., 2009), whereas certain serotypes of EHEC encode as many as 41 (Ogura et al., 2009; Tobe et al., 2006). Likewise, there is considerable variation in the number of Nle-encoded effectors among A/E animal pathogens such as REPEC and *C. rodentium* (Dean and Kenny, 2009; Deng et al., 2010). The variation in effector repertoire among A/E pathogenic species likely reflects differences in virulence phenotypes and adaptation to diverse host environments (Dean and Kenny, 2009; Tobe et al., 2006). To date, cellular functions and host binding partners have been established for some of the LEE and Nle-encoded effectors. Figure 1.1 depicts what is currently known about the site of action and function of most identified EPEC/EHEC effectors.

(Ruchaud-Sparagano et al., 2011). The remaining six LEE-encoded effectors, Map, EspF, EspG, EspZ, EspH and EspB, all have physiological roles relevant to A/E pathogen infection. Map stimulates formation of membrane filopodia and epithelial barrier disruption as well as mitochondrial dysfunction (Ma et al., 2006). Multifunctional properties have also been reported for EspF and EspG, both of which affect aquaporin localization leading to diarrhea (Guttman et al., 2007). Like Map, EspF localizes to mitochondria (Nougayrède and Sonnenberg, 2004) and has been shown to disrupt tight junctions (Guttman et al., 2006), while EspG inhibits surface receptor recycling (Clements et al., 2014; Selyunin et al., 2014) and may alter host cytoskeletal components through its interaction with tubulin (Hardwidge et al., 2005). EspZ promotes host cell survival (Shames et al., 2010) and regulates effector translocation (Berger et al., 2012). EspH affects filopodia formation, participates in actin signaling during pedestal formation (Wong et al., 2012a) and acts as a RhoGEF inhibitor (Wong et al., 2012b), while both EspH and EspB are capable of inhibiting phagocytosis of EPEC by macrophages (Dong et al., 2010; Iizumi et al., 2007).

1.3.3.2 Non-LEE-encoded effectors

Nle effector genes are located on prophages and integrative elements throughout the genomes of A/E pathogens and there is considerable variation in the number and type of Nle effectors among A/E pathogens (Dean and Kenny, 2009). The prototypical EPEC strain, E2348/69, encodes many Nle effectors involved in dampening the host immune response. NleB, NleC, NleD, NleE and NleH have all been shown to inhibit NF- κ B activation through a variety of different mechanisms (Baruch et al., 2011; Gao et al., 2009, 2013; Li et al., 2013; Nadler et al., 2010; Newton et al., 2010; Pearson et al., 2011, 2013; Sham et al., 2011; Yen et al., 2010). NleB and

NleE reduce translocation of the p65 subunit of NF- κ B to the nucleus by preventing degradation of the NF- κ B inhibitor (I κ B) (Nadler et al., 2010; Newton et al., 2010). NleB was recently identified as an N-acetyl-D-glucosamine (GlcNAc) transferase capable of inactivating several proteins in the NF- κ B activation pathway through the addition of a GlcNAc residue (Gao et al., 2013; Li et al., 2013; Pearson et al., 2013). On the other hand, NleE has been identified as an S-adenosyl-L-methionine (SAM)-dependent methyltransferase targeting various adapter proteins involved in NF- κ B activation (Zhang et al., 2012). The effectors NleC and NleD were found to cooperatively target both NF- κ B and c-Jun N-terminal kinase (JNK) pathways through zinc-dependent endopeptidase activities (Baruch et al., 2011). NleC was shown to cleave the NF- κ B p65 subunit while NleD was responsible for cleavage of JNK (Baruch et al., 2011). NleH is a Ser/Thr protein kinase and is also shown to dampen the immune response by reducing nuclear localization of ribosomal protein s3 (RPS3) (Gao et al., 2009; Wan et al., 2011) in addition to modulating the apoptotic response (Hemrajani et al., 2010). In addition to immunomodulatory functions, Nle-encoded effectors such as EspJ have anti-phagocytic properties (Marchès et al., 2008), while NleA and NleF alter host protein secretion (Kim et al., 2007; Olsen et al., 2013). NleA impairs the function of coat protein complex II (COPII) vesicles to impede anterograde transport between the endoplasmic reticulum (ER) and Golgi (Kim et al., 2007; Thanabalasuriar et al., 2012) and disrupts tight junction integrity (Thanabalasuriar et al., 2010), an effect that has been linked to its interaction with COPII vesicles during infection (Thanabalasuriar et al., 2013). Similar to NleA, NleF has also been shown to inhibit protein secretion. However, NleF interacts with the COPI vesicle receptor, Tmp21, to impair retrograde vesicle transport between the Golgi and ER (Olsen et al., 2013).

1.3.3.3 T3SS effectors and diarrhea production

The exact mechanism of A/E pathogen-induced diarrhea production is not fully understood and likely involves a combination of different mechanisms (Goosney et al., 2000). The speed of diarrhea onset implies a secretory mechanism rather than malabsorption as a more likely cause of diarrhea (Hecht, 2001). Nonetheless, the effacement of microvilli at the sites of bacterial attachment could lead to a decrease in absorptive surfaces thereby contributing to diarrhea through interference with proper absorptive channels. A number of T3SS effectors are known to impact on various water and ion channels of the intestinal epithelia and are thought to contribute collectively to EPEC-induced diarrhea but the exact contribution of each mechanism is unknown. Tir, Map, EspF, and EspH inhibit the sodium–D-glucose transporter (SGLT1), which is responsible for fluid uptake from the intestine (Dean and Kenny, 2009; Dean et al., 2006), while EspF and EspG alter localization of aquaporins, which also play a role in water transport (Guttman et al., 2007). EspG and EspG2 are also responsible for disruption of chloride transport across the apical membrane resulting in decreased Cl^-/OH^- exchange activity (Gill et al., 2007). EPEC is also known to inhibit the intestinal serotonin transporter (SERT) as well as mucosal content of 5-HT (Esmaili et al., 2009), a neurotransmitter that affects secretion and absorption of fluids and electrolytes through SERT (Gill et al., 2005). Inhibition of SERT appears to be T3SS-dependent (Esmaili et al., 2009), however, no T3SS effectors have been identified as specifically associated with this process. Additionally, disruption of tight junctions by EspF (Viswanathan et al., 2004), EspG (Matsuzawa et al., 2005), and Map (Dean and Kenny, 2004) leads to increased intestinal permeability, which could also contribute to EPEC-induced diarrhea.

1.4 Model systems for studying A/E pathogens

Recent advances in *in vitro* and *in vivo* modeling of A/E pathogens have contributed to our knowledge of how EPEC and EHEC attach to host cells and subvert host cell signaling pathways to promote infection and cause disease. EPEC and EHEC are strictly human enteric pathogens, but the availability of surrogate animal models, in addition to the advent of tissue culture, has made it possible to study the complex interactions between these pathogens and their hosts (Vallance et al., 2004). *In vitro* models such as IECs in tissue culture and *in vitro* organ culture (IVOC) have been used extensively to define, at the molecular level, T3SS-related proteins necessary for effector secretion and A/E lesion formation, as well as effector localization, function and protein interactions within host cells. Alternatively, *in vivo* models including nematodes, mice and rabbits as well as human volunteers, provide essential information with respect to virulence, host immunity and how the inflammatory response contributes to the pathology of A/E pathogen-mediated disease (reviewed in (Law et al., 2013)).

1.4.1 *In vitro* models for studying A/E pathogens

Under natural infection conditions, EPEC shows a narrow specificity for cells of the pediatric small intestine, while EHEC is usually restricted to the colon and shows no preference in the age of individuals it infects. In tissue culture however, this specificity in age and tissue tropism is lost and EPEC/EHEC are capable of interacting with a number of cells originating from a variety of tissues and species (Law et al., 2013). Unlike EHEC, EPEC rapidly infects tissue culture cells making this pathogen an ideal candidate for studies on the molecular mechanisms of A/E pathogen infection. Infection of immortalized epithelial cells provides a simple and convenient means to assess the direct relationship between the infecting organism and the intestinal epithelia

in the absence of additional host and microbial factors that would normally be present within the lumen. The nonpolarized human HeLa cell line has been used extensively to study actin pedestal biogenesis, T3SS-dependent protein translocation as well as functional analyses of effectors during A/E pathogen infections. On the other hand, Ptk2 cells derived from the kangaroo rat kidney have been useful in describing pedestal motility on the surfaces of EPEC/EHEC infected cells (Sanger et al., 1996; Shaner et al., 2005) due to their tendency to remain flat throughout the cell cycle and during infection. In comparison to nonpolarized cell lines, Caco-2 and T84 cells are capable of mimicking polarized enterocytes of the small and large intestine, respectively, and have additionally been used to study the effects of EPEC infection on tight junction integrity and overall intestinal barrier function (Dean and Kenny, 2004; McNamara et al., 2001; Thanabalasuriar et al., 2010). EPEC/EHEC are human-specific pathogens and the use of human cell lines enables the study of direct interactions between these bacteria and their natural host cells, making IEC lines an excellent tool to study A/E pathogen-host-cell dynamics. However, the physiological relevance of the findings discovered in cultured cells needs confirmation in more biologically relevant host models. Cell culture methods provide important information with respect to the cellular biology of T3SS effector function, but are of limited use in studying the interaction of A/E pathogens with the host immune system and microbiota. Related A/E animal pathogens, infecting their natural hosts, have come to serve as effective models for EPEC/EHEC pathogenesis although not all are capable of causing equivalent intestinal disease in their animal hosts.

1.4.2 *In vivo* models for studying A/E pathogens

Given the narrow host range of EPEC/EHEC, studies exploring the roles of the genes involved in A/E pathogen virulence and lesion formation have been limited by a lack of *in vivo* models reflecting the natural disease process in humans. While much information has been gathered through *in vitro* analyses with respect to localization and function of T3SS effector proteins, *in vivo* systems are the only way of assessing A/E pathogen virulence within the context of the complete intestinal environment. A/E bacteria are able to infect diverse animal species (Wales et al., 2005) from the invertebrate, *Caenorhabditis elegans* to mice, rabbits, pigs and cattle. As such, the diversity of available animal models has provided the research community with a wealth of potential hosts with which to simulate the various aspects of human infection.

1.4.2.1 The REPEC model of infection

A great deal of *in vivo* research on A/E pathogens has been performed using natural animal pathogens related to EPEC and EHEC. Infection of rabbits and mice with REPEC and *C. rodentium*, respectively, has been used to study the contributions of many translocated effectors and T3SS-related genes to EPEC virulence and disease. REPEC encompasses a number of serotypes of A/E lesion-forming, diarrheagenic *E. coli* that share many virulence characteristics with human EPEC and are capable of causing diarrheal disease in weaned rabbits (Goosney et al., 2000). Similar to human-specific EPEC strains, REPEC induces A/E lesions and intestinal pathology without invasion of the epithelia or production of enterotoxins (Robins-Browne et al., 1994). The REPEC LEE has been characterized and shares a high degree of homology with the LEE region of EPEC (Tauschek et al., 2002), thereby facilitating the discovery of LEE genes required for A/E lesion formation and disease (Abe et al., 1997; Marchès et al., 2000).

1.4.2.2 The *C. rodentium*-mouse model of infection

Similar to the LEE of REPEC, the LEE of *C. rodentium* is comparable to those of EPEC and EHEC (Deng et al., 2001), but is required to produce A/E lesions on the intestinal cells of mice (Schauer and Falkow, 1993a). Functional conservation of Tir and intimin from EPEC and *C. rodentium* has been demonstrated and confirms the usefulness of the *C. rodentium*-mouse model to study human infections with EPEC and EHEC (Deng et al., 2003; Frankel et al., 1996). Instead of causing obvious diarrhea as seen with EPEC and EHEC, *C. rodentium* infection results in colonic inflammation and hyperplasia (Barthold et al., 1978). However, studies have shown that mice infected with *C. rodentium* have an increased proportion of water in the contents of their colons which translates to a diarrhea-like phenotype (Guttman et al., 2006). In spite of any differences in disease manifestation, mouse infections with *C. rodentium* have contributed significantly to our understanding of A/E pathogen virulence and mechanisms of disease *in vivo*. Using the *C. rodentium*-mouse model 33 virulence factors were identified during a screen of all 41 genes in the *C. rodentium* LEE (Deng et al., 2004). A comprehensive analysis of the *C. rodentium* secretome has since been performed, effectively confirming secretion of many previously identified effectors while expanding the known repertoire of T3SS proteins among A/E pathogens (Deng et al., 2010). Infection of mice with *C. rodentium* mutants confirms a critical role in colonization and virulence of the LEE-encoded effectors Tir, EspB, and EspZ, as well as the Nle-encoded effectors NleA and NleB (Deng et al., 2003, 2004; Gruenheid et al., 2004; Kelly et al., 2006; Mundy et al., 2004; Newman et al., 1999), whereas others are thought to contribute collectively (Dean and Kenny, 2009).

The *C. rodentium*-mouse model has been widely used to explore the host immune response to pathogenic *E. coli* infections (Borenshtein et al., 2008; Kum et al., 2010; Luperchio and Schauer, 2001). Thus, another significant advantage to the use of *in vivo* models is the ability to assess host-generated immune responses to bacterial infections. In susceptible mice, *C. rodentium* induces colonic hyperplasia and intestinal inflammation and mice often die as a result of infection, whereas less susceptible mouse strains are generally able to clear these infections (Luperchio and Schauer, 2001) and develop a protective response against subsequent infection (Ghaem-Maghami et al., 2001). Although the clinical outcome of EPEC or EHEC infection in humans differs from that of *C. rodentium* in mice, this model remains the best for studies on host immune response to A/E pathogen infection.

A variety of infection models have been developed to provide insight into our current understanding of the virulence mechanisms employed by A/E bacterial pathogens and to explore the molecular mechanisms that contribute to virulence of pathogenic *E. coli*. No model system currently in use for the study of EPEC/EHEC pathogenesis is able to completely replicate the natural infection process in humans. However, each model does have its particular advantages and it is the combination of all these models that has advanced our knowledge on A/E pathogens tremendously over the last 20 years. The use of *in vitro* and *in vivo* model systems has given way to important advances in several areas of EPEC/EHEC pathogenesis. The best studied aspects of A/E pathogen infection include pathogen-induced effects on host immune signaling and cell death pathways as well as manipulation of the cellular cytoskeleton and associated cytoskeletal components.

1.5 A/E pathogen infection and the host cytoskeleton

For many intracellular pathogens, movement within and between host cells is accompanied by pathogen-induced cytoskeletal alterations (Stevens et al., 2006), whereas A/E pathogens deliver a set of T3SS effectors into the host that drive actin reorganization while remaining extracellular. Rearrangement of actin and other cytoskeletal components in the vicinity of attaching bacteria leads to pedestal formation, thereby tightening the interaction between the A/E pathogen and the intestinal epithelium in order to ensure colonization (Caron et al., 2006).

For all A/E pathogens, Tir is essential for intimate attachment and pedestal formation and it is thought that intimin on the bacterial cell surface is involved in clustering translocated Tir on the apical membranes of IECs (Touzé et al., 2004). Once inserted into the plasma membrane, Tir adopts a hairpin-like conformation with both the amino- and carboxy-terminal domains present in the host cell cytoplasm where they interact with a number of host cytoskeletal and signaling components (Hartland et al., 1999). Interestingly, the Tir proteins of EPEC and EHEC are not functionally interchangeable, despite similarities in the host components they associate with during actin assembly (Campellone and Leong, 2003). Tir_{EPEC} requires tyrosine phosphorylation and most often binding of Tir_{EPEC} to Nck, an adaptor protein involved in actin signaling; whereas Tir_{EHEC} does not require phosphorylation or Nck and instead uses an additional secreted effector, EspF_U, to initiate actin assembly for pedestal formation (Campellone, 2010; Campellone and Leong, 2003; DeVinney et al., 2001). Following Nck-dependent or independent initiation, Neuronal Wiskott-Aldrich syndrome protein (N-WASP) is ultimately recruited to the site of pedestal assembly where it activates the actin-related protein 2/3 (Arp2/3) complex to form densely branched actin filaments beneath adherent bacteria (Campellone, 2010).

While much is known about the proteins involved in the subversion of actin dynamics during pedestal formation (Campellone and Leong, 2003), microtubules (MTs) are also thought to be a target of T3SS effectors during A/E pathogen infection. The EPEC secreted effector EspG binds directly to tubulin heterodimers and may be involved in MT disassembly and early colonization in a mouse model of infection (Hardwidge et al., 2005; Matsuzawa et al., 2004).

Eukaryotic cells use MTs for structural support, motility, cell division and intracellular trafficking, as well as docking space for signaling molecules and cytoplasmic components (Janmey, 1998). A wide variety of proteins including the transcription factor, NF- κ B, associate with cytoplasmic MTs and it is thought that release of these factors through localized MT depolymerization can influence gene expression (Janmey, 1998). Modifications in MT dynamics have been reported during invasion of host cells by intracellular pathogens such as *Shigella flexneri* (Yoshida et al., 2006) and *Campylobacter jejuni* (Oelschlaeger et al., 1993). Interestingly, EspG shares some sequence similarity with the VirA protein of *S. flexneri* (Hardwidge et al., 2005) which has been shown to cause MT disassembly *in vitro* as well as *in vivo* (Yoshida and Sasakawa, 2003). Thus far, EspG and its homologue EspG2 are the only published EPEC or EHEC effectors known to specifically affect MTs or their accessory proteins.

1.6 Microtubule associated proteins (MAPs)

The function and stability of MTs is determined in large part by a number of accessory proteins known as microtubule associated proteins (MAPs). MAPs bind along the entire length of the MT and are involved in several important functions such as MT stabilization, growth and dynamics, as well as interactions during several steps of mitotic division. In general, MAPs can

be divided into motor or non-motor proteins. Molecular motor proteins like kinesin and cytoplasmic dynein interact directly with MTs and as such are also involved in chromosomal separation during cell division (Hirokawa and Noda, 2008; Hirokawa et al., 1998). In addition to movement of chromosomes, molecular motors use MTs as tracks for long-distance transport of a variety of cargo including mRNA, organelles and membrane bound vesicles. The binding and distribution of MAPs along MTs can be affected by post-translational modification (PTM) of the $\alpha\beta$ -tubulin heterodimers making up polymerized MTs (Bonnet et al., 2001; Konishi and Setou, 2009) or MAPs themselves may affect the PTM state of the MT through binding (Perez et al., 2009; Takemura et al., 1992). In this way, MAPs play an essential role in distribution of kinesins and contribute to spatio-temporal localization of cargo during and after mitosis. On the other hand, non-motor proteins such as ensconsin may still be involved in MT motor-dependent processes by acting as cofactors for kinesin-1 proteins (Barlan et al., 2013; Sung et al., 2008).

1.6.1 Ensconsin (MAP7 / EMAP-115)

Though never before identified as a target for microbial pathogens, the MAP ensconsin has been connected to several fundamental MT-related cellular functions. Ensconsin (E-MAP-115 or MAP7) is an 84 kDa protein originally purified from HeLa cells (Bulinski and Bossler, 1994; Masson and Kreis, 1993). Expression of this MAP occurs mainly in cells of epithelial origin and cryosections of the human small intestine show its expression is limited to the epithelial layer (Vanier et al., 2003). Ensconsin exhibits a dynamic association with MTs in cultured cells (Faire et al., 1999) and when overexpressed under *in vitro* conditions has been suggested to contribute to MT stability (Bulinski and Bossler, 1994; Masson and Kreis, 1993). However, other studies have shown that undifferentiated cells expressing increased amounts of this MAP show similar

MT dynamics to those of untransfected cells (Faire et al., 1999). More recently, the ensconsin protein of *Drosophila melanogaster* was shown to be integral for all known functions of kinesin-1 in neurons and oocytes (Sung et al., 2008). Sung and colleagues showed that distribution of kinesin-1 and kinesin-1-dependent cargo was affected in loss of function mutants as well as MT association rate and mobility of the motor (Sung et al., 2008). This effect was confirmed by a later study, showing that ensconsin appeared to control specific recruitment of kinesin-1 to MTs as well as kinesin-1 activation and transport (Barlan et al., 2013). Additionally, ensconsin is required for proper positioning of nuclei in mammalian- and *Drosophila*-derived myotubes (Metzger et al., 2012) as well as separation of centrosomes during mitosis (Gallaud et al., 2014). Given the critical role that ensconsin and other MAPs play in maintaining MT stability and motor transport, these proteins would make attractive targets for infecting pathogens though few studies have focused on this aspect of host-pathogen biology.

1.7 Summary of thesis

The field of EPEC/EHEC pathogenesis is rapidly expanding and while a significant amount of literature exists on the virulence strategies used by these pathogens in causing disease, many questions about the molecular mechanisms of specific virulence effectors have yet to be answered. The studies presented in this thesis were initiated to identify the cellular role and virulence effects of the T3SS effectors, NleB and EspL, as they relate to EPEC/EHEC pathogenesis.

Over the last decade, an area of increasing interest in the T3SS effector field has involved identifying specific targets for secreted effectors once inside host cells. Using a quantitative

mass spectrometry screen we identified host cell binding partners for a number of secreted effectors. Of these, NleB and EspL were both shown to have an affinity for the mammalian MAP, ensconsin. Our aim was to evaluate the potential roles of these effectors in altering host cytoskeletal structures or MT based processes and transport systems during infection. The focus of this work was to characterize the effector-ensconsin interactions and to determine how these effectors contribute to A/E pathogen-mediated disease. Our hypothesis is that the T3SS effectors, NleB and EspL, contribute to pathogenesis and the overall infection process through modulation of host ensconsin. The following chapters outline experiments to determine the physiological role of NleB and EspL as it relates to the function of ensconsin in epithelial cells, as well as to establish a connection between the effector-altered function of ensconsin and promotion of A/E pathogen infection. Chapters 2 and 3 detail the interaction between NleB, EspL and ensconsin and identify a novel function for these effectors in disrupting host vesicle trafficking during EPEC infections. Chapter 4 further characterizes the known virulence-associated effects of NleB and EspL through simultaneous deletion of their encoding genes in *C. rodentium* followed by infections in mice. Understanding the roles of singular effectors as well as groups of related effectors will provide insight into the pathogenic strategy of A/E pathogens and may provide unique options for therapeutic development.

Chapter 2: The type III secretion system effectors, NleB and EspL, interact with host ensconsin

2.1 Introduction

The T3SS is a complex protein structure used by many Gram negative bacterial pathogens to transfer virulence proteins directly into the host cell cytosol. These bacterial virulence proteins, also known as effectors, are central to pathogenesis as T3SS mutants are often severely hindered in their ability to colonize their hosts. Accordingly, techniques to identify effectors and characterize their interactions within host cells are paramount to understanding bacterial disease.

Our laboratory has previously used the SILAC (stable isotope labeling with amino acids in cell culture) method to effectively analyze the type III secretome of EPEC and the related A/E pathogen *C. rodentium* (Deng et al., 2010, 2012) but effector identification is only the first step in understanding A/E pathogen-mediated disease. The SILAC method was first used to identify host protein binding partners for the *Salmonella* T3SS effector SopB (Rogers et al., 2008) and has previously been used by our laboratory to identify host targets for all *Salmonella* Typhimurium secreted effectors, many of which have been confirmed through independent analyses (Auweter et al., 2011). To quantitatively identify protein-protein interactions, we used the SILAC method to differentially label the cellular proteomes of related samples by replacing essential amino acids with stable isotopes followed by mass spectrometry analysis (Ong et al., 2003). As demonstrated by Auweter and colleagues, the SILAC method is a sensitive and specific technique which could be applied to identify host targets of many effector secreting pathogens (Auweter et al., 2011).

EPEC and EHEC are gastrointestinal pathogens capable of causing severe infections that can result in life-threatening outcomes. The virulence of EPEC and EHEC is dependent on a functional T3SS as non-secreting mutants are incapable of translocating effectors, pedestal formation and virulence in mice (Deng et al., 2004; Gauthier et al., 2003). While there is variation in the number and type of effector proteins secreted by EPEC and EHEC, certain effector sequences are highly conserved among these pathogens. EPEC and EHEC are thought to encode a 'core' set of essential T3SS effectors which includes the 7 LEE-encoded effectors as well as a set of Nle-encoded effectors including NleA, NleB, NleE, NleF, NleG, NleH and EspL (Iguchi et al., 2009). Of the Nle-encoded effectors, NleA and NleB are the only two known to have a major role in virulence (Gruenheid et al., 2004; Kelly et al., 2006; Mundy et al., 2004; Wickham et al., 2006) while others are known to play minor roles (Wickham et al., 2006, 2007). For NleA, this effect has been suggested to involve disruption of intestinal barrier function, which has been linked to its influence on COPII vesicle trafficking (Thanabalasuriar et al., 2010, 2013). NleB is one of several effectors involved in dampening the immune response to infection (Gao et al., 2013; Li et al., 2013; Nadler et al., 2010; Newton et al., 2010; Pearson et al., 2013), but has not yet been connected to an effect on intracellular vesicle transport. NleB was recently identified as a GlcNAc transferase that inactivates several death domain containing proteins in the NF- κ B activation pathway (Gao et al., 2013; Li et al., 2013; Pearson et al., 2013). The *nleB* gene is conserved among A/E pathogens and is often associated with other virulence genes including the effector encoding gene, *espL* (also known as *ent*) (Wickham et al., 2006, 2007). NleB is encoded in two copies by the *nleB1* and *nleB2* genes in both EPEC and EHEC. Based on homology, *espL* is thought to be present in one functional copy in EPEC, while EHEC carries 3 putative copies of *espL* genes (Tobe et al., 2006). However, only *espL2*, which corresponds to

EPEC *espL*, has been functionally confirmed (Ogura et al., 2009; Tobe et al., 2006). In comparison to *nleB*, the presence of *espL* has a modest effect on colonization of mice (Wickham et al., 2006), but the presence of PAI O122, which harbors both genes, is correlated with higher virulence potential of EPEC and EHEC in humans (Bugarel et al., 2010; Vieira et al., 2010; Wickham et al., 2006). Similarly, EHEC EspL2 has been linked to colonization defects in tissue culture by interacting with annexin-2 to modulate F-actin aggregation beneath adherent bacteria (Miyahara et al., 2009).

EspL is one of many effectors known to target actin associated proteins during A/E pathogen infection but there has been a dearth of work examining any MAPs as potential effector targets. MAPs often serve to regulate MT dynamics or to connect MTs with other cellular components (Cassimeris and Spittle, 2001) and their influence on vesicle trafficking and distribution of cellular cargo has recently been reviewed (Atherton et al., 2013). Unlike the neuronal MAPs, Tau and MAP-2, ensconsin (EMAP-115 or MAP7) is a conserved MAP expressed mainly in epithelial cells. Ensconsin binds along the entire length of MTs and was originally identified based on its ability to tightly associate with MTs (Bulinski and Bossler, 1994; Masson and Kreis, 1993). Additionally, ensconsin has been identified as an essential cofactor of kinesin-1 involved in motor recruitment to MTs, MT growth and vesicle trafficking (Barlan et al., 2013; Gallaud et al., 2014; Metzger et al., 2012; Sung et al., 2008).

Characterization of protein-protein interactions between bacterial effectors and host receptors is a crucial step in understanding the physiological significance of T3SS proteins during A/E pathogen infection. In many cases, the multifunctional and overlapping nature of many secreted effectors hinders the discovery of novel effector functions. In this study, we used the highly

sensitive SILAC technique to quantitatively identify host interaction partners for a number of EHEC secreted effectors. We confirmed several previously determined host targets and identified ensconsin as a novel host target for the conserved effectors, NleB1 and EspL. We confirmed these interactions through co-immunoprecipitation for both EPEC and EHEC and determined that the site of effector interaction was located in the MTB region of ensconsin. Importantly, we found that the *Salmonella* homolog for NleB, namely SseK, did not interact with ensconsin, indicating that ensconsin may be a unique target for A/E pathogens. These data show that EPEC/EHEC secrete multiple effectors targeting the MAP ensconsin, suggesting that this protein may be an important target during infection.

2.2 Materials and methods

2.2.1 Tissue culture, bacterial strains and plasmids

HEK293T cells (ATCC) were maintained in Dulbecco's Modified Eagle Medium (DMEM) High Glucose (Thermo Scientific) supplemented with 10% fetal bovine serum (FBS) (Thermo Scientific), 1% Glutamax (Gibco) and 1% non-essential amino acids (NEAA) (Gibco).

For routine cloning, bacteria were grown in Lysogeny Broth (LB) broth at 37°C supplemented with appropriate antibiotics. Broth cultures were inoculated from single bacterial colonies on LB agar plates containing antibiotics where appropriate. Antibiotic concentrations were as follows: ampicillin 100 µg/ml, streptomycin 50 µg/ml and kanamycin 50 µg/ml or 100 µg/ml. A complete list of bacterial strains and plasmids used in this study are described in Tables 2.1 and 2.2, respectively.

Table 2.1 Bacterial strains used in this study

| Name | Source/Reference |
|--|-----------------------------|
| <u><i>Escherichia coli</i></u> | |
| BL21 (DE3) | Stratagene |
| <u>EPEC O127:H6 strain E2348/69</u> | |
| Wild type | (Levine et al., 1978) |
| <u>EHEC O157:H7 strain EDL933</u> | |
| Wild type | (Johnson and Lior, 1984) |
| <u><i>Salmonella</i> strain SL1344</u> | |
| Wild type | (Hoiseth and Stocker, 1981) |

Table 2.2 Plasmids used in this study

| Plasmids | Source/Reference |
|--|-------------------------|
| pGEX-6P-3 | GE Lifesciences |
| pGEX-6P-3-HA ₃ | Lab vector |
| pGEX-6P-3-HA ₃ :: <i>nleB1</i> | This study |
| pGEX-6P-3-HA ₃ :: <i>espL2</i> | This study |
| pGEX-6P-3-HA ₃ :: <i>nleB1(P)</i> | This study |
| pGEX-6P-3-HA ₃ :: <i>nleB2(P)</i> | This study |
| pGEX-6P-3-HA ₃ :: <i>espL(P)</i> | This study |
| pCMVTag4A (pCMV4A) | Stratagene |
| pmap7-FLAG | This study |
| pmap7N1-N6-FLAG | This study |
| pmap7ΔC | This study |
| pmap7ΔN | This study |
| pET28a | EMD Millipore |
| pET28a::6xHis- <i>sseK1</i> | This study |

2.2.2 Cloning of effector gene sequences into pGEX-6P-3::HA₃

For PCR, Elongase Enzyme Mix (Invitrogen) was routinely used. Effector gene sequences were amplified from EPEC strain E2348/69 or EHEC strain EDL933 genomic DNA using primer pairs as listed in Table 2.3. PCR amplified EHEC *nleB1* and *espL2* gene sequences were digested with XhoI/NotI or XmaI/XhoI respectively, and cloned in frame into XhoI/NotI- or XmaI/XhoI-digested pGEX-6P-3 (GE Lifesciences) with an upstream triple HA tag (lab vector; pGEX-6P-3::HA₃). PCR amplified EPEC *nleB1*, *nleB2* and *espL* gene sequences were digested with XhoI/NotI and inserted into XhoI/NotI digested pGEX-6P-3::HA₃. All cloned constructs were verified by DNA sequencing at the Nucleotide and Protein Sequencing (NAPS) Unit (UBC, Vancouver, Canada).

2.2.3 Generation of MAP7-FLAG fusion

The human *map7* sequence (lacking its stop codon) was amplified from cDNA clone SC322593 (OriGene Technologies, Inc.) using primers map7-F and map7-R. The resulting PCR product contained the *map7* gene with a Kozak sequence at the 5' end. Purified PCR product was then digested with BamHI and HindIII and inserted into BamHI/HindIII-digested pCMVTag4A (Stratagene) to generate pCMVTag4A::*map7*-FLAG (*pmap7*-FLAG) which was verified through sequencing.

2.2.4 Generation of MAP7-FLAG truncations

The plasmid *pmap7*-FLAG was used as a template to generate all truncations. All primers used are listed in Table 2.3. C-terminal gene truncations *map7N1* to *map7N6* were amplified using the forward primer map7-F paired with reverse primers map7N1-R, map7N2-R, map7N3-R,

map7N4-R, map7N5-R or map7N6-R. Primers map7C-F and map7-R were used to amplify *map7ΔC*. All constructs were digested with BamHI and HindIII and inserted into BamHI/HindIII digested *pmap7-FLAG*. All *map7* truncations were confirmed by DNA sequencing.

Table 2.3 Oligonucleotide primers used in this study

| Primer | Sequence (5' – 3') ^{a,b} | Restriction endonuclease |
|-----------|---|--------------------------|
| map7-F | gagggatcc acc atggcggagctaggagctg | BamHI |
| map7-R | gagaagctttataacttctgcagtctgctgtg | HindIII |
| map7ΔC-R | gagaagcttcaaggaggatgtcggctctg | HindIII |
| map7ΔN-F | gagggatcc acc atgccaccggctcagtcaaa | BamHI |
| map7-Tr1 | gagaagcttcggagcgtttgtgtacatg | HindIII |
| map7-Tr2 | gagaagcttctgccgctgcagctgctc | HindIII |
| map7-Tr3 | gagaagcttggggaccgggctggag | HindIII |
| map7-Tr5 | gagaagctttctccagacaaggcagctg | HindIII |
| map7-Tr6 | gagaagcttcttctgctcctttccattg | HindIII |
| EHnleB1-F | cacctcgagatgttatcttcattaaatgctc | XhoI |
| EHnleB1-R | gagggcgccgcttaccatgaactgcaggtatac | NotI |
| EHespL2-F | gagcccggaatgccataataa | XmaI |
| EHespL2-R | gagctcgagtactcaactgagagtgccgt | XhoI |
| EPnleB1-F | gactcctcgagatgttatcttcattaaatgcctt | XhoI |
| EPnleB1-R | gtccttacgctgcggccgcttaccatgaactgctgtatac | NotI |
| EPnleB2-F | gacgactcgagatgctttcaccgataaggac | XhoI |
| EPnleB2-R | gtccatacgctgcggccgcttaccatgaactgcatgtatac | NotI |
| EPespL-F | gagcactcgagatgccaataataaacaatcggc | XhoI |
| EPespL-R | gagggttacgctgcggccgctcaattggaataataattatataca | NotI |
| sseK1-F | tcgtcggatccatgatcccaccattaaatagatatg | BamHI |
| sseK1-R | acgacgaattcctactgcacatgcctcgcc | EcoRI |

a – Restriction endonuclease sites are underlined.

b – Kozak sequences are in red.

2.2.5 Cloning of *Salmonella sseK1* into pET28a

Salmonella strain SL1344 was used for cloning of the *sseK1* gene sequence. The *sseK1* gene sequence was amplified using primers sseK1-F and sseK1-R and the resulting PCR product was digested with BamHI and EcoRI. Purified and digested *sseK1* was then inserted into BamHI/EcoRI digested pET28a to generate pET28a::6xHis-*sseK1* which was verified by sequencing.

2.2.6 Recombinant protein expression and purification

EHEC and EPEC effector gene sequences were cloned into pGEX-6P-3::HA₃ as described above. *E. coli* BL21 DE3 was transformed with derivatives of pGEX-6P-3::HA₃ containing effector sequences and grown with shaking (225 rpm) at 37°C for ~3 hrs. Cells were induced with 1 mM IPTG and growth was continued for 16 hrs at 16°C. Cells were harvested in bacterial lysis buffer [Phosphate Buffered Saline (PBS), pH 7.4, 1 mM EDTA, 1 mM DTT, 10 µg/ml DNase, 10 µg/ml RNase and EDTA-free Complete Protease Inhibitor Cocktail (Roche)] and passed through a French Pressure cell at 10,000 p.s.i. Lysates were clarified by centrifugation for 10 minutes at 8,000 r.c.f. followed by 30 minutes at 30,000 r.c.f. Clarified lysates were added to glutathione-agarose beads (Sigma-Aldrich) and batch bound with rotation for 1 hr at 4°C. Bead-lysate mixtures were transferred to Bio-Rad Polyprep chromatography columns and columns were washed successively with 20 ml PBS + 0.1% Triton X-100, 20 ml PBS + 0.05% Triton X-100 + 0.5 M NaCl and 20 ml PBS. Proteins were eluted with 10 mM glutathione in 50 mM Tris (pH 9.5) and dialyzed using SlideAlyzer dialysis cassettes (Pierce Scientific). Purified proteins were stored at -80°C until use. For expression of *Salmonella SseK1*, *E. coli* BL21 DE3 was transformed with pET28a::6xHis-*sseK1*. Cells were grown and induced as described above.

Cells were harvested and lysed as described above. Clarified lysates were added to Ni Sepharose High Performance beads (GE Healthcare Life Sciences) and batch bound with rotation for 1 hr at 4°C. Bead-lysate mixtures were then transferred to Bio-Rad Polyrep chromatography columns and washed successively with lysis buffer + 250 mM imidazole. His-tagged proteins were eluted with lysis buffer + 500 mM imidazole and dialyzed using SlideAlizer dialysis cassettes. Protein concentrations were determined using Coomassie Plus Better Bradford Assay Reagent (Thermo Scientific) and purified protein was stored at -80°C until use.

2.2.7 SILAC labeling and analysis

For SILAC labeling, HEK293T cells were maintained as described previously (Rogers et al., 2008). Briefly, cells were split from normal growth media into lysine and arginine free DMEM (Caisson Laboratories Inc.) containing 10% dialyzed FBS, 1% Glutamax, 1% NEAA, 0.1 units/L Penicillin/Streptomycin and either 36.5 mg/L ²H₄-lysine and 21 mg/L ¹³C₆-arginine (Cambridge Isotope Laboratories) for heavy cells or normal isotopic abundance L-lysine and L-arginine (Sigma-Aldrich) for light cells. Cells were maintained in labeling media for at least 5 cell divisions to ensure complete labeling.

Light and heavy labeled cells were grown in 10 cm dishes and lysed in NP40 lysis buffer [20 mM Tris-HCl pH 7.5, 150 mM NaCl, 1% NP-40, 10 mM Na-pyrophosphate, 50 mM NaF, 1 mM Na₃VO₄, protease inhibitor cocktail (Roche)] and centrifuged at 16,000 r.c.f. Protein concentrations were determined using Coomassie Plus Bradford Assay Reagent (Thermoscientific) and 10 mg lysate was transferred to tubes containing beads bound to 20 pmol recombinant effector. Tubes were incubated with rotation for 1 hr at 4°C followed by

centrifugation at 2100 r.c.f. for 5 min. Beads were washed with cold lysis buffer followed by cold PBS and incubated in 100 μ L 50 mM Tris (pH 9.5) plus 10 mM glutathione overnight at 4°C with rotation. Tubes were centrifuged at 2100 r.c.f. for 5 min and supernatants were separated from beads using GELoader Tips (Eppendorf). Supernatants from like samples were pooled and eluted proteins were precipitated using ethanol/acetate and digested in-solution as described previously (Foster et al., 2003). The resulting peptides were acidified and analyzed by liquid chromatography-tandem mass spectrometry (LC-MS/MS) using an LTQ-OrbitrapXL as described elsewhere (Rogers et al., 2008). A schematic representation of the SILAC methodology used in this work is shown below (Figure 2.1).

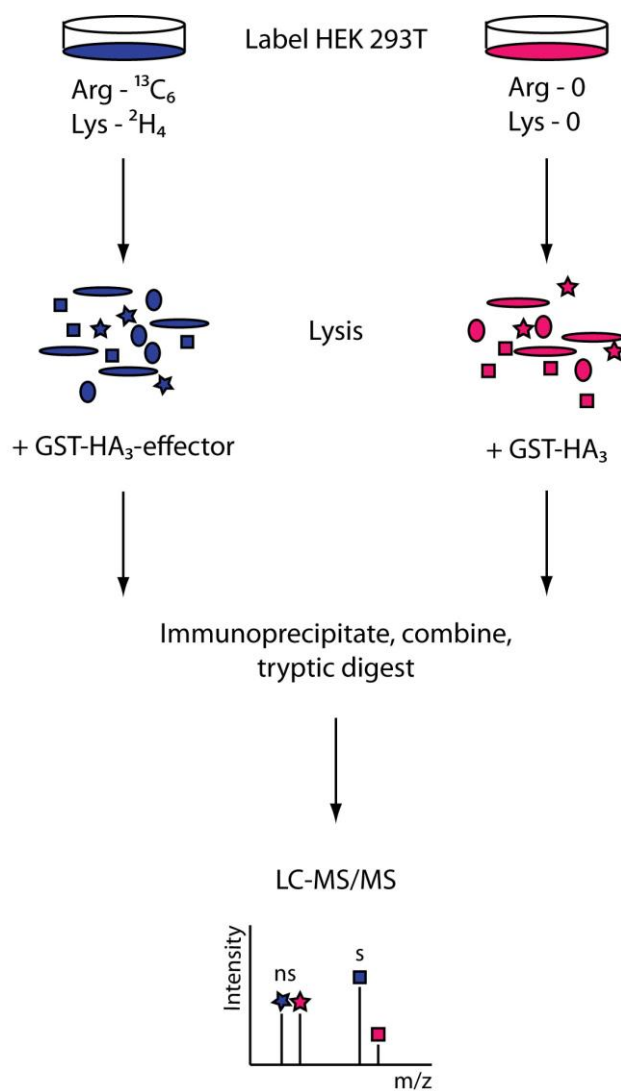


Figure 2.1 Schematic representation of SILAC methodology.

HEK293T cells are grown in SILAC medium for at least five doublings to ensure complete incorporation of heavy label. Cell lysates are mixed with purified HA₃-tagged effector; samples are combined and then processed simultaneously for identification and quantification of host peptides. Arg: arginine; Lys: lysine; LC-MS/MS; liquid chromatography tandem mass spectrometry; m/z: mass to charge ratio; ns: not significant; s: significant.

2.2.8 Co-immunoprecipitation

HEK293T cells grown in 10 cm dishes were transiently transfected by the calcium phosphate method. Lysates were generated 48 hrs post transfection in NP40 lysis buffer and centrifuged at 16,000 r.c.f. for 30 minutes at 4°C. For α -FLAG, α -His or α -HA pulldowns, 70 μ L Protein G Sepharose 4 fast Flow (GE Healthcare) was used to pre-clear samples containing ~3 mg total protein mixed with 2 μ g purified effector. Cleared supernatants were then incubated with either 1 μ g mouse- α -FLAG M2 (Sigma-Aldrich), mouse- α -HA (clone 2C16, home-made) or mouse- α -penta-His (Roche) and 40 μ L Protein G Sepharose. Beads were pelleted by centrifugation at 4°C, washed with lysis buffer and resuspended in 30 μ L SDS-PAGE loading buffer and boiled for 10 minutes prior to Western blot analysis.

2.2.9 Western blotting

Samples were separated on 12% polyacrylamide gels and transferred to Pure Nitrocellulose (Bio-Rad) using a wet transfer cell. Membranes were blocked with blocking buffer [5% w/v skim milk powder in Tris-buffered saline containing 0.1% Tween 20 (TBST)] for 30 minutes at room temperature. Membranes were incubated overnight at 4°C with primary antibodies diluted in blocking buffer. Antibodies were diluted from a 1 mg/ml stock to 1:2500 [α -HA (rat; Roche), α -FLAG M2 (mouse; Sigma)] or 1:1000 [α -penta-His (mouse; Roche)]. Three 10 minute wash steps were performed using TBST followed by room temperature incubation of membranes with secondary antibody [HRP-conjugated goat α -rat or goat α -mouse (Sigma-Aldrich)] diluted to 1:5000 in blocking buffer for 1 hr. Membranes were washed as described above and treated with Clarity™ Western ECL Substrate (Bio-Rad Laboratories, Inc.) prior to chemiluminescent developing.

2.3 Results

2.3.1 The EHEC T3SS effectors, NleB1 and EspL2, interact with host ensconsin

To identify host protein targets of EHEC T3SS effectors, we employed a highly sensitive mass spectrometry screen using lysate from SILAC-labeled HEK293T cells mixed with purified, tagged effectors. We were able to identify several candidate host targets, many of which have previously been confirmed as effector interactors (Table 2.4). Analysis of protein complexes that precipitated with HA₃-tagged effector showed that peptides derived from ensconsin, an essential cofactor of kinesin-1 (Barlan et al., 2013; Metzger et al., 2012; Sung et al., 2008), were enriched in the presence of NleB1 or EspL2 compared to controls (Figure 2.2A, B). To further confirm these interactions, we performed the reciprocal pulldown, this time using CoIP of FLAG-tagged ensconsin expressed in HEK293T cells to enrich for HA₃-NleB1 or HA₃-EspL2. HEK293T cells were transfected with full length ensconsin (*pmap7*-FLAG) or control vector (*pCMV4A*) and lysates generated from these cells were mixed with purified HA₃-NleB1 or HA₃-EspL2. Both NleB1 and EspL2 were precipitated using an α -FLAG antibody directed at FLAG-tagged ensconsin, but not with vector-only or isotype controls (Figure 2.2C, D). Based on these observations, we concluded that ensconsin is a target for the EHEC secreted proteins NleB1 and EspL2, and continued our investigation of these effectors.

Table 2.4 Summary of host targets identified by LC-MS/MS as specifically immunoprecipitated with tagged effectors in SILAC experiments

| Effector | Host target | Reference ^a |
|-----------------|--------------------------------|--|
| Map | NHERF2 | (Martinez et al., 2010) |
| Tir | None | |
| EspB | None | (Alto et al., 2007; Marchès et al., 2006) |
| EspF | SH3PX3, SNX9 | |
| EspG | α -tubulin | (Hardwidge et al., 2005; Matsuzawa et al., 2004) |
| EspL2 | Ensconsin | |
| NleA | Sec23A | (Kim et al., 2007; Thanabalasuriar et al., 2012) |
| NleB1 | Ensconsin | |
| NleB2 | None | (Shames et al., 2011) |
| NleC | Histone acetyltransferase p300 | |
| NleD | None | |
| NleF | None | |
| NleG | None | |

a – Target confirmed from published data.

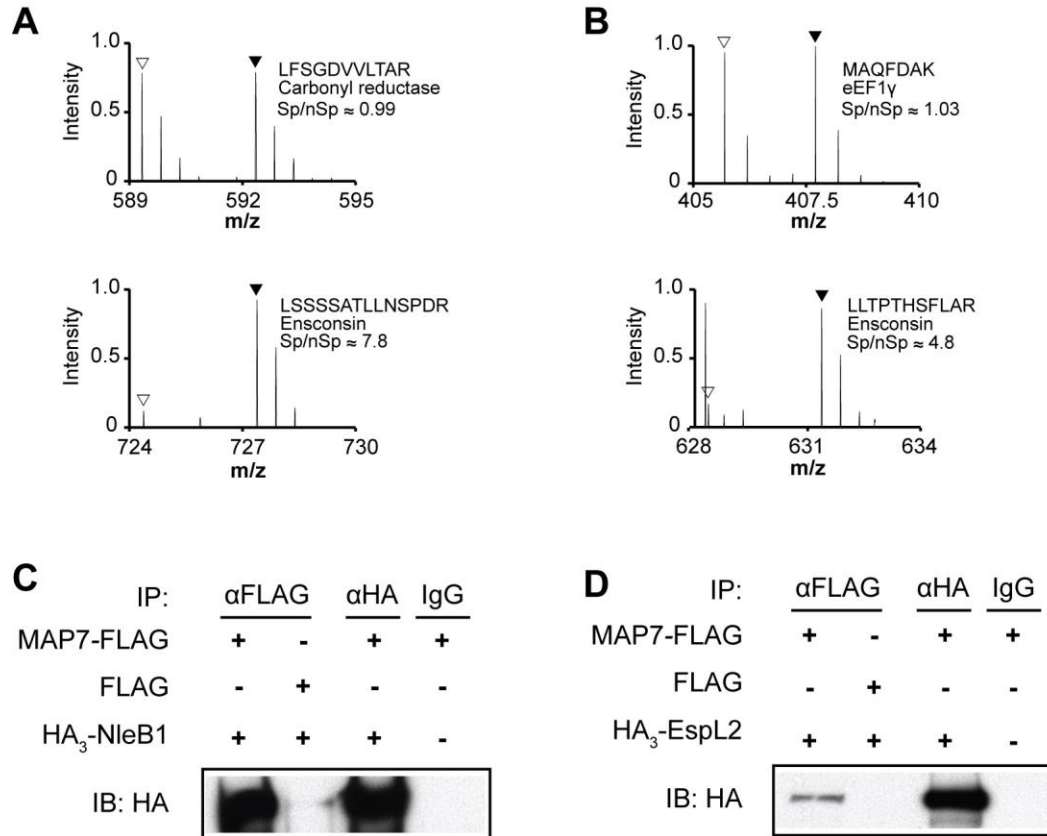



Figure 2.2 Ensconsin (MAP7) interacts with type III secreted effectors, NleB1 and EspL2.

(A) Representative mass spectra for immunoprecipitations (IP) with NleB1. (B) Representative mass spectra for IP with EspL2. Triangles indicate expected mass/charge (m/z) of light (open) and heavy (filled) forms of the given peptide. Peptide sequences are shown and m/z ratios (heavy/light) >1 signify a specific interaction. Upper panels: m/z ratios of peptides from non-specifically bound proteins in the presence (filled triangles) or absence (open triangles) of effector. Lower panels: m/z ratios of peptides from ensconsin, specifically bound in the presence of effector (filled triangles) but not in the absence of effector (open triangles). (C-D) CoIP of ensconsin and NleB1 or EspL2. Lysates of cells transfected with *pmap7*-FLAG or *pCMV4A* were incubated with purified HA₃-tagged effector followed by IP with α -FLAG or α -HA antibody and immunoblot with α -HA antibody. IP: immunoprecipitation; IB: immunoblot.

2.3.2 The EPEC T3SS effectors, NleB1, NleB2 and EspL, interact with host ensconsin

It has been suggested that the NleB and EspL families of Nle-encoded effectors may be part of a core set of essential T3SS effectors belonging to all A/E pathogens (Iguchi et al., 2009). Given the presence of these effector families in EHEC and the closely related A/E pathogen, EPEC, as well as the similarity among their gene sequences, CoIPs of EPEC NleB1, NleB2 and EspL were performed with FLAG-tagged ensconsin. Similar to what was seen with EHEC NleB1 and EspL2, the homologous EPEC effectors, NleB1 and EspL, were also precipitated with an α -FLAG antibody directed at FLAG-tagged ensconsin but not with vector-only controls (Figure 2.3). On the other hand, NleB2, which did not precipitate with a binding partner during the initial SILAC screen, interacted with ensconsin through CoIP, while NleC, another Nle-encoded effector not known to interact with ensconsin, did not (Figure 2.4), indicating that the interaction between ensconsin and the NleB/EspL families of effectors is specific. These data show that both EPEC and EHEC have evolved with multiple proteins to target the same host factor and suggest that ensconsin may be an important target for A/E pathogen manipulation during the infection process.

A

| IP: | α FLAG | | α HA | |
|------------------------|---|---|-------------|---|
| | + | - | + | + |
| MAP7-FLAG | + | - | + | + |
| FLAG | - | + | - | - |
| HA ₃ -NleB1 | + | + | + | - |
| IB: HA |  | | | |

B


| IP: | α FLAG | | α HA | |
|-----------------------|---|---|-------------|---|
| | + | - | + | + |
| MAP7-FLAG | + | - | + | + |
| FLAG | - | + | - | - |
| HA ₃ -EspL | + | + | + | - |
| IB: HA |  | | | |

Figure 2.3 The EPEC effectors, NleB1 and EspL, interact with host ensconsin (MAP7).

(A) CoIP of ensconsin and EPEC NleB1. (B) CoIP of ensconsin and EPEC EspL. Lysates of cells transfected with *pmap7*-FLAG or pCMV4A were incubated with purified HA₃-tagged effector followed by IP with α -FLAG or α -HA antibody and immunoblot with α -HA antibody. IP: immunoprecipitation; IB: immunoblot.



| IP: | α FLAG | | | | α HA | |
|------------------------|--|---|---|---|-------------|---|
| | + | + | - | + | + | + |
| MAP7-FLAG | + | + | - | + | + | + |
| FLAG | - | - | + | - | - | - |
| HA ₃ -NleB1 | + | - | - | - | - | - |
| HA ₃ -NleB2 | - | + | + | - | + | - |
| HA ₃ -NleC | - | - | - | + | - | - |
| IB:FLAG |  | | | | | |
| IB:HA |  | | | | | |

Figure 2.4 The EPEC T3SS effector, NleB2, interacts with host ensconsin (MAP7).

Lysates of cells transfected with *pmap7*-FLAG or pCMV4A were incubated with purified HA₃-tagged NleB1, NleB2 or NleC followed by IP with α -FLAG or α -HA antibody and immunoblot with α -HA or α -FLAG antibody. IP: immunoprecipitation; IB: immunoblot.

2.3.3 The NleB homolog, SseK1, does not interact with host ensconsin

In addition to the A/E pathogens, the non-A/E human intestinal pathogen *Salmonella* Typhimurium has been shown to secrete homologs of the NleB family of effectors. In *Salmonella*, these effectors are called SseK1, SseK2 and SseK3 (Brown et al., 2011). SseK1 shows the most sequence identity with NleB1 and has recently been reported to target TRADD, a host protein also targeted by NleB1 (Li et al., 2013). To determine whether NleB1 and SseK share ensconsin as a host target, a reciprocal CoIP was performed using FLAG-tagged ensconsin and 6xHis-tagged SseK1. However, unlike the NleB and EspL family effectors, SseK1 did not interact with ensconsin (Figure 2.5). These findings suggest that although NleB- and SseK-type proteins belong to the same effector family, they do not target an identical repertoire of host proteins and that the interaction with ensconsin may be unique to EPEC/EHEC effectors.

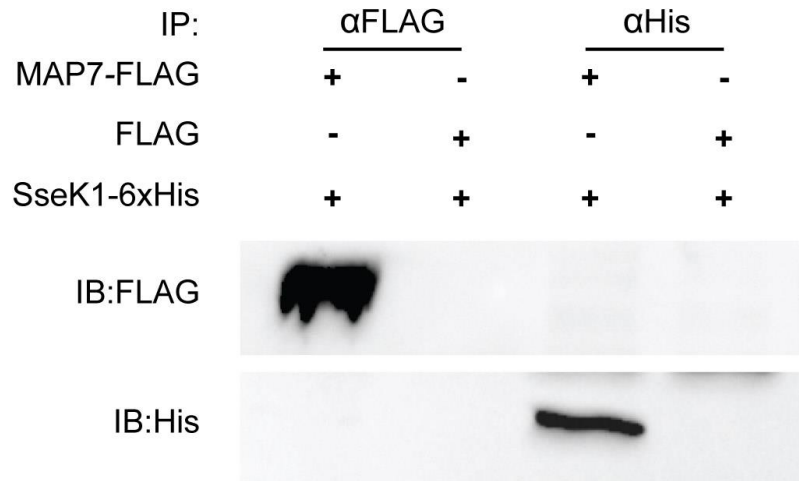


Figure 2.5 The *Salmonella* T3SS effector, SseK1, does not interact with host ensconsin.

Lysates from cells transfected with a FLAG-tagged ensconsin construct (*pmap7*-FLAG) or pCMV4A (FLAG-only control) were incubated with purified 6xHis-tagged SseK1 followed by IP with α -FLAG or α -His pulldown and immunoblot with α -His or α -FLAG antibody. IP: immunoprecipitation; IB: immunoblot.

2.3.4 The effector-ensconsin interaction is specific and mediated by the MTB region of ensconsin

Knowing that the NleB/EspL effectors of both EHEC and EPEC were capable of interacting with ensconsin, we sought to determine which regions of ensconsin were responsible for effector binding. To this end, several truncated versions of ensconsin were generated using *pmap7*-FLAG and expression in HEK293T cells was established by Western blot analysis (Figure 2.6).

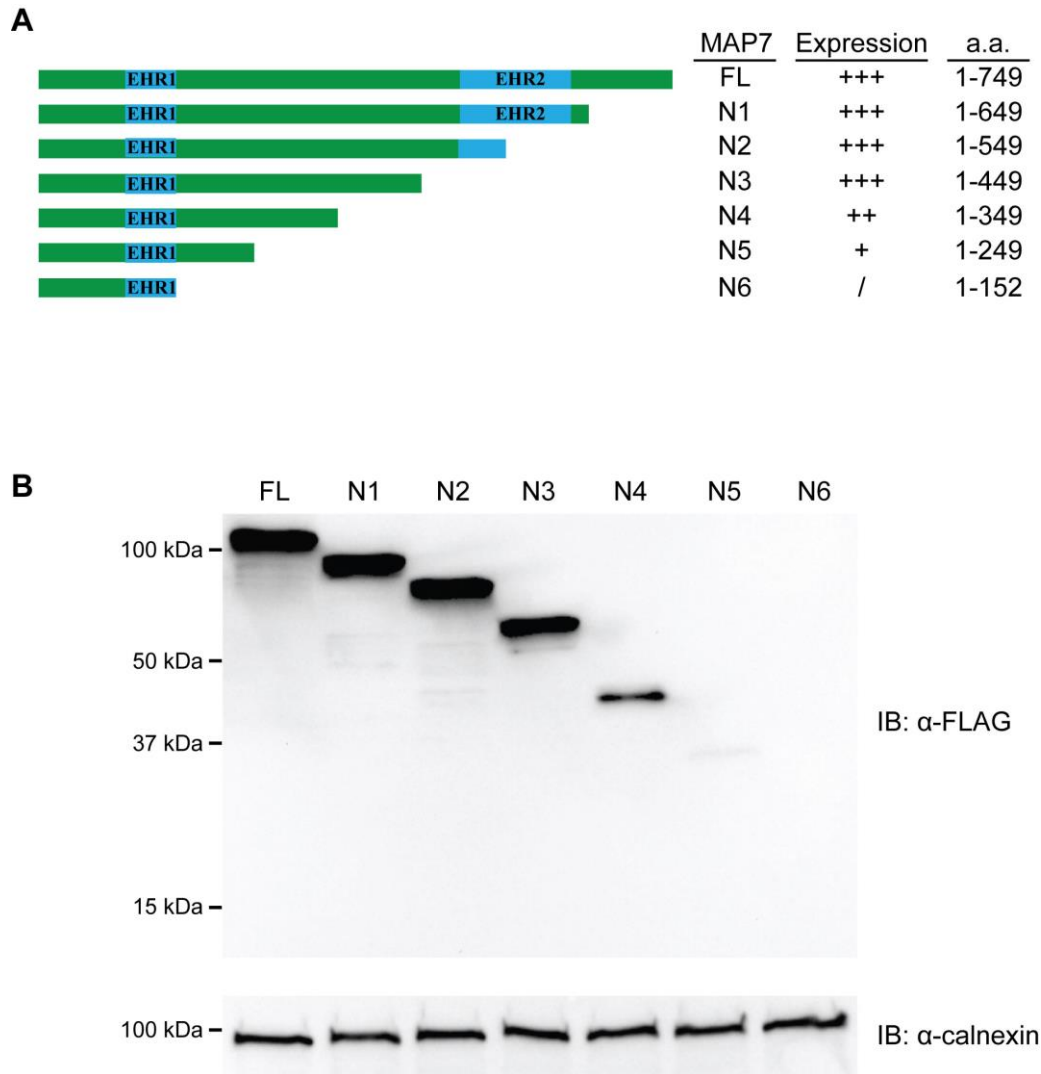


Figure 2.6 Protein expression levels of ensconsin truncations in HEK293T cells.

(A) Schematic diagram depicting truncations of ensconsin (MAP7) cloned into *pmap7*-FLAG. Expression level shown in right panel (+++, high; ++, moderate; +, low; /, none). (B) Western blot of full length MAP7-FLAG and truncations N1-N6. HEK293T cells transfected with *pmap7*-FLAG constructs were lysed and subjected to immunoblot analysis with α -FLAG antibody or α -calnexin antibody as a loading control. EHR1: ensconsin homology region 1; EHR2: ensconsin homology region 2; FL: full length; a.a.: amino acids; IB: immunoblot.

Reciprocal CoIPs were performed using the shortest *pmap7*-FLAG construct with a reasonably high level of expression (*pmap7*N4-FLAG). For simplicity, *pmap7*N4-FLAG was renamed

pmap7ΔC since nearly the entire C-terminal half of the protein had been deleted. Using this construct, we narrowed down the area of effector interaction as roughly corresponding to the MT binding (MTB) region of *ensconsin* (Barlan et al., 2013; Masson and Kreis, 1993), as the truncation mutant (MAP7ΔC) was enriched only in the presence of NleB1 or EspL (Figure 2.7). As an additional control, HA₃-NleC was again used to confirm that the observed interaction with *ensconsin* was specific to NleB and EspL effectors. Based on these results, an additional truncation mutant was made (MAP7ΔN) containing the C-terminal “activity” domain of *ensconsin* but missing the MTB region (Figure 2.8). Contrary to what was seen with MAP7ΔC, CoIP analysis of purified effector with MAP7ΔN showed that neither NleB1 nor EspL interacted efficiently with the C-terminal portion of *ensconsin* (Figure 2.9). These data confirm that NleB1 and EspL interact specifically with *ensconsin* and that this interaction is localized to an area of the protein that roughly corresponds to its MTB region.

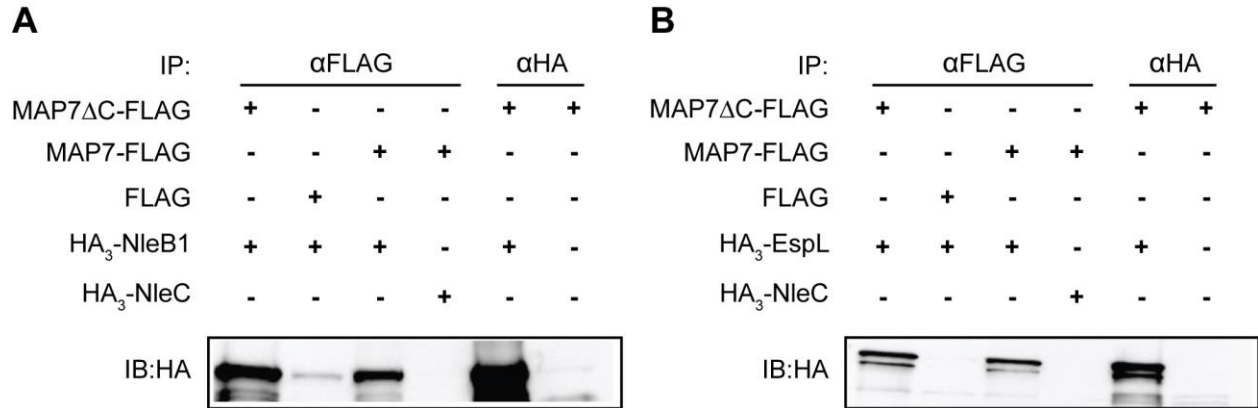


Figure 2.7 NleB1 and EspL interact with the microtubule binding (MTB) region of ensconsin.

(A) CoIP of MAP7 Δ C and NleB1. (B) CoIP of MAP7 Δ C and EspL. Lysates from cells expressing FLAG-tagged ensconsin (MAP7-FLAG) constructs or FLAG-only control were incubated with purified HA₃-tagged effector followed by IP with α -FLAG or α -HA antibody and immunoblot with α -HA antibody. IP: immunoprecipitation; IB: immunoblot.

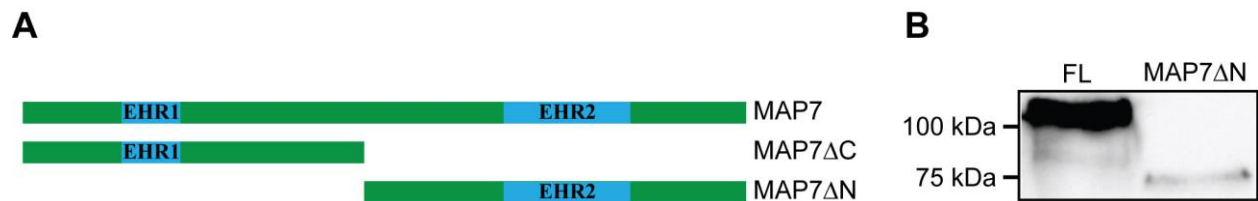


Figure 2.8 Protein expression of the ensconsin truncation mutant, MAP7 Δ N.

(A) Schematic diagram showing MAP7 Δ N in relation to full length ensconsin (MAP7) and the MAP7 Δ C truncation mutant. (B) Western blot of full length MAP7 and MAP7 Δ N. HEK293T cells transfected with *pmap7*-FLAG constructs were lysed and subjected to immunoblot analysis with α -FLAG antibody. EHR1: ensconsin homology region 1; EHR2: ensconsin homology region 2; FL: full length.

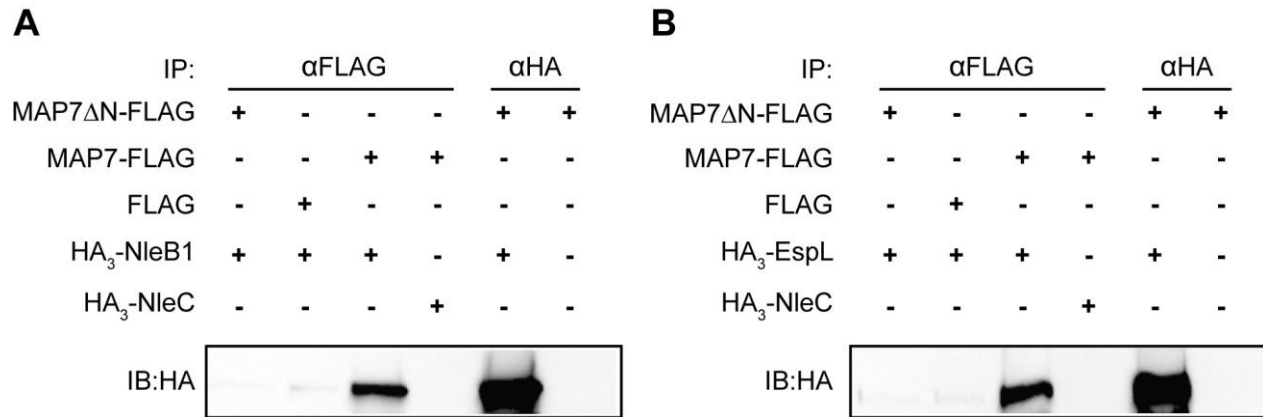


Figure 2.9 NleB1 and EspL do not interact with the C-terminal “activity” region of ensconsin.

(A) CoIP of MAP7 Δ N and NleB1. (B) CoIP of MAP7 Δ N and EspL. Lysates from cells expressing FLAG-tagged ensconsin (MAP7-FLAG) constructs or FLAG-only control were incubated with purified HA₃-tagged effector followed by IP with α -FLAG or α -HA antibody and immunoblot with α -HA antibody. IP: immunoprecipitation; IB: immunoblot.

2.4 Discussion

Many medically and agriculturally relevant pathogens including *Salmonella*, *Shigella* and pathogenic *E. coli* utilize T3SSs to further infection and disease progression (Coburn et al., 2007; Cornelis, 2006; Kaper et al., 2004). Diarrheal illnesses caused by EPEC and EHEC are dependent on the efficient delivery of several secreted effectors directly into host cells. Bacterial effectors manipulate a variety of cellular processes to promote colonization and survival. Due to the multifunctional and cooperative nature of many T3SS effectors, the specific functions of many of these proteins are still poorly understood. The key to combatting enteric diseases caused by EPEC and EHEC lies in a better understanding of how these pathogens evade the host immune response and cause disease.

In this study, we employed the SILAC labeling technique paired with LC-MS/MS analysis to identify novel host protein targets for a number of EHEC T3SS effectors. Through differential labeling of the host proteome, we were able to quantitatively measure differences in host protein abundance inferred from isotopic peptide ratios in the presence or absence of purified effector. We identified host targets for several LEE- and Nle-encoded effectors with binding partners involved in several cellular processes including gene transcription, endocytosis, protein secretion and cellular trafficking as well as components of the cytoskeleton. The sensitivity of the SILAC method in identifying effector targets is supported by the fact that several of our identified targets have been confirmed through independent methods. For example, the Nle-encoded effector, NleC, was shown to interact with the nuclear histone acetylase p300 through SILAC and this was confirmed by CoIP (Shames et al., 2011). Additionally, several targets were identified that have been confirmed by independent laboratory studies. The interactions of NleA, EspF and Map with COPII vesicle proteins, sorting nexin 9 (SNX9) and Na⁺/H⁺ exchange regulatory factor (NHERF2), respectively, have all been confirmed by work from independent laboratories (Kim et al., 2007; Marchès et al., 2006; Martinez et al., 2010).

In addition to confirmed interactions, we were also able to establish a novel binding partner for both NleB1 and EspL2 during our screen of EHEC secreted effectors. NleB1 and EspL2 both showed a strong affinity for the MAP, ensconsin, with peptide ratios well above controls and we were able to confirm these interactions via CoIP. We were also able to confirm that the homologous EPEC secreted effectors, NleB1, NleB2 and EspL, all interacted with ensconsin indicating that ensconsin is a conserved target among A/E pathogens. Although ensconsin was first identified over 20 years ago, it has never been shown to be a target for any bacterial or viral

pathogen. Initially, ensconsin was thought to be involved in MT stabilization (Bulinski and Bossler, 1994) but recent work shows that it functions primarily as a cofactor of kinesin-1 (Barlan et al., 2013; Sung et al., 2008). Given that MTs are important in cell division, differentiation, structural stabilization and intracellular transport processes, it is conceivable that A/E pathogens could manipulate any of these functions by targeting ensconsin.

Little is known about the three dimensional structure of ensconsin but its MTB region has been localized to the N-terminus of the protein (Barlan et al., 2013; Masson and Kreis, 1993). It has also been shown that the C-terminus of the protein is responsible for kinesin-1 binding and activation of transport (Barlan et al., 2013). We were able to show that both NleB1 and EspL interacted with ensconsin in an area roughly corresponding to its MTB region. On the other hand, we showed that neither NleB1 nor EspL specifically interacted with the C-terminal domain of ensconsin which includes the ‘activity’ region of this MAP. This may mean that NleB and EspL family effectors affect the MT-binding ability of ensconsin or its proposed effect on MT stability. On the other hand, it is possible that while these effectors interact with the MTB region of ensconsin, they may still exert an enzymatic or steric effect on the activity domain of the protein, thereby interfering with normal ensconsin trafficking functions.

We also showed that interaction with ensconsin was specific to NleB and EspL since NleC, another Nle-encoded effector, did not bind to ensconsin. Interestingly, SseK1, an NleB homolog found in *Salmonella* (Brown et al., 2011), was also incapable of interacting with ensconsin. This was shown not only from our CoIP data but also in a similar SILAC-based screen to identify host targets of *Salmonella* secreted effectors. In this study, neither SseK1 nor SseK2 showed any evidence of interaction with ensconsin (Auweter et al., 2011). Additionally, EspL shares some

sequence homology with the *Shigella* enterotoxin OspD3/ShET2 which has shown some involvement in cytokine secretion in epithelial cells infected with *Shigella* (Farfán et al., 2011). However, it remains to be determined whether these proteins are functionally similar to EspL during infections with these pathogens.

NleB and SseK have recently been shown to possess the same GlcNAc transferase activity with similar host targets in the NF- κ B activation pathway (Li et al., 2013; Pearson et al., 2013). However, the fact that the SseK family of effectors do not interact with ensconsin may indicate a novel function for NleB. This is supported by the fact that EspL also interacts with ensconsin but shows no homology to NleB or SseK nor has it been identified as having GlcNAc transferase activity. Furthermore, the host proteins targeted for GlcNAcylation by NleB and SseK all contain death domains while ensconsin does not, thus giving more credence to the idea of a novel additional mechanism of activity for NleB. Further work is needed to fully define the mechanism of action of these conserved A/E pathogen effectors as well as to identify their effect on host ensconsin as it relates to infection.

In summary, we have identified two different EPEC/EHEC effectors with no prior indication of similar or related functions, both targeting the MAP, ensconsin. We show that both NleB1 and EspL interact with the MTB region but not the activity domain of ensconsin and that interaction with this protein is thus far specific to A/E pathogen effectors. Ensconsin is a novel host target for microbial pathogens and given that EPEC/EHEC encode multiple effectors that interact with this protein, it could indicate that manipulation of ensconsin function is an essential aspect of infection. The following chapter focuses on the cellular roles of the NleB and EspL proteins during infection as they relate to ensconsin function.

Chapter 3: EPEC disrupts host transferrin receptor trafficking using NleB/EspL

3.1 Introduction

Identifying the specific functions of individual effectors is important to understand the disease mechanisms exploited by EPEC and EHEC, but the vast majority of effectors have only been cursorily explored. These microbes employ between 20 and 50 T3SS effectors during their infections and although much work on a handful has been pursued, their multifunctional and cooperative nature has made their functional classification difficult.

The effectors involved in the subversion of actin dynamics, immune signaling and cell death pathways during A/E pathogen infection have been well studied, but only recently, has vesicle trafficking gained interest as an important target for some bacterial and viral pathogens as part of their pathogenic strategy (reviewed in (Sharp and Estes, 2010)). Intracellular trafficking is a critical process involved in maintaining cellular homeostasis, promoting cell survival and responding to the presence of pathogens. Directed delivery of transport vesicles requires the concerted action of a number of cargo adaptors, molecular motors and their cytoskeletal tracks, which presents pathogenic microbes with several targets against which to mount an efficient attack. Human Norovirus is capable of antagonizing COPII vesicle transport between the endoplasmic reticulum (ER) and Golgi (Sharp et al., 2010). Similarly, EPEC/EHEC inhibit COPII/COPI vesicle transport via the T3SS effectors, NleA and NleF, respectively (Kim et al., 2007; Olsen et al., 2013; Thanabalasuriar et al., 2012). Adenovirus-2 blocks protein secretion by interfering with endosomal recycling which leads to Golgi dispersion (Landry et al., 2009), an

activity and phenotype comparable to that seen with the EspG family of EPEC/EHEC secreted effectors (Clements et al., 2014; Selyunin et al., 2014).

Long-range active transport systems use MTs and associated motor proteins to maintain proper spatio-temporal distribution of a variety of cellular cargo (Hirokawa et al., 2009). The navigation, loading and delivery of specialized cargo are highly regulated processes within the cell and involve multiple host factors including a variety of adaptors, modifying enzymes and MT associated proteins (Atherton et al., 2013). *Salmonella* is known to specifically recruit kinesin to the site of bacterial replication where it exploits motor activity to promote bacterial spreading (Boucrot et al., 2005; Kaniuk et al., 2011). Despite the importance of these regulatory mechanisms in managing differential delivery of transport vesicles, there has been little done in examining these factors as potential targets during infection.

To explore A/E pathogen-induced perturbations in the spatio-temporal movement of intracellular vesicles we used a combination of time-lapse microscopy and multiple particle tracking. We show that host transferrin receptor trafficking is halted during live EPEC infections and that this arrest is due to the cooperative actions of two conserved T3SS effectors (NleB and EspL). We found that both NleB and EspL interact with ensconsin and that ensconsin physically interacts with Kif5b, a mammalian kinesin-1 motor protein. In addition, we found that the vesicle movement blockade occurred in the absence of any observable MT destruction. Our findings demonstrate the first live-infection evidence of targeted trafficking inhibition through bacterial effectors and present a novel strategy to hijack host cells without destroying their cytoskeletal tracts.

3.2 Materials and methods

3.2.1 Tissue culture, bacterial strains and plasmids

HeLa and HEK293T cells (ATCC) were maintained in Dulbecco's Modified Eagle Medium (DMEM) High Glucose (Thermo Scientific) supplemented with 10% fetal bovine serum (FBS) (Thermo Scientific), 1% Glutamax (Gibco) and 1% non-essential amino acids (NEAA) (Gibco). Ptk2 cells were maintained in MEM/F-12 (1:1) + 10% FBS (Gibco).

For routine cloning and infections, bacteria were grown in LB broth at 37°C supplemented with appropriate antibiotics. Broth cultures were inoculated from single bacterial colonies on LB agar plates containing antibiotics where appropriate. Antibiotic concentrations were as follows: streptomycin 50 µg/ml, ampicillin 100 µg/ml, kanamycin 50 µg/ml, chloramphenicol 30 µg/ml. Bacterial strains used in this study are described in Table 3.1.

Table 3.1 Bacterial strains used in this study

| Name | Source/Reference |
|-------------------------------------|------------------------------|
| <u><i>Escherichia coli</i></u> | |
| SM10λ <i>pir</i> | (Miller and Mekalanos, 1988) |
| DH10B | Life Technologies |
| EC100D <i>pir</i> + | Epicentre Biotechnologies |
| MFD <i>pir</i> | (Ferrières et al., 2010) |
| <u>EPEC O127:H6 strain E2348/69</u> | |
| Wild type | (Levine et al., 1978) |
| Δ <i>escN</i> | (Gauthier et al., 2003) |
| Δ <i>nleB1</i> | This study |
| Δ <i>nleB2</i> | This study |
| Δ <i>nleB1</i> Δ <i>nleB2</i> | This study |
| Δ <i>espL</i> | This study |
| Δ <i>nleB</i> Δ <i>espL</i> | This study |

3.2.2 Generation of *pnleB1* and *pespL*

For PCR, Elongase Enzyme Mix (Invitrogen) was routinely used. EPEC *nleB1* and *espL* gene sequences were amplified from EPEC strain E2348/69 genomic DNA using primer pairs PnleB1c-F/PnleB1c-R and PespLc-F/PespLc-R. The resulting PCR fragments were then digested with BamHI/SalI or BamHI/XhoI for *nleB1* and *espL*, respectively, and inserted into BamHI/SalI or BamHI/XhoI-digested pACYC184 to generate *pnleB1* and *pespL*. A complete list of oligonucleotide primers and plasmids used in this study can be found in Table 3.2 and Table 3.3, respectively.

3.2.3 Green fluorescent protein (GFP) fusion to NleB1 and EspL

EPEC E2348/69 *nleB1* and *espL* gene sequences were amplified from genomic DNA using primer pairs PnleB1GFP-F/PnleB1GFP-R and PespLGFP-F/PespLGFP-R for *nleB1* and *espL*, respectively. The resulting PCR fragments were digested with KpnI/BamHI and inserted into KpnI/BamHI-digested pEGFPC1 (Clontech Laboratories, Inc.) to generate pEGFPC1::*nleB1* (pEGFP-*nleB1*) and pEGFPC1::*espL* (pEGFP-*espL*).

Table 3.2 Oligonucleotide primers used in this study

| Primer | Sequence (5' – 3')^a | Restriction endonuclease |
|---------------|--|---------------------------------|
| HuACTB-F | tgtgcaaggccggcttcg | N/A |
| HuACTB-R | gtgaggatgcctctcttcg | N/A |
| HuMAP7-F | gatgatgaagggacacttgg | N/A |
| HuMAP7-R | agcaggaaaggaattccattaa | N/A |
| EPnleB1-1F | <u>gggtaccaca</u> agaggtgagataatcag | KpnI |
| EPnleB1-DR | <u>cgctagca</u> actttctggagaagtgtac | NheI |
| EPnleB1-DF | <u>ggctagct</u> ttaactattcatcgttacac | NheI |
| EPnleB1-2R | <u>cgagctca</u> acagttcgggtgattcaac | SacI |
| EPnleB2-1F | <u>cggtagcc</u> gcatattccagagcaggac | KpnI |
| EPnleB2-DR | <u>ggctagcc</u> gtttgacaggggaactctg | NheI |
| EPnleB2-DF | <u>ggctagcc</u> agtatacatgcagttcatgg | NheI |
| EPnleB2-2R | <u>ggagctcg</u> attacccatcatcaactccg | SacI |
| EPespL-1F | <u>gagggtagc</u> catattcaacataatttgatgccg | KpnI |
| EPespL-DR | <u>gagggtagc</u> tacctaagcgagttcagcgg | NheI |
| EPespL-DF | <u>gagggtagc</u> ttgttctaataatcatgtaatatcg | NheI |
| EPespL-2R | <u>gagggtagc</u> ttgttctaataatcatgtaatatcg | SacI |
| nleB1c-F | <u>gagggtagc</u> ccacaagaggaattttatgttatctt | BamHI |
| nleB1c-R | <u>gagggtagc</u> acttaccatgaactgctggatac | SalI |
| espLc-F | <u>gagggtagc</u> ccagaaaggatacaaacatatgcc | BamHI |
| espLc-R | <u>gagggtagc</u> gaattggaataataattatatacat | XhoI |
| nleB1mut-F | gtagcggatgtatatatcttgctgccgcatgattattaccgataaat | N/A |
| nleB1mut-R | atttatcggtaataatcatggcggcagcaagatatatacatccgctac | N/A |
| nleB1GFP-F | <u>ttaggtaccat</u> gttatcttcattaaatgtcctt | KpnI |
| nleB1GFP-R | ctc <u>ggatcct</u> taccatgaactgctggatacat | BamHI |
| espLGFP-F | <u>ttaggtaccat</u> gccataataaacaatcgg | KpnI |
| espLGFP-R | ctc <u>ggatcct</u> caattggaataataattatataca | BamHI |

a – Restriction endonuclease sites are underlined; N/A: not applicable.

Table 3.3 Plasmids used in this study

| Plasmids | Source/Reference |
|-----------------------------------|---------------------------|
| <i>pmap7-6xHis</i> | This study |
| <i>pCMV6-Entry::kif5B-myc-DDK</i> | OriGene Technologies Inc. |
| <i>pRE112</i> | (Edwards et al., 1998) |
| <i>pACYC184</i> | New England Biolabs |
| <i>pnleB1</i> | This study |
| <i>pespL</i> | This study |
| <i>pTfR-mCherry</i> | (Silverman Lab, SFU) |
| <i>pEGFP-nleB1</i> | This study |
| <i>pEGFP-espL</i> | This study |

3.2.4 Generation of EPEC effector deletion mutants

EPEC strain E2348/69 was used to generate all deletion mutants used in this study. In-frame deletion of *nleB1*, *nleB2* and *espL* genes was carried out using *sacB*-based allelic exchange and the sucrose selection method. The suicide plasmid, *pRE112* (Edwards et al., 1998), was used to generate in-frame effector deletion mutants. Briefly, PCR was used to generate two ~1 kb fragments of effector flanking DNA for each effector gene using primer pairs as indicated in Table 3.2. Upstream fragments were cloned with *KpnI* and *NheI* restriction sites at the 5' and 3' ends, respectively, while downstream fragments were cloned with *NheI* and *SacI* restriction sites at the 5' and 3' ends, respectively. PCR fragments were then cloned into *pCR2.1-TOPO* (Invitrogen) and digested with *KpnI/NheI* or *NheI/SacI*. Digested fragments were inserted into *KpnI/SacI* digested *pRE112* in a three-way ligation. The resulting gene deletion plasmid was verified by sequencing. *pRE112* deletion plasmids were transformed into *E. coli* donor strain SM10 λ *pir* (Simon et al., 1983) or MFD*pir* (Ferrières et al., 2010) for conjugation with recipient

strain E2348/69 to create $\Delta nleB1$, $\Delta nleB2$, $\Delta espL$, $\Delta nleB1\Delta nleB2$ and $\Delta nleB1\Delta nleB2\Delta espL$ ($\Delta nleB\Delta espL$). After sucrose selection, transconjugants that were resistant to sucrose and sensitive to chloramphenicol were screened by colony PCR and verified for chromosomal deletion by sequencing at the NAPS Unit (UBC).

3.2.5 Generation of *nleB1mut*

The plasmid pRE112::*nleB1* was used as a template for site directed mutagenesis using PfuUltra (Agilent Technologies). PCR was performed according to the manufacturer's directions using primers *nleB1mut-F* and *nleB1mut-R* (Table 3.2). Mutation of Asp221 and Asp223 to Ala221 and Ala223 was confirmed through DNA sequencing. pRE112::*nleB1mut* was then transformed into MFD*pir* for conjugation with EPEC $\Delta nleB2$ and sucrose selection performed as described above. EPEC *nleB1mut* $\Delta nleB2$ (*nleB1mut*) mutants were confirmed by DNA sequencing (NAPS Unit, UBC).

3.2.6 Co-immunoprecipitation

HEK293T cells grown in 10 cm dishes were transiently co-transfected with *pmap7-6xHis* and pCMV6-Entry::*kif5B-myc-DDK* (OriGene Technologies Inc.) by the calcium phosphate method. Lysates were collected 48 hrs post transfection in NP40 lysis buffer and centrifuged at 16,000 r.c.f. for 30 minutes at 4°C. Twenty five μ L of Ni Sepharose High Performance (GE Healthcare) beads were incubated with ~3 mg total protein for 2 hrs at 4°C with rotation. Beads were pelleted by centrifugation at 4°C, washed twice with lysis buffer + 50 mM imidazole and eluted with 25 μ L lysis buffer + 500 mM imidazole (to a final imidazole concentration of 250 mM).

Ten μ L SDS-PAGE loading buffer was added to protein samples and samples were boiled for 10 minutes prior to Western blot analysis.

3.2.7 Western blotting

Samples were separated on 12% polyacrylamide gels and transferred to Pure Nitrocellulose (Bio-Rad) using a wet transfer cell. Membranes were blocked with blocking buffer [5% w/v skim milk powder in Tris-buffered saline containing 0.1% Tween 20 (TBST)] for 30 minutes at room temperature. Membranes were incubated overnight at 4°C with primary antibodies diluted in blocking buffer. Antibodies were diluted from a 1 mg/ml stock to 1:1000 [α -Penta-His (mouse; Roche)] or 1:2500 [α -FLAG M2 (mouse; Sigma)]. Three 10 minute wash steps were performed using TBST followed by room temperature incubation of membranes with secondary antibody [HRP-conjugated goat α -mouse (Sigma-Aldrich)] diluted to 1:5000 in blocking buffer for 1 hr. Membranes were washed as described above followed by addition of Clarity™ Western ECL Substrate (Bio-Rad Laboratories, Inc.) prior to chemiluminescent developing.

3.2.8 RNA extraction

Total RNA was extracted from HeLa cells grown in 6 well plates using an RNeasy Mini Kit (Qiagen) according to the manufacturer's instructions and quantified using a NanoDrop ND-1000 spectrophotometer (NanoDrop Technologies). One μ g RNA was used as template for reverse transcription with the Quantitect RT kit (Qiagen) to generate cDNA according to the manufacturer's instructions.

3.2.9 Real-time PCR

Real-time PCR was performed using Quantitect SYBR-Green Mastermix (Qiagen) and the Applied Biosystems (Foster City, USA) 7500 system. Beta-actin (ACTB) was used for normalization of ensconsin gene expression. Fold difference in expression was calculated as threshold cycle ($2^{-\Delta\Delta CT}$). Primer sequences are listed in Table 3.2.

3.2.10 Transfection of HeLa cells with pEGFP-*nleB1* or pEGFP-*espL*

HeLa cells were transiently transfected with pEGFP-*nleB1* or pEGFP-*espL* using FuGENE HD (Roche) in DMEM with a ratio of 2:3 (μ g DNA to μ L reagent) according to the manufacturer's instructions. Cells were imaged by confocal microscopy at 24 hr post-transfection.

3.2.11 Confocal microscopy

HeLa cells were grown on coverslips in 6 well plates for 48 hrs prior to infection with EPEC or for 24 hrs prior to transfection with EGFP-effector fusion plasmids. Coverslips were washed with PBS and fixed with 4% paraformaldehyde followed by 0.2% Triton X-100 permeabilization. Cells were blocked for 1 hr at room temperature with Antibody Diluent (DAKO S3022). Mouse α -MAP7 (Abnova), mouse α -tubulin (Sigma-Aldrich) and Alexa 488-conjugated goat α -mouse (Life Technologies) antibodies were diluted in Antibody Diluent from a 1 mg/ml stock solution and used at a concentration of 1/200. Coverslips were incubated in primary antibody solution at 4°C overnight and in secondary antibody at 4°C for 1 hr. Wash steps with PBST/BSA were carried out at room temperature after each antibody step. Coverslips were mounted on glass slides using ProLong Gold Antifade Reagent with DAPI (Invitrogen). Fluorescent images were obtained using an Olympus Fluoview 10i laser scanning confocal

microscope or an Olympus FV1000 MPE microscope with Olympus FV 2.1 software at the UBC Bioimaging facility.

3.2.12 Live cell imaging and analysis

Approximately 1×10^5 Ptk2 cells were seeded onto 18 mm glass coverslips in 12 well plates containing MEM/F-12 (1:1) + 10% FBS (Gibco). Following overnight incubation, cells were transfected with 2 μ g plasmid DNA using jetPEI transfection reagent (Polyplus Transfection) and protein expression allowed to proceed for 24 hrs. At 3 hrs post-infection, coverslips were washed with PBS +/- (calcium 0.9 mM / magnesium 0.49 mM), spent media replaced with fresh growth media, and incubation continued for an additional 1.5 hrs. Samples were imaged with a Leica DMI4000 B microscope connected to a humidified live cell chamber (CU-109) [Chamlide] set at 37°C, 60 mmHg of CO₂. Images were acquired with continuous shooting at 200 ms/frame for ~200 frames using Metamorph v7.8.2 (Molecular Devices) and analyzed with u-track multiple particle tracking software (Jaqaman et al., 2008). Prior to particle detection and tracking, a background estimate was subtracted from each raw movie frame. Each frame was passed through a difference of Gaussians filter and a suitable intensity threshold was applied to the filtered images. The threshold was at least 8 standard deviations in absolute pixel intensity above the mean absolute pixel intensity and guaranteed that no more than the brightest 0.2% of pixels were retained after its application. Tracks were obtained for detected particles in at least 3 representative cells per infection condition and particle speeds were calculated for all tracks with at least 10 visible track segments as follows: for any given track with ≥ 10 visible track segments, the lengths of all visible track segments (in pixels) were added together and divided by the total number of track segments (frames) for which the particle was detected to give an

average particle speed for each track in pixels/frame, which was then converted to $\mu\text{m/s}$. Mean squared displacements (MSDs) were calculated for all particles with tracks persisting ≥ 10 frames based on 5-frame intervals. For each relevant track, the particle's scalar displacement was calculated for every 5 frame interval and then averaged to give the MSD/5 frames.

3.2.13 Statistical analyses

All statistical analyses were performed using Prism 4.0 Software (GraphPad). Unpaired two-tailed *t*-tests were used for comparisons of two component data sets and one-way ANOVA with appropriate multiple comparisons tests were applied to identify statistically significant differences for comparisons of grouped data.

3.3 Results

3.3.1 EPEC blocks transferrin receptor transport in a T3SS-dependent manner

Fixed sample analyses have previously been used to demonstrate that EPEC/EHEC target host secretory and receptor recycling pathways during infection (Clements et al., 2014; Kim et al., 2007; Olsen et al., 2013; Selyunin et al., 2014; Thanabalasuriar et al., 2012). We used a novel approach to examine the kinetics of conventional intracellular transport during A/E pathogen infections. Given that NleB1 and EspL of EPEC and EHEC were found to interact with the kinesin-1 cofactor, ensconsin, we used the transferrin receptor (TfR), which is a classical marker for kinesin-based endosomal trafficking (Schmidt et al., 2009), to track the spatio-temporal movement of vesicles during live EPEC infections. Ptk2 cells ectopically expressing a TfR-mCherry fusion were infected with wild type EPEC or a T3SS mutant (ΔescN) and examined using fluorescent time-lapse imaging. When compared to uninfected cells, wild type EPEC

infection drastically reduced TfR-mCherry movement throughout the cell (Figure 3.1A) and quantification of this difference displayed a marked reduction in individual particle speeds during wild type EPEC infection (Figure 3.1B). We also saw significantly more particle movement in $\Delta escN$ -infected cells compared to wild type infection, confirming involvement of the T3SS. These data show that EPEC not only controls the spatial localization of intracellular TfR vesicles, but also the speeds at which they travel during infection, and clearly demonstrate the dramatic effect EPEC has on this cellular pathway.

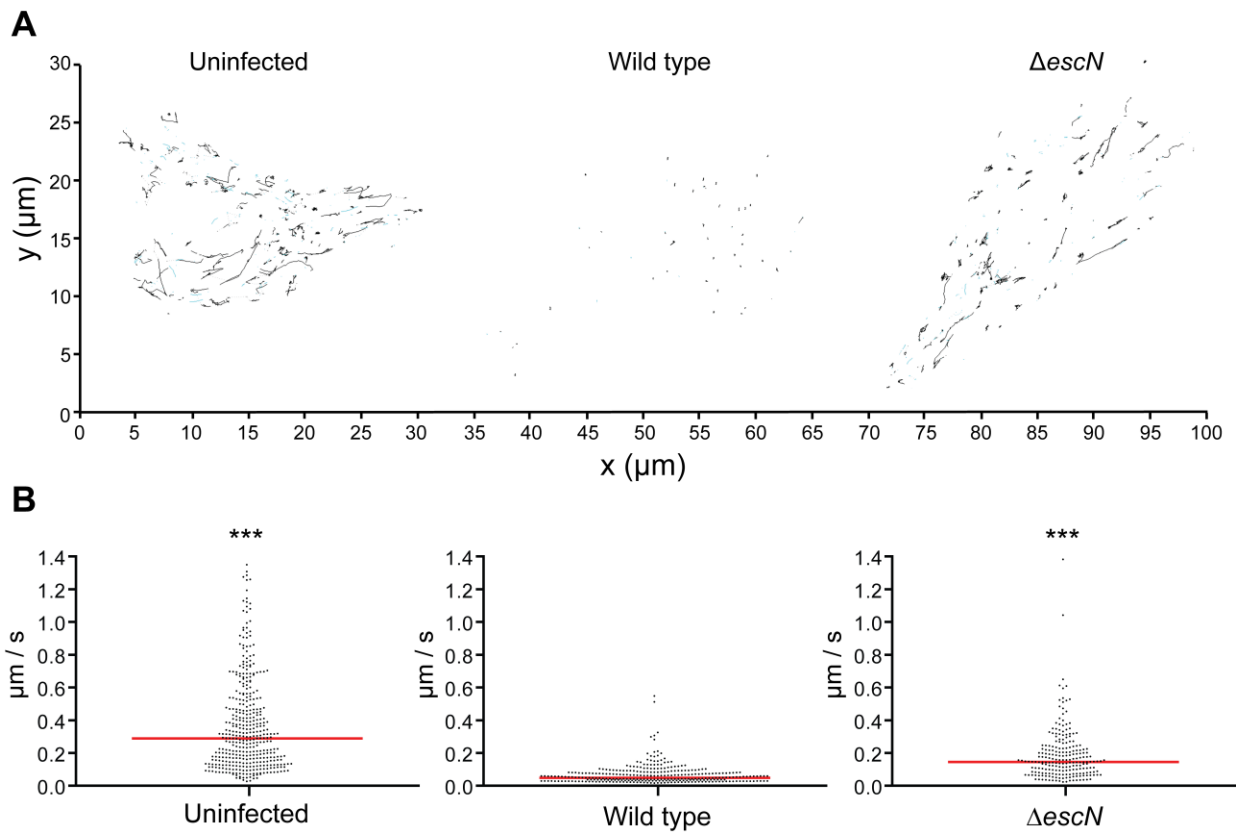


Figure 3.1 Enteropathogenic *E. coli* (EPEC) infection halts TfR-mCherry transport in a type III secretion system-dependent manner.

(A) Tracks of TfR-mCherry containing vesicles from a representative Ptk2 cell during infection with wild type EPEC or T3SS mutant ($\Delta escN$). Ptk2 cells transfected with pTfR-mCherry were

infected with EPEC or left uninfected and fluorescent TfR containing vesicles were imaged using time lapse microscopy. U-track multiple particle tracking software was used to track fluorescent vesicle movement. Particle trajectories persisting ≥ 10 frames are solid black; < 10 frames are solid cyan; inferred gap closing (linking two tracks together) are dotted gray. (B) Particle speeds of tracked TfR-mCherry containing vesicles following infection with wild type EPEC or the T3SS mutant. Dot plots represent all track speeds calculated from at least 3 cells per infection condition. Particle speeds were calculated for all tracks with ≥ 10 visible segments. Red bar denotes median particle speed in $\mu\text{m/s}$ (0.2889, 0.0487, 0.1453) for uninfected, wild type and ΔescN , respectively. Asterisks indicate significant differences from wild type infection using one-way ANOVA with Tukey's multiple comparisons test ($P < 0.001$).

3.3.2 NleB1 and EspL inhibit TfR vesicle trafficking in EPEC-infected cells

Given that the EPEC/EHEC effectors NleB1 and EspL interacted with the kinesin-1 cofactor ensconsin (Chapter 2) and knowing that TfR-mCherry transport was significantly affected in a T3SS-dependent manner, we sought to determine whether this effect was mediated by NleB1 and/or EspL during EPEC infection. We infected Ptk2 cells with EPEC effector mutants and again examined movement of TfR-mCherry through fluorescent time-lapse imaging. We observed a distinct increase in TfR-mCherry vesicle movement during infection with ΔnleB1 and ΔespL (Figure 3.2A) similar to what was seen with T3SS-deficient EPEC. In contrast, cells infected with ΔnleB2 continued to display disrupted movement of TfR vesicles nearly indistinguishable from wild type EPEC (Figure 3.2A). Particle velocities determined for TfR-mCherry vesicles further demonstrated the profound effect that both NleB1 and EspL had on restricting vesicle movement during EPEC infections (Figure 3.2B). To further compare TfR-mCherry movement during infection with EPEC, we calculated the MSD of tracked particles for 5-frame intervals. Again, we observed a substantial reduction in vesicle movement during infection with ΔnleB2 or wild type EPEC compared to the attenuated effector mutant strains (Figure 3.3).

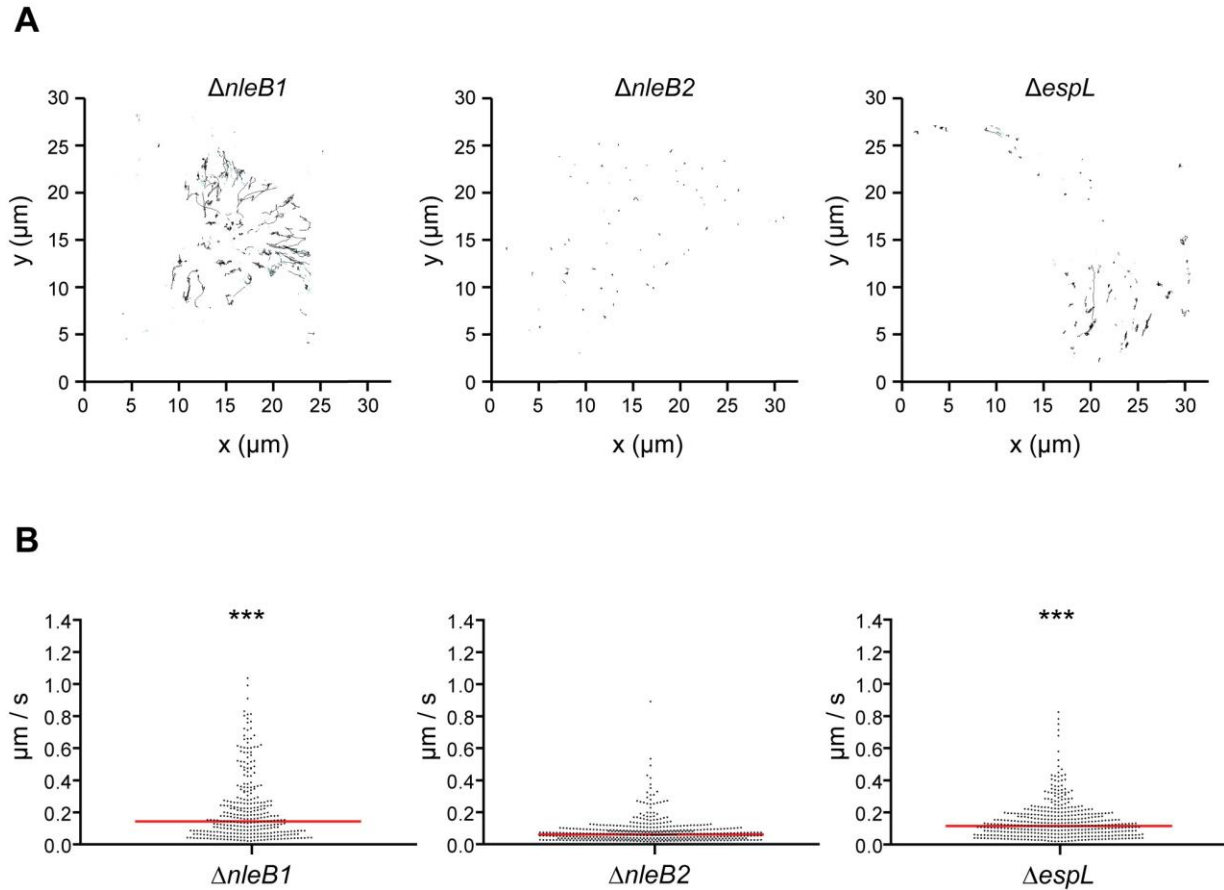


Figure 3.2 Enteropathogenic *E. coli* (EPEC) infection halts TfR-mCherry transport in an NleB1/EspL-dependent manner.

(A) Tracks of TfR-mCherry containing vesicles from a representative Ptk2 cell following infection with EPEC $\Delta nleB1$, $\Delta nleB2$ or $\Delta espL$ mutant. Ptk2 cells transfected with pTfR-mCherry were infected with EPEC and fluorescent TfR containing vesicles were tracked using u-track multiple particle tracking software. Particle trajectories persisting ≥ 10 frames are solid black; < 10 frames are solid cyan; inferred gap closing (linking two tracks together) are dotted gray. (B) Particle speeds for TfR-mCherry vesicles during EPEC infection. Dot plots represent all speeds calculated from at least 3 cells per infection condition. Particle speeds were calculated for all tracks with ≥ 10 visible segments. Red bar denotes median particle speed in $\mu\text{m/s}$ (0.1424, 0.0613, 0.1147) for $\Delta nleB1$, $\Delta nleB2$, and $\Delta espL$ respectively. Asterisks indicate significant differences from $\Delta nleB2$ using one-way ANOVA with Tukey's multiple comparisons test ($P < 0.001$).

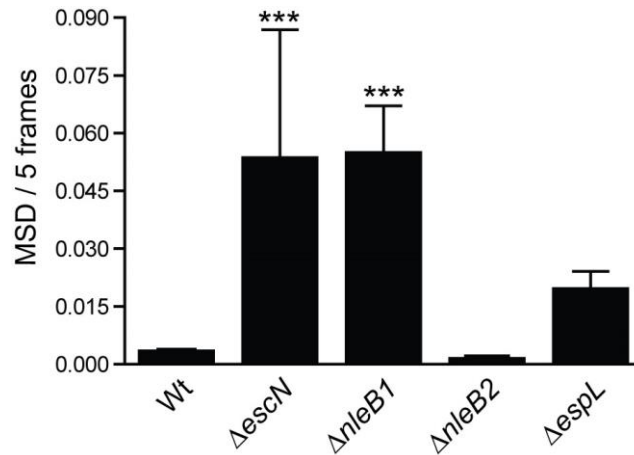


Figure 3.3 Mean squared displacements of TfR-mCherry particles in EPEC-infected cells.

Mean squared displacement (MSD) of pooled tracks showing severely disrupted TfR-mCherry movement in wild type EPEC or $\Delta nleB2$ mutant-infected Ptk2 cells. MSD/5 frames with 95% CI is shown for each infection for all particle trajectories with ≥ 10 visible track segments. Asterisks indicate significant differences from wild type using one-way ANOVA with Tukey's multiple comparisons test ($P < 0.001$).

3.3.3 Trans-complementation of the EPEC $\Delta nleB1$ and $\Delta espL$ mutants

To confirm that the observed trafficking inhibition of TfR-mCherry containing vesicles was specific to NleB1 and EspL, we complemented a $\Delta nleB1\Delta nleB2$ double mutant with *pnleB1* and the $\Delta espL$ single mutant with *pespL* and tested the ability of these strains to perturb TfR-mCherry movement. We found that infection with $\Delta nleB1\Delta nleB2/pnleB1$ or $\Delta espL/pespL$ significantly reduced TfR vesicle trafficking compared to infection with their uncomplemented counterpart strains (Figure 3.4). Thus, complementation of *nleB1* and *espL* in trans at least partially restored TfR trafficking inhibition seen during infection with wild type EPEC. To show that differences in TfR trafficking were not dependent on the specific parameters used to link individual particles between successive movie frames, a second tracking analysis was performed for each movie using an additional, more stringent set of tracking parameters (Appendix B

Figure B.1, B.2). Collectively, these data confirm that both NleB1 and EspL have a significant impact on TfR transport during infection.

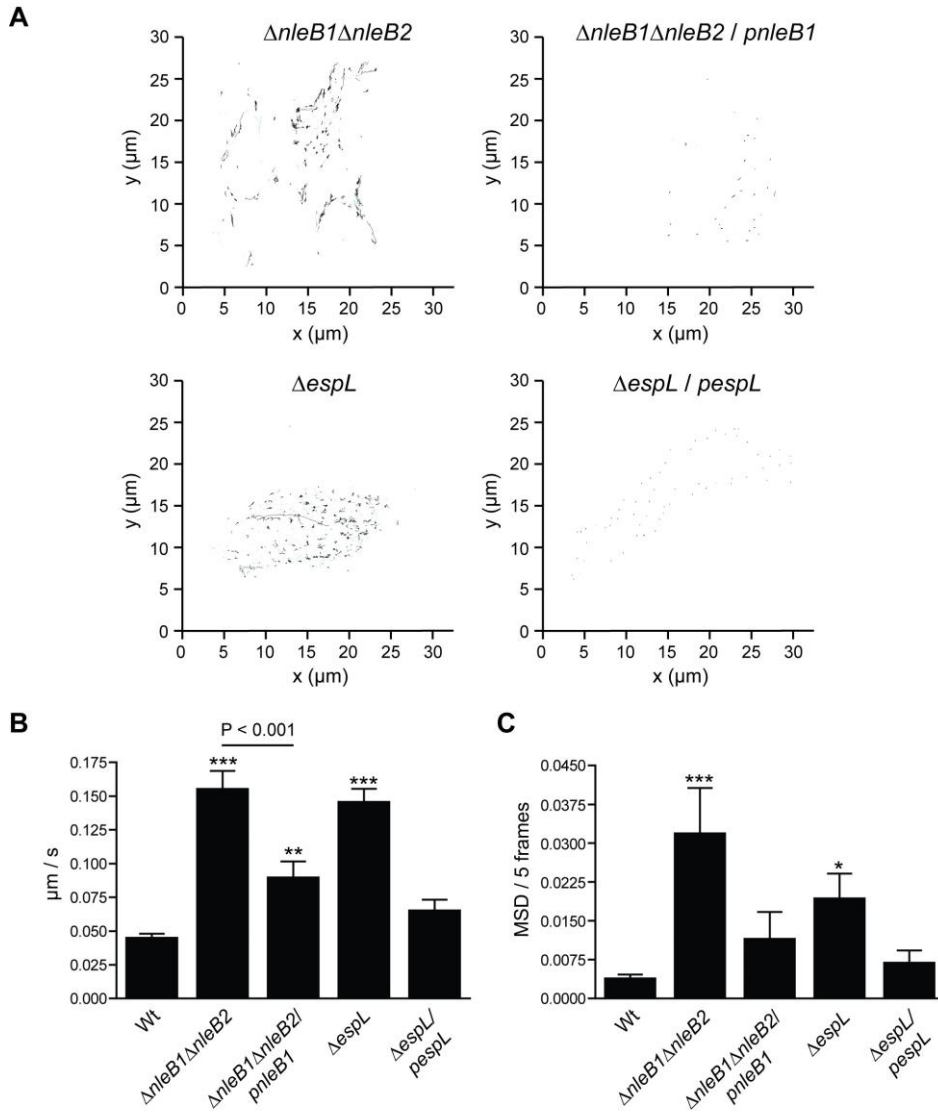


Figure 3.4 Trans complementation of *nleB1* and *espL* restores trafficking inhibition during EPEC infection.

(A) Tracks of TfR-mCherry containing vesicles from a representative Ptk2 cell following infection with EPEC *nleB1* or *espL* complemented strains. Ptk2 cells transfected with pTfR-mCherry were infected with EPEC and fluorescent TfR containing vesicles were tracked using u-track multiple particle tracking software. Particle trajectories persisting ≥ 10 frames are solid

black; < 10 frames are solid cyan; inferred gap closing (linking two tracks together) are dotted gray. (B) Mean particle speed with 95% CI of tracked TfR-mCherry containing vesicles during infection with *nleB1* or *espL* complemented strains. (C) Average MSD/5 frames with 95% CI for each infection. Pooled tracks show disrupted TfR-mCherry vesicle movement during infection with $\Delta nleB1$ or $\Delta espL$ complemented strains. Particle speeds and MSDs were calculated for all particle trajectories with ≥ 10 visible track segments. Asterisks indicate significant differences from wild type using one-way ANOVA with Tukey's multiple comparison's test ($P < 0.001$; $P < 0.01$; $P < 0.05$).

3.3.4 Effector overexpression does not affect TfR vesicle trafficking

Effector translocation is a highly regulated process and it is thought that this tight regulation is a means by which EPEC protects the host from increased cytotoxicity resulting from effector imbalance (Berger et al., 2012; Mills et al., 2008). For this reason, data from effector overexpression studies can sometimes lead to artificial results. Nevertheless, an analysis of TfR-mCherry movement in Ptk2 cells co-transfected with pTfR-mCherry and pEGFP-*nleB1* was conducted in an effort to further confirm the effect NleB1 had on vesicle trafficking. However, time lapse analyses of effector transfected vs control cells showed an extremely high density of fast moving TfR particles that could not be reliably tracked using computer analysis software. Therefore, a qualitative analysis of TfR-mCherry trafficking was conducted by visually inspecting live imaging data from effector transfection studies. No obvious differences in movement of TfR-mCherry containing vesicles were observed in cells expressing GFP-NleB1 compared to cells expressing GFP alone (Table 3.4). Based on this analysis, it was concluded that effector translocation may be a vital component of *nleB1*-mediated inhibition of transport.

Table 3.4 Movement of TfR-mCherry particles is unaffected by NleB1 overexpression

| Plasmid | Vesicle movement* | |
|---------------------|-------------------|----------|
| | Sample 1 | Sample 2 |
| pEGFPC1 | +++ | +++ |
| pEGFP- <i>nleB1</i> | +++ | +++ |

*Vesicle speed (/ , no movement; +, slow/slight; ++, moderate; +++, rapid)

3.3.5 EPEC targets kinesin-1-based vesicle motility in Ptk2 cells

Based on previously identified interactions between multiple EPEC effectors and the kinesin-1 cofactor, ensconsin, we used TfR-mCherry transport as an indicator for kinesin-1-based trafficking disruption. To determine whether this effect was indeed specific to TfR vesicle movement, we assessed trafficking of ssNPY-mCherry, a marker of Golgi-derived vesicles, in Ptk2 cells infected with wild type EPEC compared to TfR-mCherry. Indeed, both the speeds and MSDs of TfR-mCherry containing vesicles were drastically reduced compared to those of the generalized ssNPY-mCherry containing cargo vesicles (Figure 3.5 and Appendix B Figure B.3). These data indicate that EPEC specifically interferes with the trafficking of a subset of intracellular vesicles during infection and provide further evidence for targeted disruption of kinesin-1-based vesicle motility.

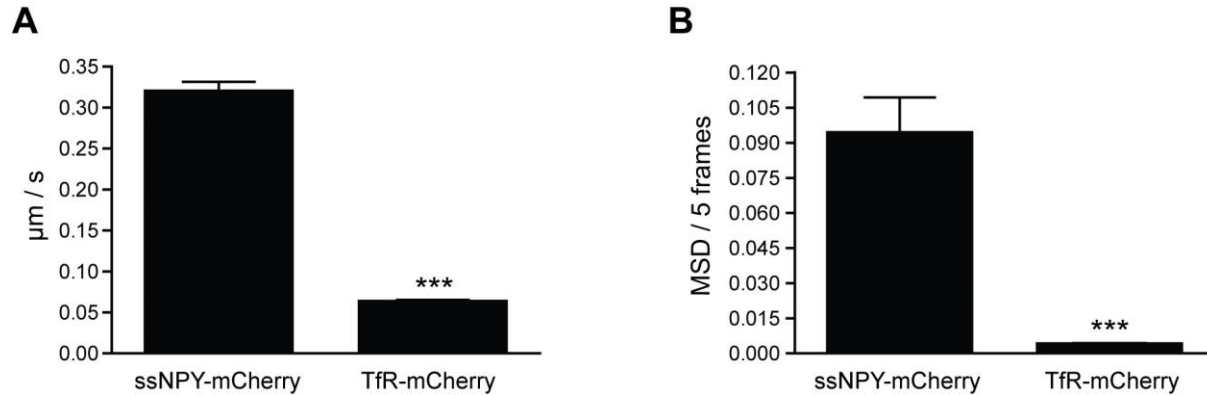


Figure 3.5 EPEC specifically inhibits kinesin-1-based vesicle motility.

Ptk2 cells infected with wild type EPEC show reduced movement of TfR-mCherry in comparison to the general vesicle marker, ssNPY-mCherry. (A) Mean particle speed with 95% CI of tracked TfR-mCherry containing vesicles during EPEC infection. (B) Average MSD/5 frames with 95% CI showing disrupted TfR-mCherry movement compared to ssNPY-mCherry during EPEC infection. Particle speeds and MSDs were calculated for all particle trajectories with ≥ 10 visible track segments. Asterisks indicate significant differences using an unpaired *t*-test ($P < 0.0001$).

3.3.6 NleB and EspL do not affect Kif5b binding to ensconsin in EPEC-infected cells

In addition to its interaction with MTs, ensconsin has recently been shown to interact with the kinesin-1 family motor, Kif5b, using murine C2C12 myoblasts (Metzger et al., 2012). Given the necessity of ensconsin for kinesin-1-based trafficking in *Drosophila*, we hypothesized that NleB1 and EspL could be acting on ensconsin to disrupt kinesin-1-based transport during infection. To confirm whether there was a physical interaction between the human ensconsin and Kif5b proteins and to determine whether this interaction might be affected during EPEC infection, we co-transfected HEK293T cells with *pmap7-6xHis* and *pCMV6-kif5b-myc-DDK* (OriGene Technologies, Inc.) prior to infection and lysis. Lysates were then subjected to nickel bead pulldown followed by Western blot analysis. Kif5b was enriched in the presence of MAP7-

6xHis compared to bead-only controls (Figure 3.6A), demonstrating that human ensconsin and Kif5b interact. However, this interaction was unaffected by EPEC infection, as similar amounts of Kif5b precipitated with MAP7-6xHis regardless of the presence of EPEC (Figure 3.6B). These results show that ensconsin and Kif5b interact in human cells and that EPEC infection does not interfere with this interaction, suggesting that if NleB1 and EspL mediate inhibition of vesicle trafficking via ensconsin, they do so without directly affecting the interaction between ensconsin and Kif5b. Thus, EPEC infection may impact the functional rather than physical relationship between ensconsin and kinesin via NleB1 and EspL. Further experimentation was therefore focused on identifying the cellular activity of these effectors with respect to ensconsin.

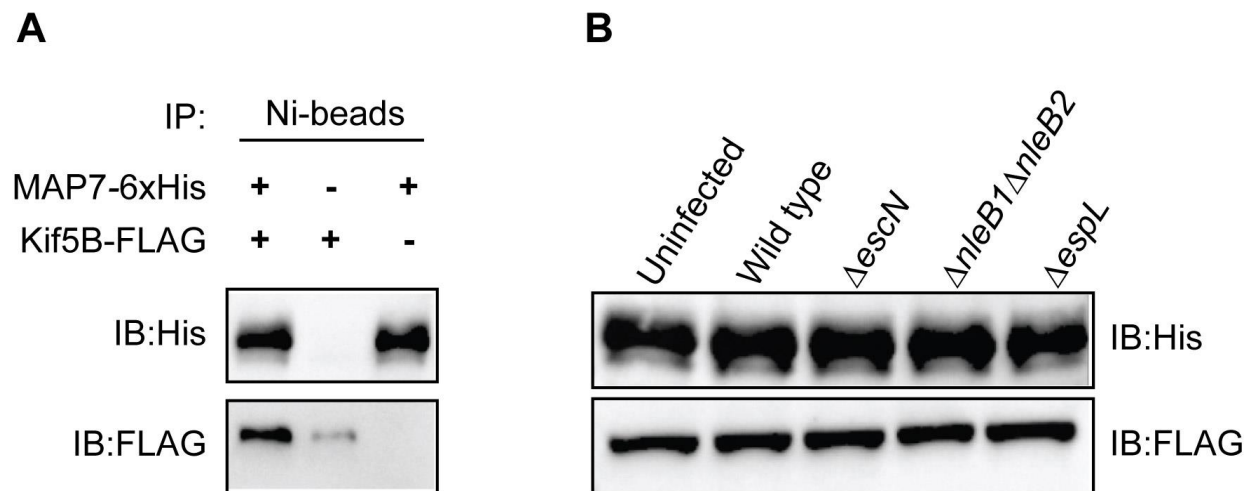


Figure 3.6 Enteropathogenic *E. coli* (EPEC) infection does not affect ensconsin (MAP7)-kinesin (Kif5b) interaction.

(A) Co-immunoprecipitation of MAP7-6xHis and Kif5b-FLAG. (B) Co-immunoprecipitation of MAP7-6xHis and Kif5b-FLAG following infection with wild type EPEC or effector mutants. HEK293T cells were co-transfected with *pmap7-6xHis* and *pCMV6-Entry::kif5B-myc-DDK* (FLAG) for 48 hrs to allow for protein expression followed by infection with EPEC for a further 1.5 hrs. Cell lysates were subjected to Nickel bead pulldown followed by immunoblot analysis with α -His or α -FLAG antibodies. IP: immunoprecipitation; IB: immunoblot.

3.3.7 Ensconsin expression is not affected by infection with EPEC

In an effort to determine how NleB1 and EspL might impact the function of ensconsin, endogenous expression levels of ensconsin were compared between uninfected cells and those infected with EPEC. Total RNA was extracted from uninfected or EPEC-infected HeLa cells and used as a template for cDNA synthesis. Real-time PCR was then performed to assess ensconsin relative expression following infection with EPEC. Relative to beta-actin, ensconsin gene expression was comparable across infection conditions (Figure 3.7A). Likewise, expression of ensconsin at the protein level was also unchanged in response to infection (Figure 3.7B). These data suggest that any effect NleB1 and EspL have on ensconsin is likely to be at the level of protein function rather than expression or stability.

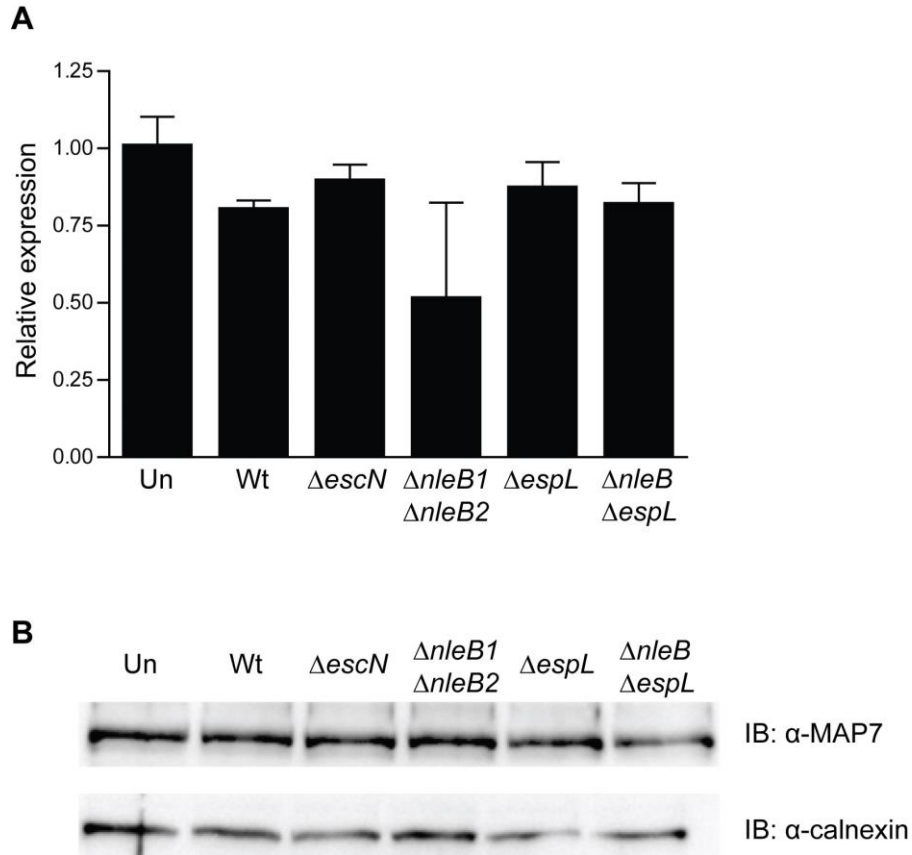


Figure 3.7 EPEC infection does not affect ensconsin expression.

HeLa cells were examined for ensconsin expression at 1.5 hrs post infection with EPEC. (A) Quantitative RT-PCR analysis of ensconsin gene expression relative to beta-actin in uninfected or EPEC infected HeLa cells. No statistically significant differences were identified using one-way ANOVA. (B) Protein expression of ensconsin (MAP7) in uninfected or EPEC-infected HeLa cells. Lysates were collected in NP40 buffer and subjected to Western blot analysis using α -MAP7 antibody or α -calnexin antibody as a loading control. Un: uninfected; Wt: wild type; IB: immunoblot.

3.3.8 Localization of ensconsin is unaffected by EPEC infection

Given that EPEC infection did not affect the levels of cellular ensconsin, we next hypothesized that binding of ensconsin by NleB1 and EspL could lead to mislocalization of the protein. We have already shown that both NleB1 and EspL interact with the MTB region of ensconsin. We

therefore used immunofluorescence (IF) to investigate the possibility that these effectors could be disrupting canonical localization of ensconsin to affect vesicle trafficking. Ensconsin staining was observed throughout the cytoplasm and appeared associated with the MT network as has been previously reported (Bulinski and Bossler, 1994; Masson and Kreis, 1993). However, no differences in ensconsin localization were detected between uninfected and EPEC-infected cells (Figure 3.8).

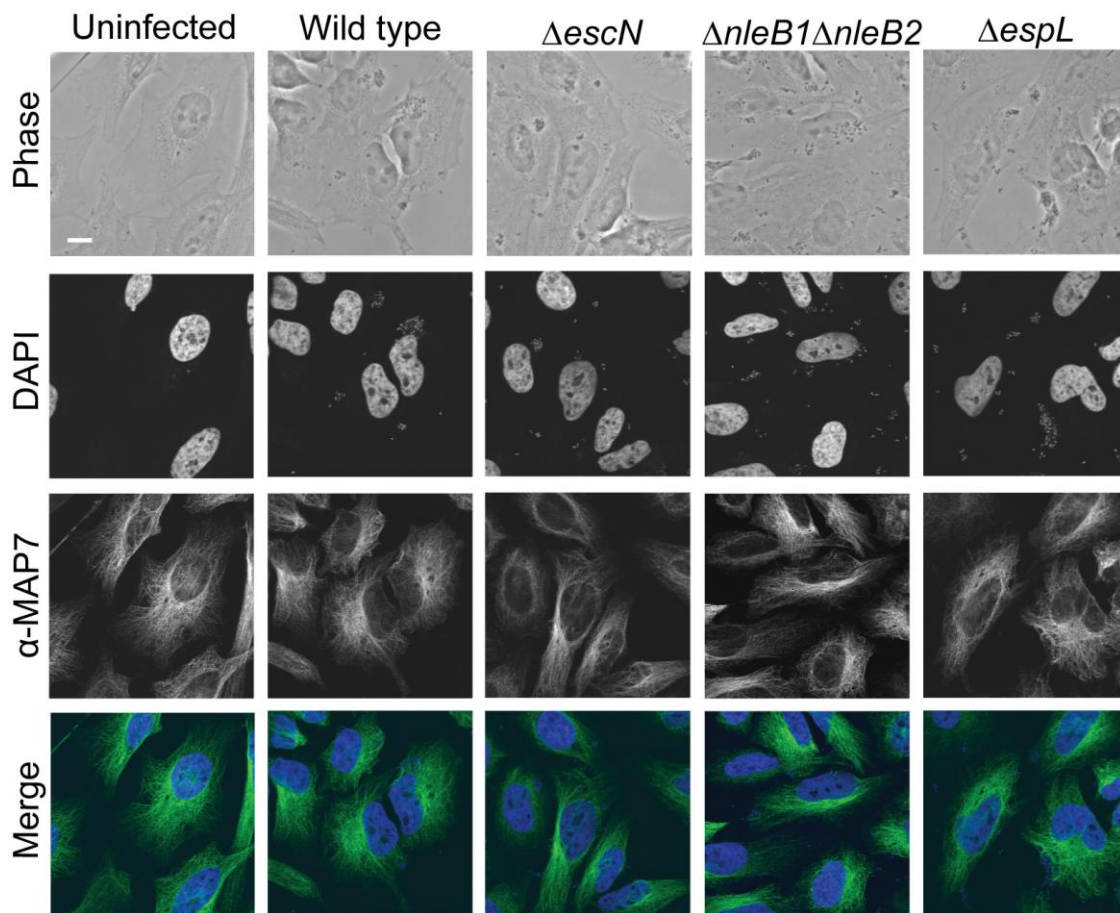


Figure 3.8 Localization of ensconsin during EPEC infection.

HeLa cells infected with EPEC for 3 hrs were stained with α -ensconsin (MAP7) antibody (green) and mounted using ProLong Gold plus DAPI to stain DNA (blue). Scale bar, 10 μ m. Images were acquired using an Olympus Fluoview 10i laser scanning confocal microscope with Olympus FV 2.1 software.

3.3.9 Microtubule structure is unaffected by NleB and EspL during EPEC infection

The function and stability of MTs is determined in large part by a number of MT associated proteins and early studies of ensconsin suggested that it may play a role in stabilizing MTs (Bulinski and Bossler, 1994; Masson and Kreis, 1993). To explore the possibility that NleB1 and EspL may be interfering with MT structure via ensconsin we performed IF analysis of α -tubulin. HeLa cells were again infected with EPEC for 1.5 hrs or left uninfected and imaged following IF staining. IF of α -tubulin demonstrated that the MTs of EPEC-infected HeLa cells remained unchanged in comparison to uninfected controls (Figure 3.9) despite the presence of EspG, a T3SS effector reported to interact directly with tubulin (Hardwidge et al., 2005; Shaw et al., 2005; Tomson et al., 2005). These data suggest that neither NleB nor EspL family effectors have any detectable effect on MT structure through their interaction with ensconsin, or that the effect may be too subtle to detect by infection alone. An additional analysis of the MT network was therefore conducted using effector overexpression.

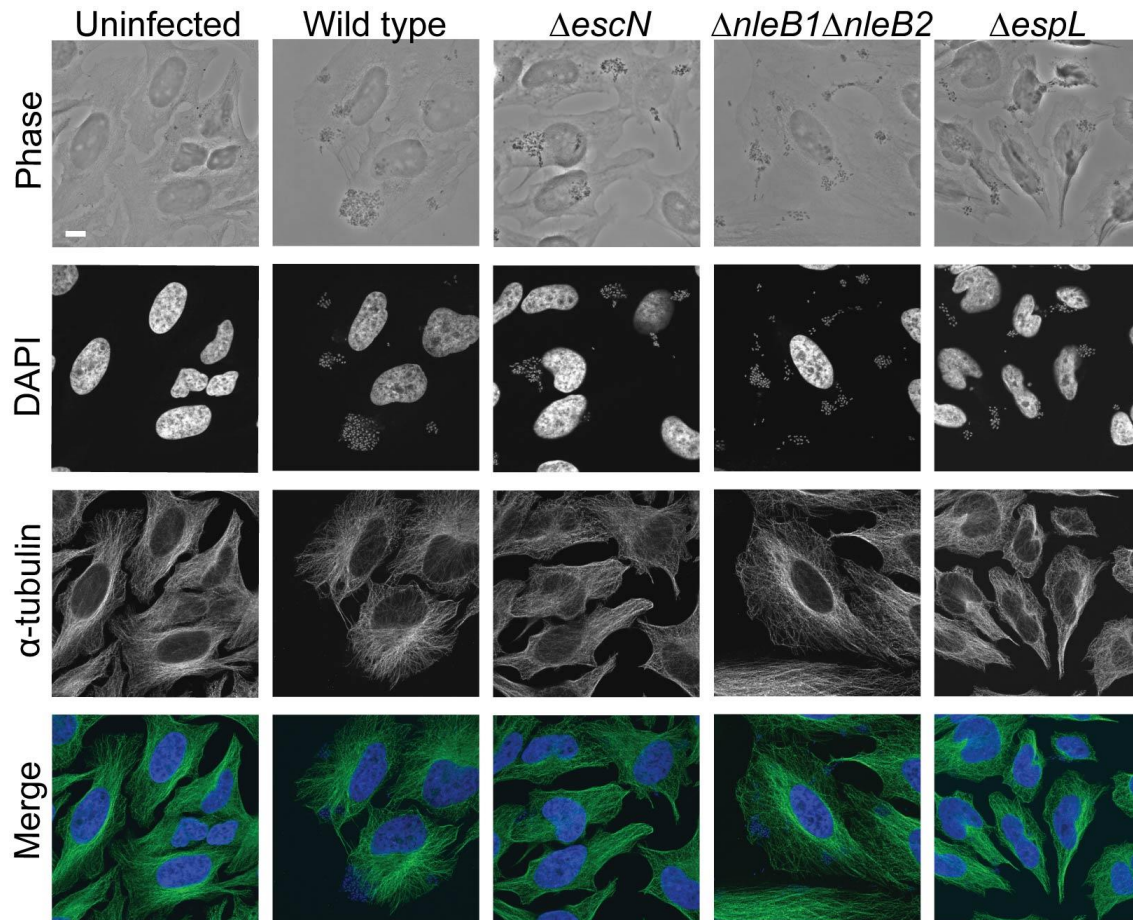


Figure 3.9 EPEC infection does not affect microtubule stability.

HeLa cells infected with EPEC for 3 hrs were stained with α -tubulin antibody (green) and mounted using ProLong Gold plus DAPI to stain DNA (blue). Scale bar, 10 μ m. Images were acquired using an Olympus Fluoview 10i laser scanning confocal microscope with Olympus FV 2.1 software.

3.3.10 Overexpression of NleB1 and EspL does not affect microtubule structure

The functions of individual effectors can be difficult to determine due to functional redundancy during infection or because subtle effects may be difficult to observe. Since no differences were detected in the MT networks of EPEC-infected cells compared to uninfected controls, we used HeLa cells ectopically expressing GFP-tagged NleB1 or EspL to assess changes in MT structure

as a result of effector overexpression. Similar to what was seen during infection, no discernable differences in the MT network were detected in cells overexpressing NleB1 or EspL compared to EGFP-only controls (Figure 3.10). Taken together, these data imply that neither NleB1 nor EspL affects MT stability via their interaction with ensconsin and that if NleB1 and EspL inhibit host TfR trafficking via ensconsin, inhibition occurs without disrupting canonical localization of ensconsin or the cytoskeletal tracks of its associated kinesin-1 motors.

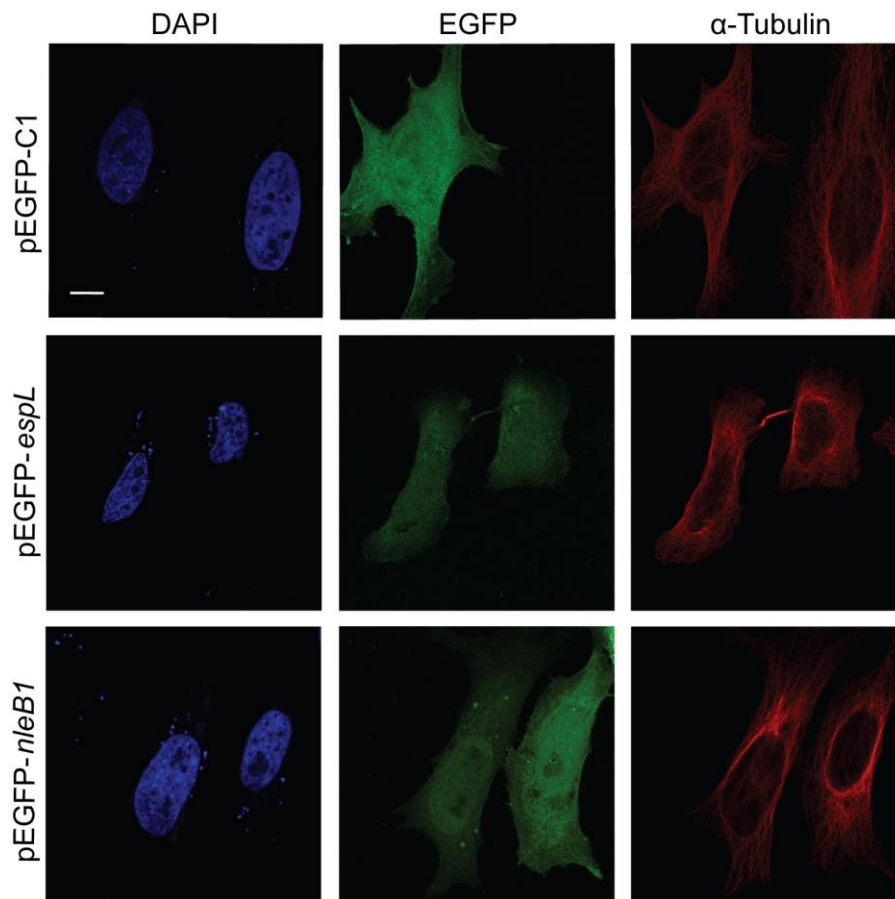


Figure 3.10 Overexpression of NleB1 or EspL does not affect microtubule structure.

HeLa cells overexpressing EGFP-tagged effectors (green) were stained with α -tubulin antibody (red) and mounted using ProLong Gold plus DAPI to stain DNA (blue). Scale bar, 10 μ m. Images were acquired using an Olympus FV1000 MPE confocal microscope with Olympus FV 2.1 software.

3.3.11 Separate roles for NleB1 during infection with EPEC

The NleB effectors were recently identified as GlcNAc transferases with catalytic residues identified in NleB1 at Asp221 and Asp223 (Gao et al., 2013; Li et al., 2013; Pearson et al., 2013). Given that the MT network and localization of ensconsin appeared unaffected by EPEC infection, we next hypothesized that NleB1 could be acting on ensconsin as a GlcNAc transferase to impair TfR-mCherry trafficking. However, infection of Ptk2 cells with an NleB1 catalytic mutant did not completely rescue the cell's ability to transport TfR (Figure 3.11 and Appendix B Figure B.4). While the particle speeds (Figure 3.11A) and tracks (Figure 3.11C) of TfR-mCherry vesicles in *nleB1mut*-infected cells showed no statistically significant differences from $\Delta nleB2$ infection, MSDs were not significantly different from either $\Delta nleB2$ or the attenuated double mutant (Figure 3.11B). As such, it remains to be determined whether GlcNAcylation and ensconsin binding are distinct functions of NleB, and if NleB1 and EspL perform an as yet undiscovered enzymatic or regulatory role in altering the ability of ensconsin to mediate vesicle trafficking.

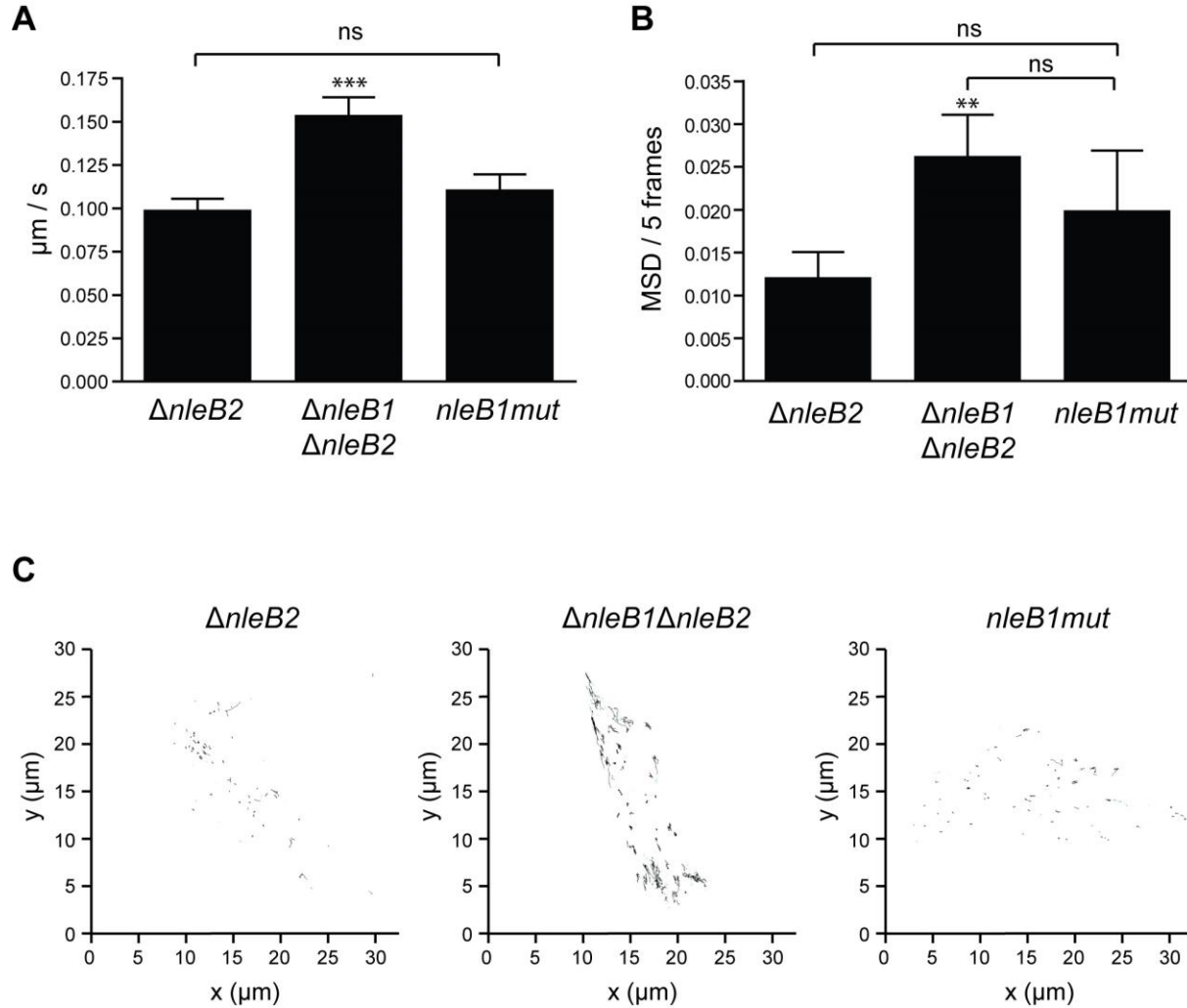


Figure 3.11 NleB1 GlcNAcylation activity does not affect TfR-mCherry vesicle trafficking.

Ptk2 cells infected with an NleB1 catalytic mutant-expressing strain show intermediate reduction in TfR-mCherry movement in comparison to controls. (A) Mean particle speed with 95% CI of TfR-mCherry containing vesicles following infection with EPEC $\Delta nleB2$, $\Delta nleB1 \Delta nleB2$ or $nleB1mut$. (B) Average MSD/5 frames with 95% CI showing intermediate disruption of TfR-mCherry movement during infection with $nleB1mut$. Particle speeds and MSDs were calculated for all particle trajectories with ≥ 10 visible track segments. Asterisks indicate significant differences from $\Delta nleB2$ using one-way ANOVA with Tukey's multiple comparisons test ($P < 0.001$; $P < 0.01$); ns: not significant. (C) Particle tracks of TfR-mCherry containing vesicles following infection with EPEC mutants. Particle tracks persisting ≥ 10 frames are solid black; particle tracks persisting < 10 frames are solid cyan; inferred gap closing, linking two tracks together are dotted gray. U-track multiple particle tracking software was used to track fluorescent vesicle movement.

3.4 Discussion

In the highly compartmentalized environment of a eukaryotic cell, precise control over intracellular trafficking is absolutely required to maintain the organized and continuous flow of an assortment of micro- and macromolecules throughout the cell. In the context of infection, however, trafficking pathways can be manipulated to alter normal intracellular transport to facilitate infection or for directed delivery of microbial proteins to a variety of cellular locations. Clearly, the ability to commandeer the host components involved in these pathways would provide a major advantage to pathogens.

Until recently, exploitation of intracellular vesicle transport by EPEC and EHEC has not been well studied, but the fact that these pathogens secrete multiple effectors to manipulate this pivotal host cell function demonstrates its importance during infection. Differential cargo delivery within host cells is spatially and temporally controlled by MT-dependent motors (Hirokawa and Noda, 2008) and while EPEC is known to spatially alter the localization of vesicles and surface receptors, its effects on temporal control of cargo delivery have not been studied (Clements et al., 2014; Kim et al., 2007; Olsen et al., 2013; Selyunin et al., 2014; Thanabalasuriar et al., 2012). We were able to demonstrate perturbations in the kinetics of kinesin-1-based vesicle motility by tracking fluorescent TfR during live EPEC infections. We showed that TfR-mCherry transport is almost completely blocked during infection with wild type EPEC and that the T3SS effectors NleB1 and EspL were responsible for this phenotype. We also showed that TfR trafficking was greatly reduced in comparison to that of the general vesicle marker, ssNPY, suggesting that EPEC targets specific routes of transport during infection rather than globally inhibiting vesicle trafficking.

In Chapter 2 we identified ensconsin as a novel target for both NleB1 and EspL of EPEC/EHEC and now present evidence for a previously unknown role for this MAP during bacterial infection. Early reports suggested that ensconsin may contribute to MT stability (Bulinski and Bossler, 1994; Masson and Kreis, 1993) but we showed that the MT network was unaffected by EPEC infection despite the presence of EspG, a T3SS effector reported to interact directly with tubulin (Hardwidge et al., 2005; Shaw et al., 2005; Tomson et al., 2005). However, EspG also inhibits membrane transport exclusive of MT destabilization (Selyunin et al., 2014), implying that EPEC employs a variety of effectors with different cellular targets to fine tune its influence on vesicular transport, independent of MT disruption. Since the goal of infection is to achieve a balance between efficient colonization and host survival, this would allow EPEC to tightly control motor-based transport without obstructing other MT functions.

Ensconsin is required for kinesin-1-based motility in the neurons and oocytes of *Drosophila* (Barlan et al., 2013; Sung et al., 2008). The exact mechanism by which ensconsin facilitates recruitment and activation of kinesin-1 is unknown, but it has been suggested that its C-terminal domain is involved in relieving the autoinhibition of kinesin-1 to stimulate its motor activity (Barlan et al., 2013). Consistent with this, we showed that while NleB1 and EspL interacted with the MTB region of ensconsin (Chapter 2), this interaction did not affect localization of ensconsin to MTs. It is then reasonable to speculate that these effectors block TfR vesicle transport either by interfering with kinesin-1-ensconsin interactions or by inducing conformational changes in the activity domain of ensconsin that precludes activation of kinesin-1. In line with this, we investigated the possibility that the GlcNAc transferase activity of NleB was required for inhibition of TfR transport. However, our data indicate that GlcNAcylation and

obstruction of vesicle transport may be independent functions of NleB. This is supported by the fact that EspL, which also interacts with ensconsin and inhibits vesicle transport, is not known to possess GlcNAc transferase activity, suggesting a novel mechanism whereby NleB1 and EspL oppose vesicle trafficking (Figure 3.12).

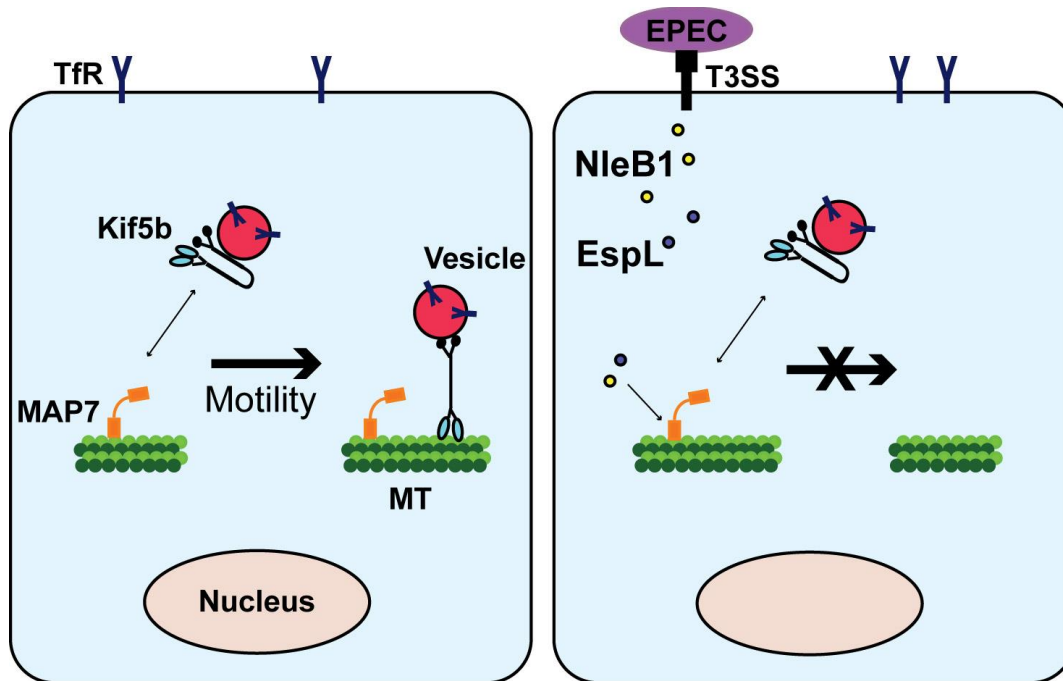


Figure 3.12 Schematic model of proposed NleB1/EspL function during infection with EPEC.

NleB1 and EspL target the critical kinesin-1 cofactor, ensconsin, and inhibit transferrin receptor trafficking. NleB1 (yellow) and EspL (Blue) interact with the microtubule (MT) binding region of ensconsin (orange) without disrupting MT structure or ensconsin (MAP7)-kinesin-1 (Kif5b) interaction. Thus, NleB1 and EspL are likely to perturb TfR trafficking through inhibition of Kif5b activation.

The pathogenesis of EPEC and EHEC can be enhanced by disrupting cellular trafficking of immune system mediators, brush border enzymes and surface receptors. In this way it is conceivable that A/E pathogens might further dampen the host's response to infection by

reducing trafficking and secretion of cytokines, by preventing release of antimicrobial factors to extracellular adherent organisms, or by interfering with membrane recycling, thereby allowing bacterial receptors to remain surface-located.

In summary, we have potentially identified a broad-based system whereby A/E pathogens could control transport of specific vesicle populations during infection by targeting an essential motor protein cofactor. We have shown that EPEC blocks vesicle trafficking during live infections and we have identified the MAP, ensconsin, as a unique target of two bacterial effectors with no previous connection to intracellular trafficking. We propose that inhibition of vesicle trafficking is a critical step in the overall infection process and that this activity is precisely controlled by multiple secreted effectors.

Chapter 4: Distinct virulence-associated phenotypes of the type III secretion system effectors, NleB and EspL, in the cecum of *C. rodentium*-infected mice

4.1 Introduction

In vitro studies elucidating the cellular functions and host targets of T3SS effectors have substantially improved our understanding of the molecular mechanisms of A/E pathogen virulence. However, to fully appreciate how these molecular interactions contribute to disease, *in vivo* studies are required to demonstrate the direct impact specific effectors have on A/E pathogen virulence. Thus far, no animal model currently available for A/E pathogens research can completely replicate infections caused by EPEC/EHEC. However, surrogate hosts can provide important information regarding host responses to infection and involvement of the host microbiome that cannot be obtained from tissue culture methods alone. For this reason, a considerable amount of *in vivo* A/E pathogens research has been performed using natural animal infection models, such as the *C. rodentium*-mouse model.

Upon ingestion, *C. rodentium* colonizes the cecum with progression to the distal colon within 2-3 days (Mundy et al., 2005). The most prominent symptoms of infection are colonic inflammation and hyperplasia (Barthold et al., 1978) but loose stool with increased luminal water content also accompanies *C. rodentium* infections (Guttman et al., 2006, 2007). Other features of *C. rodentium* infection include intestinal barrier disruption and, in highly susceptible mouse strains, mortality (Mundy et al., 2005).

Approximately 60% of the genes found in *C. rodentium* are shared with both EPEC and EHEC, including those encoding the LEE T3SS and several secreted effectors (Petty et al., 2010). *C.*

rodentium is capable of inducing A/E morphology similar to that of EPEC/EHEC (Schauer and Falkow, 1993a) and shares several virulence determinants with human pathogenic strains (Deng et al., 2001). Similar to the LEE genes of EPEC and EHEC, the *C. rodentium* LEE is required to produce A/E lesions in mouse intestinal cells (Schauer and Falkow, 1993b) and functional conservation between Tir and intimin from *C. rodentium* and EPEC demonstrates the usefulness of this model for studying human infections (Deng et al., 2003). A comprehensive analysis of the *C. rodentium* secretome effectively expanded the known repertoire of T3SS proteins among A/E pathogens (Deng et al., 2010) and using the *C. rodentium*-mouse model, 33 virulence factors have been uncovered in the *C. rodentium* LEE (Deng et al., 2004).

Infection studies in mice have identified several effectors that critically influence *C. rodentium* virulence including Tir, EspB, EspZ, NleA and NleB (Deng et al., 2003, 2004; Gruenheid et al., 2004; Kelly et al., 2006; Mundy et al., 2004; Newman et al., 1999), while other effectors, like EspJ, NleE and EspL, play a minor role in colonization and are thought to contribute to virulence collectively (Dahan et al., 2005; Kelly et al., 2006; Wickham et al., 2006, 2007).

Of the Nle-encoded effectors, NleA and NleB have the strongest effect on virulence with mice displaying reduced intestinal colonization and pathology when infected with *C. rodentium* $\Delta nleA$ or $\Delta nleB$ mutants. Similarly, cattle infected with EHEC $\Delta nleA$ or $\Delta nleB$ strains also show strongly reduced colonization potential (Misyurina et al., 2010). In comparison, the presence of *espL* has only a modest effect on colonization of mice (Wickham et al., 2006). Interestingly, the genetic arrangement of *nleB* and *espL* is conserved across EPEC E2348/69, EHEC O157:H7 EDL933 and EHEC O157:H7 Sakai as well as the animal pathogens, REPEC 83/39 and *C. rodentium* (Kelly et al., 2006); and the presence of PAI O122, which harbours both genes, is

correlated with higher virulence potential of EPEC/EHEC in humans (Bugarel et al., 2010; Vieira et al., 2010; Wickham et al., 2006).

We have shown that NleB and EspL of EPEC/EHEC interact with the same host target, ensconsin (Chapter 2), and that these effectors perform similar roles during infection in tissue culture (Chapter 3). Given their common activity and association with ensconsin, as well as their conserved genetic placement among A/E pathogenic strains, it is possible that EspL and NleB perform synergistic or antagonistic roles during A/E pathogen infection. To investigate the combined effects of NleB and EspL during infection *in vivo*, this chapter examines the colonization potential and virulence associated effects of a double $\Delta nleB\Delta espL$ *C. rodentium* deletion strain in C3H/HeJ mice.

4.2 Materials and methods

4.2.1 Generation of *C. rodentium* deletion mutants

The *C. rodentium* strain DBS100 was used to generate all mutants described in this study (Table 4.1). Creation of *C. rodentium* $\Delta nleB$ has been previously described (Wickham et al., 2006). In-frame deletion of *espL* was carried out using *sacB*-based allelic exchange and the sucrose selection method. Briefly, Pfu Turbo DNA polymerase (Stratagene) was used to PCR amplify ~600 bp on either side of *espL* using primer pairs crespL-F/crespL-DR and crespL-DF/crespL-R, respectively (Table 4.2). Upstream and downstream fragments were then joined using splice overlap extension PCR to create the *espL* deletion product. The deletion product was digested with KpnI/SacI and cloned into KpnI/SacI digested pRE112 to generate pRE112- $\Delta espL$. The plasmid pRE112- $\Delta espL$ was then transformed into *E. coli* donor strain MFD $_{pir}$ for conjugation

with recipient strain DBS100 or DBS100 Δ *nleB* to create DBS100 Δ *espL* and DBS100 Δ *nleB* Δ *espL*, respectively. After sucrose selection, transconjugants that were resistant to sucrose and sensitive to chloramphenicol were screened by colony PCR and verified for deletion by DNA sequencing (NAPS Unit, UBC).

Table 4.1 Bacterial strains used in this study

| Name | Source/Reference |
|---|------------------------|
| <u><i>C. rodentium</i> strain DBS100</u> | |
| Wild type | (Schauer et al., 1995) |
| Δ <i>escN</i> | (Deng et al., 2004) |
| Δ <i>nleB</i> | (Wickham et al., 2006) |
| Δ <i>espL</i> | This study |
| Δ <i>nleB</i> Δ <i>espL</i> | This study |

Table 4.2 Primers used in this study

| Primer | Sequence (5' – 3') ^a |
|-----------|---|
| crespL-F | <u>gggtacc</u> ggatgagtctgaagtgattccg (KpnI) |
| crespL-DR | tactactggcatatattcatctcc |
| crespL-DF | ggagatgaatatatgccagtagtaggtattactctaataataaca |
| crespL-R | <u>ggagctc</u> cccactgtatcgacgtagtag (SacI) |
| actBms-F | cagttcgccatggatgacg |
| actBms-R | tcaccacataggagtcctt |
| map7ms-F | agcaccatggcggagcag |
| map7ms-R | ttgtcctgaaactgtagaagt |

a – Restriction endonuclease sites are underlined.

4.2.2 Infection of mice with *C. rodentium* and effector mutants

Six- to eight-week-old female C3H/HeJ mice (Jackson Laboratories) were housed at the UBC animal facility in accordance with the guidelines of the University of British Columbia's Animal Care Committee and the Canadian Council on the use of laboratory animals. Mice received a

standard diet of sterile chow (laboratory rodent diet 5001; Purina Mills, St.Louis, MO) and sterilized water ad libitum throughout the experiment. Infections were carried out by oral gavage with 0.1 ml of an overnight culture of *C. rodentium* DBS100 or an effector mutant derivative in LB containing approximately $2-3 \times 10^8$ colony forming units (CFU). Retrospective serial dilution in PBS followed by plating on MacConkey agar was carried out to verify viable inoculum counts for each culture.

4.2.3 *C. rodentium* CFU and cytokine determination

Stool samples were collected at 2, 4, and 6 days post-infection (DPI). Tissues (cecum and spleen) were collected from mice at 6 DPI into 1 mL of sterile PBS supplemented with complete ethylenediaminetetracetic acid-free protease inhibitor cocktail (Roche Diagnostics) at a final concentration recommended by the manufacturer. Tissues were weighed, and then homogenized in a MixerMill 301 bead miller (Retch) for 5 minutes at 30 Hz at room temperature. For CFU determination, fecal homogenates were serially diluted in PBS and plated onto MacConkey Agar (Difco), incubated overnight at 37°C, and bacterial colonies were enumerated the following day, (normalized to tissue weight - per gram). *C. rodentium* colonies were clearly identified by their unique characteristic of being round with a red centre and white rim.

Cecum and spleen homogenates were centrifuged twice at 21,000 r.c.f. for 20 min at 4°C to remove cell debris and supernatants were aliquoted and stored at -80°C. Cytokine levels in cecum and spleen homogenates were determined with the BD Cytometric Bead Array Mouse Inflammation Kit (BD Biosciences) according to the manufacturer's recommendations (normalized to tissue weight - per gram).

4.2.4 RNA isolation and cDNA synthesis

Cecum sections were immediately submerged in RNeasy lysis buffer (Qiagen) and stored overnight at 4°C and then at -80°C until further processing. Cecum RNA was extracted using an RNeasy minikit (Qiagen) according to the manufacturer's instructions and quantified using a NanoDrop ND-1000 spectrophotometer (NanoDrop Technologies). One µg RNA was used as template for reverse transcription with the Quantitect RT kit (Qiagen) to generate cDNA according to the manufacturer's directions.

4.2.5 Real-time PCR

Real-time PCR was performed using Quantitect SYBR-Green Mastermix (Qiagen) and the Applied Biosystems (Foster City, USA) 7500 system. Beta-actin (ACTB) was used for normalization of *ensconsin* gene expression. Fold difference in expression was calculated as threshold cycle ($2^{-\Delta\Delta CT}$). Primer sequences are listed in Table 4.2.

4.2.6 Immunohistochemistry

Tissues for histological analysis were placed in 10% neutral buffered formalin upon collection. Fixed tissues were embedded in paraffin and cut into 5 µm sections using standard techniques by the UBC Histology Laboratory. Cecal sections were deparaffinized, rehydrated, and then placed in 10 mM citric acid (pH 6.0) at 90-100°C for 20 min, followed by room temperature cooling. Samples were blocked with BSA and normal goat serum and then incubated with a *C. rodentium* specific rat α -Tir antibody (Deng et al., 2003) overnight at 4°C, followed by 1 hr incubation with Alexa 488-conjugated goat α -rat secondary antibody (Invitrogen) at room temperature. Tissues

were mounted on glass slides using ProLong Gold Antifade Reagent with DAPI (Invitrogen) for DNA staining.

4.2.7 Pathology scoring

Cecal tissues were fixed in 10% neutral buffered formalin overnight and then placed into 70% ethanol. Fixed tissues were then embedded in paraffin, cut into 5 µm sections, and stained with hematoxylin-eosin (HE) by the UBC Histology Laboratory. Histopathology scores were determined as described elsewhere (Wlodarska et al., 2011). Briefly, lumen pathology was scored based on presence of necrotic epithelial cells (0, none; 1, scant; 2, moderate; 4, dense); surface epithelium was scored as the sum of regenerative change (0, none; 1, mild; 2, moderate; 3, severe), desquamation (0, none; 1, <10 cells; 2, 11-20 cells), and epithelial ulceration (3, ulceration; 4, ulceration plus severe crypt destruction); mucosa was scored for hyperplasia based on crypt length (0, <140 µm; 1, 141-285 µm; 2, 286-430 µm; 3, >431 µm) and goblet cell depletion (0, >50; 1, 25-50; 2, 10-25; 3, <10); and submucosa was scored for edema (0, none; 1, mild; 2, moderate; 3, profound).

4.3 Results

4.3.1 Infection analysis of a *C. rodentium* $\Delta nleB\Delta espL$ mutant in C3H/HeJ mice

NleB is required for *C. rodentium* to colonize the colons of C57BL/6 mice and to cause mortality in the more susceptible C3H/HeJ strain (Kelly et al., 2006; Wickham et al., 2006). On the other hand, EspL seems to contribute only slightly to mortality *in vivo* (Wickham et al., 2006). Although the genes encoding these effectors have been studied individually with respect to virulence, their simultaneous contribution to intestinal colonization and pathology has not been

considered. Based on the conserved and close genetic placement of *nleB* and *espL* among A/E pathogens and our observation that these effectors performed related roles during infection of tissue culture cells (Chapter 3), we sought to determine whether knocking these genes out in tandem would produce additive or redundant effects during infection of the cecum. To this end, C3H/HeJ mice were infected with wild type *C. rodentium* or effector deletion mutants to test the ability of $\Delta nleB\Delta espL$ to colonize relative to single deletion strains. Tissue from the ceca and spleens of C3H/HeJ mice were harvested at 6 DPI and the CFU per gram of tissue was calculated. As expected, the *nleB* mutant was significantly attenuated in its ability to colonize both the cecum and spleen (Figure 4.1). On the other hand, the *espL* mutant showed a similar level of cecum colonization as wild type *C. rodentium* but did show a statistically significant reduction in its ability to colonize the spleen (Figure 4.1). Similarly, the double mutant displayed significant attenuation in its ability to colonize the spleen but did not show a statistically significant difference in CFU/g of cecum compared to wild type *C. rodentium* (Figure 4.1). As an additional measure of colonization potential, stool samples were collected at 2, 4 and 6 DPI and mice were assessed for differences in their ability to shed *C. rodentium* (Figure 4.2). However, no statistically significant differences in the number of shed bacteria were observed among *C. rodentium* strains. These data show that deletion of *nleB* and *espL* in tandem does not affect the luminal content of *C. rodentium* in the cecum and suggest that EspL does not contribute to cecum colonization under the conditions tested.

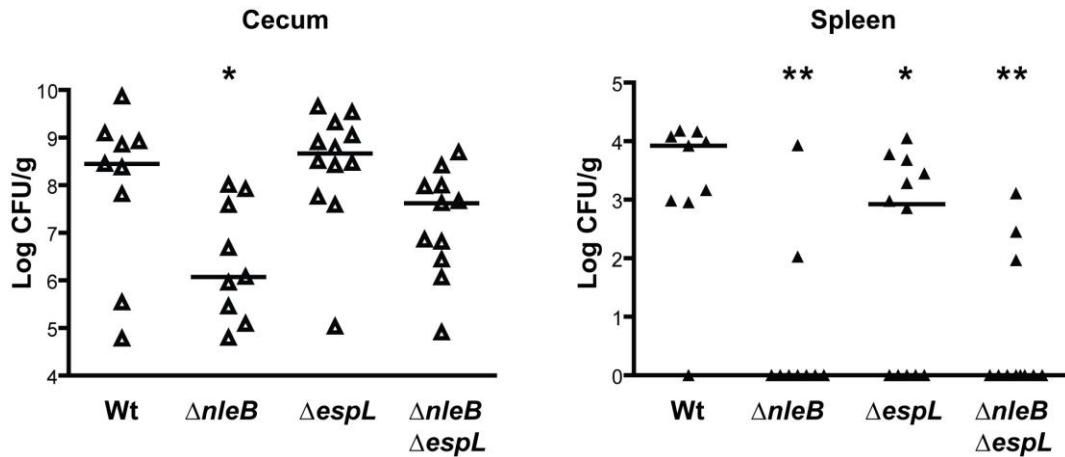


Figure 4.1 A *C. rodentium* $\Delta nleB \Delta espL$ mutant is attenuated in its ability to colonize the spleens, but not the ceca of C3H/HeJ mice.

Mice were infected with approximately 2×10^8 CFU of *C. rodentium* or effector mutant derivatives. Live bacteria were quantified from cecum or spleen homogenates collected from C3H/HeJ mice at 6 DPI and bacterial counts are represented as the \log_{10} CFU per gram of tissue. Median number of CFU per organ is shown. Asterisks indicate significant differences from wild type infection using one-way ANOVA with Dunnett's multiple comparisons test ($P < 0.05$ or $P < 0.01$).

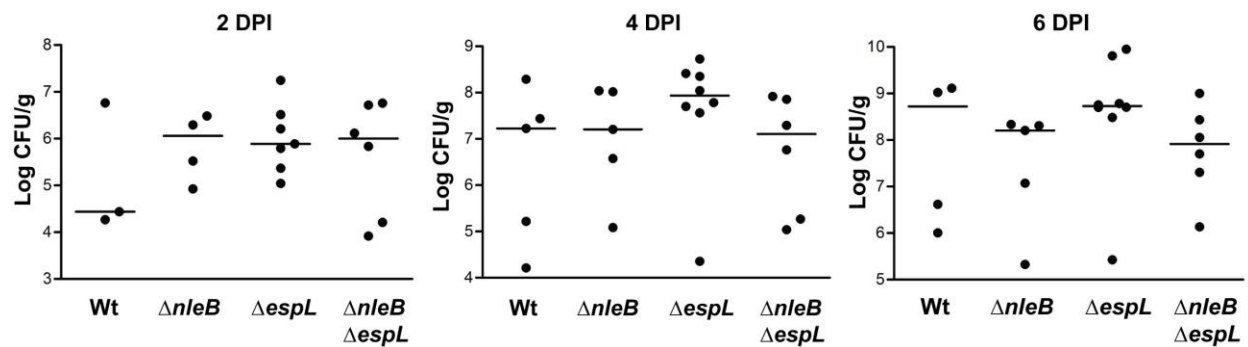


Figure 4.2 Fecal shedding of wild type *C. rodentium* or effector mutant derivatives from C3H/HeJ mice.

Mice were infected with 2×10^8 CFU of *C. rodentium* or effector mutant derivatives. Shed bacteria were quantified from feces collected at indicated time points and are represented as CFU per gram of feces per mouse. Median CFU per mouse is shown. No significant differences were identified using one-way ANOVA.

4.3.2 Tir-adherent *C. rodentium* is reduced in the cecum during infection with the $\Delta nleB\Delta espL$ mutant

Upon contact with host IECs, assembly of the T3SS is activated followed by effector translocation. Tir is one of the first T3SS effectors to be secreted (Mills et al., 2008) and is essential for intestinal colonization and hyperplasia in mice (Deng et al., 2003). For this reason, Tir expression can give an indication of the amount of adherent, T3SS-expressing *C. rodentium* in the intestines of infected mice. To compare the abilities of our *C. rodentium* deletion mutants to attach to and infect C3H/HeJ mice, cecal tissues were excised from infected mice and stained using the α -*C. rodentium* infection marker, Tir (Deng et al., 2003). In agreement with our cecum CFU data, immunostaining of infected tissue showed a greater surface area of Tir-positive tissue in wild type- or *espL* mutant-infected mice compared to those infected with the *nleB* mutant (Figure 4.3). Tissue from mice infected with the double mutant exhibited considerably less Tir staining than that seen during wild type infection or infection with the *espL* mutant (Figure 4.3) even though we saw no significant differences in cecum CFU counts among these strains (Figure 4.1). In fact, the double mutant appeared to be similarly attenuated in its ability to infect as was the *nleB* single mutant strain. These data suggest that deletion of *nleB*, but not *espL*, limits the rate of *C. rodentium* colonization in the cecum and that simultaneous deletion of *nleB* and *espL* does not produce an effect significantly different from what is observed with $\Delta nleB$ alone.

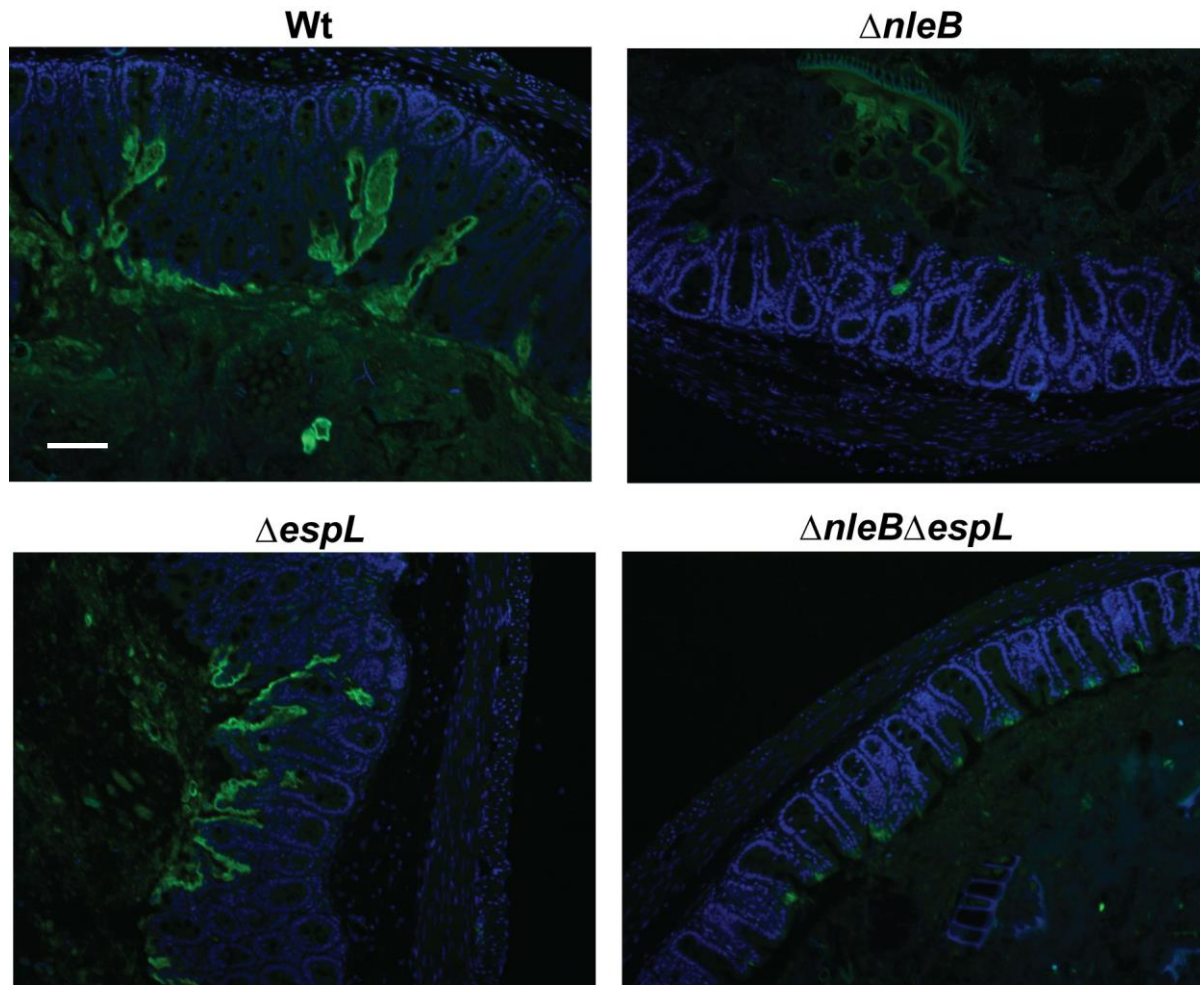


Figure 4.3 The *C. rodentium* $\Delta nleB\Delta espL$ mutant is attenuated in its ability to attach to and infect the mouse intestine.

C3H/HeJ mice were infected orally with *C. rodentium* or effector mutant derivatives and cecal tissues were harvested at 6 DPI. Immunostaining was performed using an α -Tir antibody specific to *C. rodentium* (green) with DAPI (blue) as a counterstain for host DNA. Magnification 100x; scale bar 100 μ m.

4.3.3 NleB, but not EspL, is essential for pathological changes in the cecum of *C. rodentium*-infected mice

The epithelial cells lining the cecum are the first to be colonized during infection by *C. rodentium* (Mundy et al., 2005). As a result, the cecum exhibits tissue pathology and inflammation prior to tissues of the colon and rectum. To assess the effect of an $\Delta nleB\Delta espL$

double deletion on *C. rodentium*-induced disease, pathological changes in cecal tissues of mice infected with *C. rodentium* and effector mutants were examined at 6 DPI. Compared to wild type *C. rodentium* or the *espL* mutant, mice infected with the double deletion strain showed a significant reduction in cumulative pathological changes in cecum-derived tissue (Figure 4.4). These changes were characterized by reduced submucosal edema and mucosal surface damage, as well as a reduction in mucosal hyperplasia. The observed reduction in cumulative damage scores for the *nleB* and double deletion mutants was consistent with the cecum α -Tir immunostain which showed that both of these mutants were less infective than wild type *C. rodentium* or the *espL* single mutant (Figure 4.3). These data indicate that a reduction in colonization potential corresponds to a diminished ability to cause pathological changes in the cecal tissues of infected mice and that these changes were dependent on the presence of *nleB* but not *espL*.

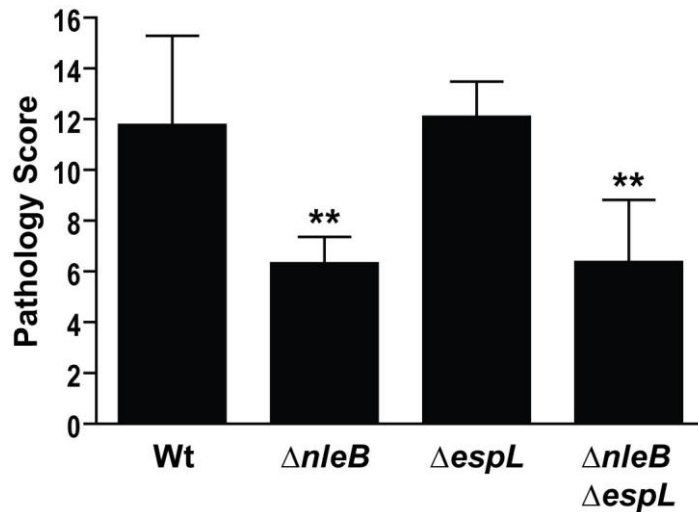


Figure 4.4 The *C. rodentium* $\Delta nleB\Delta espL$ mutant causes reduced histological damage in the cecal tissues of C3H/HeJ mice.

Microscopic examination of the ceca of *C. rodentium* infected mice at 6 DPI shows reduced histological damage in mice infected with either the single *nleB* mutant or the double effector deletion strain in comparison to mice infected with wild type *C. rodentium*. Scores were determined under blind conditions as cumulative damage to the mucosa, submucosa, surface epithelium and lumen of infected animals. Attenuation was statistically significant in comparison to wild type infection as determined by one-way ANOVA with Dunnett's multiple comparisons test ($P < 0.01$).

4.3.4 Infection with *C. rodentium* $\Delta nleB\Delta espL$ does not result in weight differences of the cecum or spleen compared to wild type controls

A shrunken cecum can be symptomatic of intestinal inflammation and damage caused by *C. rodentium* infection. On the other hand, spleen size can increase during infection in response to immune cell infiltration (Smith et al., 2011). To examine whether infection with our effector mutant derivatives would result in differences in mouse spleen/cecum weights, organs were excised and compared by weight to those of mice infected with wild type *C. rodentium*. However, no major differences were identified among mice infected with wild type *C. rodentium* or effector mutant strains and no statistically significant differences were observed (Figure 4.5).

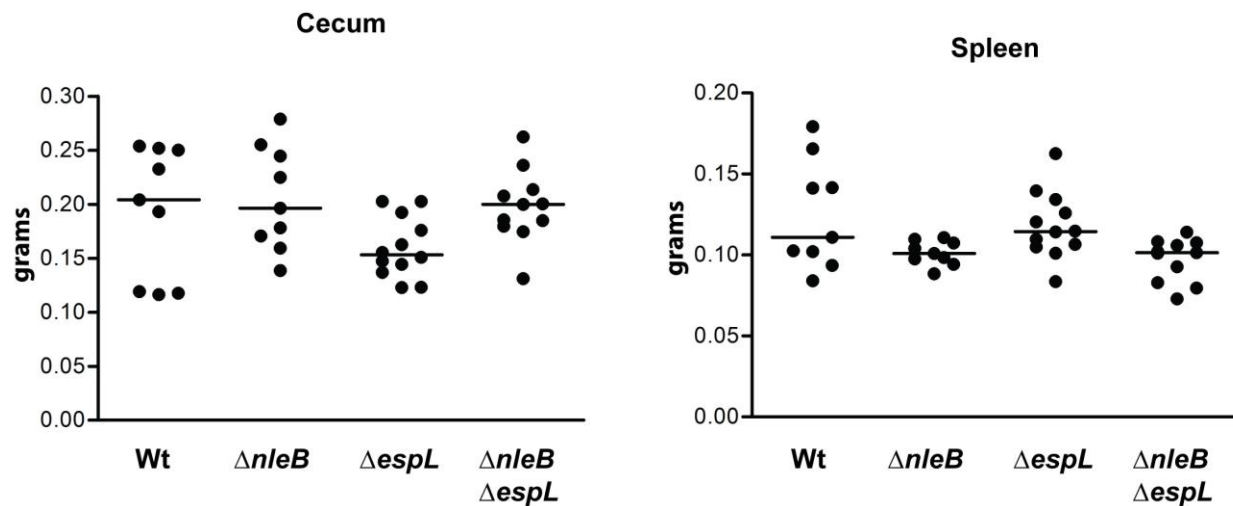


Figure 4.5 Organ weights of C3H/HeJ mice infected with wild type *C. rodentium* or effector mutant strains.

The spleens and ceca of mice infected with *C. rodentium* were removed at 6 DPI, weighed, and analyzed using one-way ANOVA with Dunnett's multiple comparisons test to identify statistically significant differences from wild type. Median organ weight is shown. No statistically significant differences were identified. Results are representative of samples collected from two separate infection experiments.

4.3.5 Reduced inflammation in the spleen and cecum correlates with attenuated colonization of the $\Delta nleB\Delta espL$ mutant

To further examine the murine inflammatory response to the double effector mutant, a cytometric bead array (CBA) was performed to compare cytokine production in the spleens and ceca of mice infected with wild type *C. rodentium* or effector mutant strains. Similar to the trend observed for *C. rodentium*-induced pathological changes (Figure 4.4), the levels of inflammatory cytokines produced in the cecum and spleen seemed to correlate with the degree of *C. rodentium*

infection. Supernatants collected from cecum and spleen homogenates showed a similar profile with an increased trend towards TNF- α , IFN- γ , and MCP-1 in wild type- and *espL* mutant-infected mice compared to mice infected with the *nleB* single mutant or the double mutant strain (Figure 4.6 and Figure 4.7). However, due to the spread in data, no statistically significant differences were detected in mean cytokine levels in either the ceca or spleens of infected mice. Nevertheless, there does appear to be a trend towards reduced amounts of all three cytokines in mice infected with the $\Delta nleB\Delta espL$ and $\Delta nleB$ mutants.

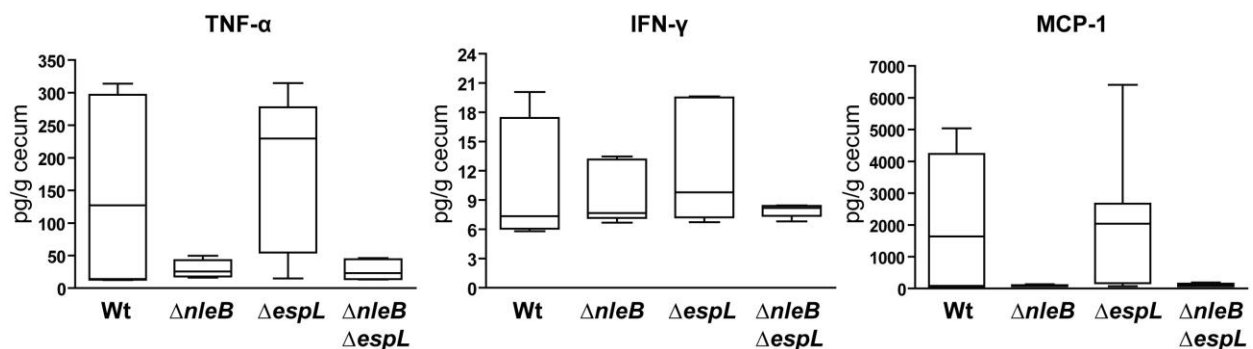


Figure 4.6 Cecum cytokine production in *C. rodentium* infected C3H/HeJ mice.

A cytometric bead array (CBA) was performed using supernatants from cecal tissues removed from mice at 6 DPI with *C. rodentium* or effector mutant derivatives. Boxes represent interquartile range and median (inner line). Whiskers represent minimum and maximum values. Samples were collected from two separate infection experiments. No statistically significant differences from wild type were identified using one-way ANOVA with Dunnett's multiple comparisons test.

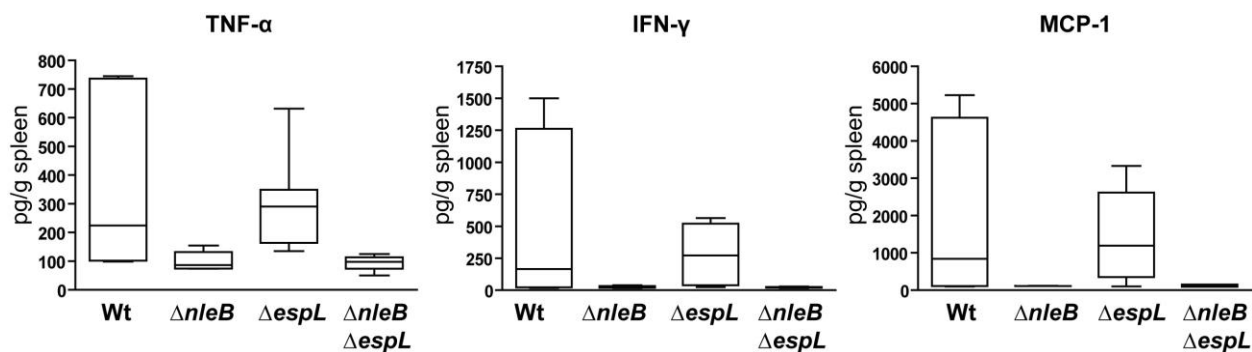


Figure 4.7 Spleen cytokine production in *C. rodentium* infected C3H/HeJ mice.

A cytometric bead array (CBA) was performed using supernatants from spleens harvested from mice at 6 DPI with *C. rodentium* or effector mutant derivatives. Boxes represent interquartile range and median (inner line). Whiskers represent minimum and maximum values. Samples were collected from two separate infection experiments. No statistically significant differences from wild type were identified using one-way ANOVA with Dunnett's multiple comparisons test.

4.3.6 *C. rodentium* infection does not affect ensconsin relative expression

Given that the double $\Delta nleB \Delta espL$ knockout did not display any additional differences in colonization or disease progression from C3H/HeJ mice infected with the *nleB* single mutant, attention was turned towards effects that NleB and EspL might have on their cellular interaction partner, ensconsin (identified in Chapter 2). Following a 6 day infection, gene expression analyses were conducted on total RNA from cecum sections extracted from C3H/HeJ mice. Quantitative RT-PCR analysis showed that relative expression of ensconsin was roughly similar across all infection conditions and no statistically significant differences were identified (Figure 4.8). These results correspond with relative expression data collected from HeLa cells infected with EPEC (Section 3.3.7) and point towards a possible effect on ensconsin at the protein activity level similar to what has been shown in tissue culture (Chapter 3).

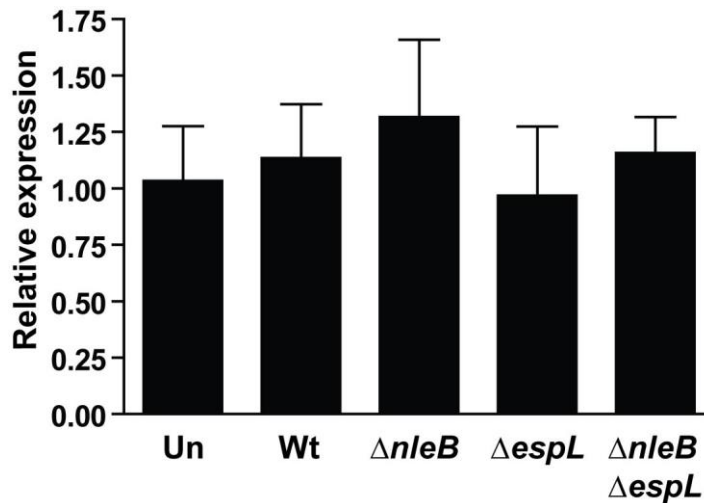


Figure 4.8 Real-time analysis of ensconsin relative gene expression in mice infected with *C. rodentium* or effector mutant derivatives.

Total RNA was extracted from the ceca of mice at 6 DPI for quantitative RT-PCR analysis. Expression of ensconsin was normalized using beta-actin and the fold difference in expression was calculated as threshold cycle ($2^{-\Delta\Delta CT}$). Data represent mean expression and 95% CI from samples collected from two separate infection experiments. No statistically significant differences were identified using one-way ANOVA. Un: uninfected; Wt: wild type.

4.4 Discussion

Diarrheagenic *E. coli* present a significant risk to human health worldwide, and due to the severity of symptoms associated with infections caused by EPEC and EHEC, few opportunities have presented themselves to study host susceptibility to these microbes and disease pathogenesis in the human host. For this reason, a variety of infection models have been developed to provide insight into our current understanding of the virulence mechanisms employed by A/E bacterial pathogens and to explore the molecular mechanisms that contribute to virulence of pathogenic *E. coli*.

Infection of mice with *C. rodentium* provides an excellent model with which to study host colonization and virulence determinants of A/E pathogens. In Chapter 2, we identified a common host target for two conserved A/E pathogen effectors that are known to contribute to *C. rodentium* colonization of mice (Kelly et al., 2006; Wickham et al., 2006). We have also shown that NleB and EspL genetically or functionally inhibit TfR vesicle transport during infection in tissue culture and that this effect may be due to the interaction between these effectors and ensconsin (Chapter 3). Given that vesicle trafficking is strongly involved in host cell signaling and immune response pathways and could be manipulated by A/E pathogens to promote colonization, we sought to determine whether simultaneous deletion of these effectors would lead to increased attenuation of *C. rodentium* infection in mice.

Using the highly susceptible C3H/HeJ mouse strain, which lacks an immune response to lipopolysaccharide and is rapidly colonized by *C. rodentium* (Vallance et al., 2003), we show that NleB is predominately responsible for virulence attenuation in the cecum compared to EspL and that simultaneous deletion of both effector genes does not increase attenuation of virulence. We used the ceca of infected mice to measure the colonization potential and virulence of *C. rodentium* effector mutants as this is the initial site of colonization for this pathogen (Mundy et al., 2005). Others have shown that infection with an *nleB* mutant results in reduced fecal shedding and colonization of colonic tissues and that this reduction is associated with lower total colon weights in comparison to wild type *C. rodentium* (Kelly et al., 2006). In agreement with these studies, we showed that the *nleB* single mutant was significantly attenuated in its ability to colonize the cecal tissue of C3H/HeJ mice, although this difference did not correlate with a significant reduction in total cecum weights. Surprisingly, the $\Delta nleB\Delta espL$ double mutant did

not display the same reduction in CFU/g of cecal tissue as mice infected with the attenuated *nleB* mutant strain and seemed to show similar bacterial loads as tissues from mice infected with wild type *C. rodentium*. However, immunofluorescence of α -Tir in the cecal tissues of *C. rodentium*-infected mice showed significantly less Tir-positive adherent bacteria during infection with both the *nleB* and double effector mutant. Likewise, the double mutant was significantly attenuated in its ability to induce pathological changes in the cecum compared to wild type *C. rodentium* or the *espL* mutant and was attenuated in its ability to cause systemic infection of the spleen. Thus, our data show that NleB plays an essential role during colonization of the cecum in susceptible mice and that the double mutant appears to be comparably attenuated in its ability to attach to the intestinal epithelium and cause tissue damage leading to systemic infection. These data are consistent with previous studies that have shown that *nleB* is critically involved in colon colonization during infection but differ from others that have identified a role for *espL* during intestinal colonization (Kelly et al., 2006; Wickham et al., 2006).

We did not observe any attenuation in the ability of the *espL* mutant to colonize the cecum or to induce pathological changes. Accordingly, immunofluorescence of α -Tir showed comparable amounts of Tir-positive adherent wild type *C. rodentium* and the *espL* mutant, indicating that deletion of this gene does not affect the ability of *C. rodentium* to attach to and infect cecum epithelial cells. The observed increase in intestinal damage was also consistent with increased levels of inflammatory cytokines in cecum and spleen supernatants of mice infected with wild type *C. rodentium* or the *espL* mutant when compared to attenuated strains. However, it should be noted that we did observe a slight attenuation in the ability of the *espL* mutant to colonize the

spleen in comparison to wild type *C. rodentium*, which is usually indicative of a reduction in barrier damage that can lead to systemic infection.

Interestingly, Wickham et al. have shown that an *espL* mutant displays some degree of attenuation in colonization and pathogenesis of *C. rodentium* in the distal colon (Wickham et al., 2006). The fact that our study showed no significant difference in the ability of an *espL* mutant to colonize and induce pathological changes in comparison to wild type *C. rodentium*, may be due to differences in the sites of infection analyzed or the mouse strains used. It is possible that EspL does not contribute to colonization of the highly susceptible C3H/HeJ strain but does play a minor role in colonization of more resistant C57BL/6 mice. It is also possible that EspL does not contribute significantly to initial colonization of the cecum but that it has some involvement in colonization of the distal colon. These data suggest that NleB is required for efficient colonization of the cecum and induction of intestinal damage and that EspL does not contribute significantly to *C. rodentium* colonization during *in vivo* infections. In line with this, we saw no additive effect on colonization or virulence of the $\Delta nleB\Delta espL$ double mutant, indicating that the aforementioned disruption in vesicle trafficking caused by NleB/EspL (Chapter 3) may be an independent function of these effectors with respect to colonization. It remains to be determined whether effector interaction with ensconsin plays any role in colonization but future work using suitable ensconsin knockout animal models to study *C. rodentium* infection will hopefully answer these important questions.

In summary, we show that NleB affects colonization and virulence potential of *C. rodentium* during cecum infection. We also show that despite having a similar cellular effect in tissue culture, NleB and EspL do not display equivalent roles during pathogenesis *in vivo* suggesting

that their molecular effects in cell culture may not directly link to colonization and pathological effects *in vivo*. The use of knockout mice or other relevant infection models will be required to further explore the relationship between the molecular effects of NleB and EspL in tissue culture and virulence *in vivo*. Future work in this area will shed more light on the roles of specific and related groups of effectors as they contribute to A/E pathogen virulence and what role (if any) *ensconsin* plays during infection *in vivo*.

Chapter 5: Conclusions

5.1 Relevance and contributions to the field

In this thesis, the function and disease relevance of two A/E pathogen effectors were explored using a combination of *in vitro* biochemical techniques, tissue culture analyses as well as surrogate host infections. When this work began in 2009, very little was known about the host interaction partners and cellular functions of either NleB or EspL. NleB was known to be an important contributor to A/E pathogen virulence, however, no interaction or mechanistic studies had yet been published. It was not until 2010 that research on NleB began to flourish with two publications detailing the involvement of this protein in dampening the immune response (Nadler et al., 2010; Newton et al., 2010). These were followed by three significant studies detailing the enzymatic mechanism responsible for the identified phenotype (Gao et al., 2013; Li et al., 2013; Pearson et al., 2013). On the other hand, only one study has so far been published identifying a cellular interaction partner and phenotype for EspL, but no mechanistic data have been provided (Miyahara et al., 2009). Our work adds to the growing pool of knowledge on T3SS effector function among A/E pathogens. This thesis details a novel protein target and never before seen impact on cellular function during A/E pathogen infection. In Chapter 2, we identified and confirmed ensconsin as a novel target for multiple effector proteins of both EPEC and EHEC, which was the first evidence of A/E pathogen manipulation of a MT associated protein. Ensconsin was identified from mammalian cell lines and was initially characterized in the early 1990's, since then however, little work has been published on the effects of this protein using *in vivo* mammalian models. In mice, ensconsin was shown to be important for spermatogenesis based on its interaction with MTs of the spermatid manchette (Komada et al., 2000; Penttilä et

al., 2003), but functional analyses of its role in mammalian *in vivo* active transport have yet to be explored. In this work we have generated the first link between active kinesin-based vesicular transport and ensconsin function in mammalian cells. Additionally, this is the first work identifying this MAP as an important target of any pathogen and the fact that EPEC/EHEC have retained distinct effectors that interact with ensconsin, demonstrates the importance of this protein during infection. This constitutes a major contribution to the fields of bacterial pathogenesis as well as cellular biology and provides the ground work for additional studies on the transport-related function of ensconsin in human cells. Others have used static, fixed sample analyses to show that host secretion and transport functions are affected by EPEC. Our work is unique to these studies in that we used a novel automated tracking system for live infection analyses of cellular transport and were able to identify a directed effect on spatial and temporal transport of specific vesicle populations. The work in this thesis supports the hypothesis that ensconsin is a critical target for manipulation by A/E pathogens and that NleB and EspL contribute to the pathogenesis of these microbes through their interaction with ensconsin. Additionally, our work shows that A/E pathogen effectors have varying roles in importance with respect to virulence during animal infections. However, the fact that certain effectors, like EspL, do not present a significant effect on disease pathogenesis in mouse models does not necessarily negate their importance during infection. EPEC and EHEC have an extensive repertoire of secreted effectors which could play varying roles during infection of different tissues or infection of different hosts as certain effectors have already been shown to behave differently depending on the cell line in which they are studied (Raymond et al., 2011). Indeed, the future of A/E pathogens research will necessarily have to include further analyses on effector interplay and coordination during infection of various hosts and tissues.

Ultimately, the work presented in this thesis has contributed new insight to the field of A/E pathogens research with an emphasis on intracellular functions of secreted effectors. Our work further demonstrates the multifunctional and cooperative nature of these proteins during infection and highlights a novel means of tracking infections using live microscopic analyses. Additionally, our work provides a basis for subsequent studies on the discrete mechanisms used by bacterial pathogens to control essential cellular functions and could be used as a platform to study related virulence proteins of other human and animal pathogens.

5.2 Future research directions

This thesis defines ensconsin as a conserved target of A/E pathogen effectors and provides evidence for its manipulation as a motor transport cofactor during infection. The data presented in this thesis address novel aspects of EPEC/EHEC pathogenesis that are only beginning to be explored; and while a combination of *in vitro* and *in vivo* models were used to investigate the functional details of NleB/EspL's role during infection, many mechanistic details remain undefined.

Chapters 2 and 3 describe the identification of ensconsin as a conserved interactor of the EPEC/EHEC effectors, NleB1 and EspL, and correlate these effectors with an inhibition of kinesin-1-based vesicle trafficking during EPEC infections. A number of mechanisms by which these effectors could be acting on ensconsin to disrupt vesicle trafficking have been ruled out. These include disruption of MT-based tracks and mislocalization of ensconsin, as well as inhibition of ensconsin-Kif5b binding. We have suggested that NleB1 and EspL may be altering ensconsin function through enzymatic modification, induction of conformational changes that

prevent activation of kinesin-1, or through steric hindrance of the kinesin motor. Future work should focus on identifying the specific molecular mechanisms of action of both effectors as they relate to ensconsin's function in human cells. Structural analyses of the effector-ensconsin interactions could be conducted to gain insight into the steric or conformational hindrance these interactions may place on kinesin-1 activation. Our data indicate that the GlcNAc transferase activity of NleB1 is not primarily responsible for disruption of trafficking, but we were not able to conclusively show that ensconsin is not a target for GlcNAc modification by NleB1. Therefore, further biochemical analyses will be required to definitively determine whether ensconsin is post-translationally modified in this fashion. As well, our data indicate that inhibition of trafficking is a result of effector driven manipulation and identify ensconsin as the most likely target. However, we cannot ignore the possibility that interaction of these effectors with ensconsin is unrelated to the observed effects on TfR vesicle transport. For this reason, additional analysis of the host factors involved should be further explored. For example, tracking analyses following additional kinesin motors and cytoplasmic dynein as well as a variety of cargo types should be conducted in response to EPEC infection in order to identify whether this effect is truly a kinesin-1 specific interruption or whether multiple motors may be targeted.

The majority of functional data on ensconsin comes from work using the *Drosophila* model but additional questions of how these studies might relate to mammalian systems must be tested within the context of infection. We showed that NleB and EspL have disparate effects on pathology and inflammation of the mouse cecum during infection with *C. rodentium*, indicating that the observed effects on cellular trafficking may not be related to the ability of the bacteria to

colonize the intestine. However, this could also indicate NleB and EspL perform different mechanistic roles during infection of mice than during infection of other models. Future work in this area should focus on connecting the functional properties of ensconsin *in vitro* to infection analyses *in vivo*, thereby providing an important link between molecular function and infection. Ensconsin knockout mice do exist but the deletion renders the males sterile, making experimentation with these animals expensive and difficult. The possibility of using additional animal models exists as putative copies of the ensconsin gene have been found in numerous species but functional studies have been carried out in very few.

Our work highlights the need for additional tools and models with which to study ensconsin in both infectious and non-infectious conditions. Until recently, research on ensconsin and the tools for studying it in mammalian systems has been severely lacking. Hopefully, our study, in combination with recent work using *Drosophila*, will spur renewed interest in studying the biology of this understudied MAP both as a target for pathogen subversion and as a key player in mammalian cellular trafficking and may prompt additional research in the field of cell biology to tease out the mechanism or additional mechanisms of ensconsin function.

5.3 Challenges facing A/E pathogens research

A/E pathogens have been associated with severe diarrheal illnesses for many years, imposing a significant health and financial burden worldwide. The seriousness of infections caused by EPEC/EHEC is best exemplified by the dedicated surveillance systems and long term epidemiological studies that have been established to monitor and track the spread of infections they cause as well the severity of their associated diseases. However, differences in the methods

used to properly detect and diagnose infections can lead to incorrect diagnoses, thereby making an accurate accounting of the disease burden caused by A/E pathogens difficult to obtain.

In addition to accuracy of detection and disease reporting, another challenge facing A/E pathogens research is the development of suitable models to accurately reflect the pathogenesis and disease state observed during natural human infection. Much of what is currently known regarding the molecular mechanisms of A/E pathogen infection has come from *in vitro* analyses which do not always mimic what is observed *in vivo* (Schüller et al., 2007). In addition, the redundant and interdependent nature of many effectors has hampered the identification of novel effector functions in these systems. Great strides have been made in identifying the virulence determinants involved in causing disease, but a comprehensive understanding of the molecular mechanisms of A/E pathogen infection remains in progress.

No model currently available for use in A/E pathogens research can fully replicate natural infections by EPEC/EHEC. Cell culture methods provide important information with respect to the cellular biology of T3SS effector function, but are of limited use in studying the interaction of A/E pathogens with the host immune system and microbiota. On the other hand, animal models provide a convenient means to study virulence of A/E pathogens, yet the symptoms and severity of diarrheal disease can vary significantly between animal hosts. Although much has been accomplished in the field of A/E pathogens research, many aspects of A/E pathogen infection remain poorly understood including the precise mechanisms that lead to diarrhea and the relationship between A/E pathology and disease, as well as reservoirs and transmission dynamics of EPEC (Donnenberg and Finlay, 2013).

5.4 The future of A/E pathogens research

New and rapidly evolving genomic tools are emerging, allowing for novel revelations of how differences in gut microbial composition and variability of the human metagenome among individuals correlate with human health and disease states (Arumugam et al., 2011; Pflughoeft and Versalovic, 2012). In the future, global surveys of the human metagenome should address how the composition of the microflora and the genome of the individual contribute to host susceptibility to A/E pathogens, whether in a carrier state or during acute infection. Studies of this nature should provide information that will lead to a better understanding of the infection process as it relates to host–pathogen–microbiota interplay. Thus far, no *in silico* models exist to directly simulate EPEC or EHEC infection (Vallance et al., 2004), however, publication of the EPEC E2348/69 (Iguchi et al., 2009), EHEC O157:H7 (Hayashi et al., 2001; Perna et al., 2001), and *C. rodentium* (Petty et al., 2010) genome sequences has facilitated identification of conserved and unique T3SS related proteins and effectors and should contribute to the development of microarray databases and other computer-based technologies to identify and study A/E bacterial pathogens.

It has become apparent that many pathogens use related virulence strategies to evade the host immune response and to promote infection and spread. Our knowledge of the various mechanisms used by A/E pathogens in causing disease is continuously evolving. In the future, knowing what, when and how bacterial effectors target within the host could ultimately help to develop more effective therapeutics for these as well as other enteric pathogens.

Bibliography

- Abe, A., Kenny, B., Stein, M., and Finlay, B.B. (1997). Characterization of two virulence proteins secreted by rabbit enteropathogenic *Escherichia coli*, EspA and EspB, whose maximal expression is sensitive to host body temperature. *Infect. Immun.* 65, 3547–3555.
- Afset, J.E., Bergh, K., and Bevanger, L. (2003). High prevalence of atypical enteropathogenic *Escherichia coli* (EPEC) in Norwegian children with diarrhoea. *J. Med. Microbiol.* 52, 1015–1019.
- Afset, J.E., Bevanger, L., Romundstad, P., and Bergh, K. (2004). Association of atypical enteropathogenic *Escherichia coli* (EPEC) with prolonged diarrhoea. *J. Med. Microbiol.* 53, 1137–1144.
- Alikhani, M.Y., Mirsalehian, A., and Aslani, M.M. (2006). Detection of typical and atypical enteropathogenic *Escherichia coli* (EPEC) in Iranian children with and without diarrhoea. *J. Med. Microbiol.* 55, 1159–1163.
- Alto, N.M., Weflen, A.W., Rardin, M.J., Yarar, D., Lazar, C.S., Tonikian, R., Koller, A., Taylor, S.S., Boone, C., Sidhu, S.S., et al. (2007). The type III effector EspF coordinates membrane trafficking by the spatiotemporal activation of two eukaryotic signaling pathways. *J. Cell Biol.* 178, 1265–1278.
- Arumugam, M., Raes, J., Pelletier, E., Le Paslier, D., Yamada, T., Mende, D.R., Fernandes, G.R., Tap, J., Bruls, T., Batto, J.M., et al. (2011). Enterotypes of the human gut microbiome. *Nature* 473, 174–180.
- Atherton, J., Houdusse, A., and Moores, C. (2013). MAPping out distribution routes for kinesin couriers. *Biol. Cell* 105, 465–487.
- Auweter, S.D., Bhavsar, A.P., de Hoog, C.L., Li, Y., Chan, Y.A., van der Heijden, J., Lowden, M.J., Coombes, B.K., Rogers, L.D., Stoykov, N., et al. (2011). Quantitative mass spectrometry catalogues *Salmonella* pathogenicity island-2 effectors and identifies their cognate host binding partners. *J. Biol. Chem.* 286, 24023–24035.
- Avery, L.M., Williams, A.P., Killham, K., and Jones, D.L. (2008). Survival of *Escherichia coli* O157:H7 in waters from lakes, rivers, puddles and animal-drinking troughs. *Sci. Total Environ.* 389, 378–385.
- Badea, L., Doughty, S., Nicholls, L., Sloan, J., Robins-Browne, R.M., and Hartland, E.L. (2003). Contribution of Efa1/LifA to the adherence of enteropathogenic *Escherichia coli* to epithelial cells. *Microb. Pathog.* 34, 205–215.

- Baldini, M.M., Kaper, J.B., Levine, M.M., Candy, D.C., and Moon, H.W. (1983). Plasmid-mediated adhesion in enteropathogenic *Escherichia coli*. *J. Pediatr. Gastroenterol. Nutr.* 2, 534–538.
- Barlan, K., Lu, W., and Gelfand, V.I. (2013). The microtubule-binding protein ensconsin is an essential cofactor of kinesin-1. *Curr. Biol.* 23, 317–322.
- Barthold, S.W., Coleman, G.L., Jacoby, R.O., Livestone, E.M., and Jonas, A.M. (1978). Transmissible murine colonic hyperplasia. *Vet. Pathol.* 15, 223–236.
- Baruch, K., Gur-Arie, L., Nadler, C., Koby, S., Yerushalmi, G., Ben-Neriah, Y., Yogev, O., Shaulian, E., Guttman, C., Zarivach, R., et al. (2011). Metalloprotease type III effectors that specifically cleave JNK and NF- κ B. *EMBO J.* 30, 221–231.
- Behiry, I.K., Abada, E.A., Ahmed, E.A., and Labeeb, R.S. (2011). Enteropathogenic *Escherichia coli* associated with diarrhea in children in Cairo, Egypt. *Sci. World J.* 11, 2613–2619.
- Bell, B.P., Goldoft, M., Griffin, P.M., Davis, M.A., Gordon, D.C., Tarr, P.I., Bartleson, C.A., Lewis, J.H., Barrett, T.J., and Wells, J.G. (1994). A multistate outbreak of *Escherichia coli* O157:H7-associated bloody diarrhea and hemolytic uremic syndrome from hamburgers. The Washington experience. *JAMA* 272, 1349–1353.
- Bentancor, A.B., Ameal, L.A., Calviño, M.F., Martinez, M.C., Miccio, L., and Degregorio, O.J. (2012). Risk factors for Shiga toxin-producing *Escherichia coli* infections in preadolescent schoolchildren in Buenos Aires, Argentina. *J. Infect. Dev. Ctries.* 6, 378–386.
- Berger, C.N., Crepin, V.F., Baruch, K., Mousnier, A., Rosenshine, I., and Frankel, G. (2012). EspZ of enteropathogenic and enterohemorrhagic *Escherichia coli* regulates type III secretion system protein translocation. *mBio* 3, e00317–12.
- Bieber, D., Ramer, S.W., Wu, C.Y., Murray, W.J., Tobe, T., Fernandez, R., and Schoolnik, G.K. (1998). Type IV pili, transient bacterial aggregates, and virulence of enteropathogenic *Escherichia coli*. *Science* 280, 2114–2118.
- Blanco, M., Blanco, J.E., Mora, A., Dahbi, G., Alonso, M.P., González, E.A., Bernárdez, M.I., and Blanco, J. (2004). Serotypes, virulence genes, and intimin types of Shiga toxin (verotoxin)-producing *Escherichia coli* isolates from cattle in Spain and identification of a new intimin variant gene (*eae-xi*). *J. Clin. Microbiol.* 42, 645–651.
- Bonnet, C., Boucher, D., Lazereg, S., Pedrotti, B., Islam, K., Denoulet, P., and Larcher, J.C. (2001). Differential binding regulation of microtubule-associated proteins MAP1A, MAP1B, and MAP2 by tubulin polyglutamylation. *J. Biol. Chem.* 276, 12839–12848.
- Borenshtein, D., McBee, M.E., and Schauer, D.B. (2008). Utility of the *Citrobacter rodentium* infection model in laboratory mice. *Curr. Opin. Gastroenterol.* 24, 32–37.

Boucrot, E., Henry, T., Borg, J.P., Gorvel, J.P., and Méresse, S. (2005). The intracellular fate of *Salmonella* depends on the recruitment of kinesin. *Science* 308, 1174–1178.

Bray, J. (1945). Isolation of antigenically homogenous strains of *Bact. coli* from summer diarrhoea of infants. *J. Pathol. Bacteriol.* 57, 239–247.

Brown, N.F., Coombes, B.K., Bishop, J.L., Wickham, M.E., Lowden, M.J., Gal-Mor, O., Goode, D.L., Boyle, E.C., Sanderson, K.L., and Finlay, B.B. (2011). *Salmonella* phage ST64B encodes a member of the SseK/NleB effector family. *PloS One* 6, e17824.

Bugarel, M., Beutin, L., and Fach, P. (2010). Low-density microarray targeting non-locus of enterocyte effacement effectors (nle genes) and major virulence factors of Shiga toxin-producing *Escherichia coli* (STEC): a new approach for molecular risk assessment of STEC isolates. *Appl. Environ. Microbiol.* 76, 203–211.

Bulinski, J.C., and Bossler, A. (1994). Purification and characterization of ensconsin, a novel microtubule stabilizing protein. *J. Cell Sci.* 107 (Pt 10), 2839–2849.

Campellone, K.G. (2010). Cytoskeleton-modulating effectors of enteropathogenic and enterohaemorrhagic *Escherichia coli*: Tir, EspF_U and actin pedestal assembly. *FEBS J.* 277, 2390–2402.

Campellone, K.G., and Leong, J.M. (2003). Tails of two Tirs: actin pedestal formation by enteropathogenic *E. coli* and enterohemorrhagic *E. coli* O157:H7. *Curr. Opin. Microbiol.* 6, 82–90.

Caron, E., Crepin, V.F., Simpson, N., Knutton, S., Garmendia, J., and Frankel, G. (2006). Subversion of actin dynamics by EPEC and EHEC. *Curr. Opin. Microbiol.* 9, 40–45.

Cassimeris, L., and Spittle, C. (2001). Regulation of microtubule-associated proteins. *Int. Rev. Cytol.* 210, 163–226.

CDC. (2012). Foodborne disease active surveillance network (FoodNet): FoodNet surveillance report for 2011 (final report). CDC, Atlanta, GA.

Clements, A., Stoneham, C.A., Furniss, R.C.D., and Frankel, G. (2014). Enterohaemorrhagic *Escherichia coli* inhibits recycling endosome function and trafficking of surface receptors. *Cell. Microbiol.* 16, 1693–1705.

Coburn, B., Sekirov, I., and Finlay, B.B. (2007). Type III secretion systems and disease. *Clin. Microbiol. Rev.* 20, 535–549.

Cornelis, G.R. (2006). The type III secretion injectisome. *Nat. Rev. Microbiol.* 4, 811–825.

Croxen, M.A., and Finlay, B.B. (2010). Molecular mechanisms of *Escherichia coli* pathogenicity. *Nat. Rev. Microbiol.* 8, 26–38.

- Croxen, M.A., Law, R.J., Scholz, R., Keeney, K.M., Wlodarska, M., and Finlay, B.B. (2013). Recent advances in understanding enteric pathogenic *Escherichia coli*. *Clin. Microbiol. Rev.* *26*, 822–880.
- Dahan, S., Wiles, S., La Ragione, R.M., Best, A., Woodward, M.J., Stevens, M.P., Shaw, R.K., Chong, Y., Knutton, S., Phillips, A., et al. (2005). EspJ is a prophage-carried type III effector protein of attaching and effacing pathogens that modulates infection dynamics. *Infect. Immun.* *73*, 679–686.
- Dean, P., and Kenny, B. (2004). Intestinal barrier dysfunction by enteropathogenic *Escherichia coli* is mediated by two effector molecules and a bacterial surface protein. *Mol. Microbiol.* *54*, 665–675.
- Dean, P., and Kenny, B. (2009). The effector repertoire of enteropathogenic *E. coli*: ganging up on the host cell. *Curr. Opin. Microbiol.* *12*, 101–109.
- Dean, P., Maresca, M., and Kenny, B. (2005). EPEC's weapons of mass subversion. *Curr. Opin. Microbiol.* *8*, 28–34.
- Dean, P., Maresca, M., Schüller, S., Phillips, A.D., and Kenny, B. (2006). Potent diarrheagenic mechanism mediated by the cooperative action of three enteropathogenic *Escherichia coli*-injected effector proteins. *Proc. Natl. Acad. Sci. U. S. A.* *103*, 1876–1881.
- Deng, W., Li, Y., Vallance, B.A., and Finlay, B.B. (2001). Locus of enterocyte effacement from *Citrobacter rodentium*: sequence analysis and evidence for horizontal transfer among attaching and effacing pathogens. *Infect. Immun.* *69*, 6323–6335.
- Deng, W., Vallance, B.A., Li, Y., Puente, J.L., and Finlay, B.B. (2003). *Citrobacter rodentium* translocated intimin receptor (Tir) is an essential virulence factor needed for actin condensation, intestinal colonization and colonic hyperplasia in mice. *Mol. Microbiol.* *48*, 95–115.
- Deng, W., Puente, J.L., Gruenheid, S., Li, Y., Vallance, B.A., Vázquez, A., Barba, J., Ibarra, J.A., O'Donnell, P., Metalnikov, P., et al. (2004). Dissecting virulence: systematic and functional analyses of a pathogenicity island. *Proc. Natl. Acad. Sci. U. S. A.* *101*, 3597–3602.
- Deng, W., de Hoog, C.L., Yu, H.B., Li, Y., Croxen, M.A., Thomas, N.A., Puente, J.L., Foster, L.J., and Finlay, B.B. (2010). A comprehensive proteomic analysis of the type III secretome of *Citrobacter rodentium*. *J. Biol. Chem.* *285*, 6790–6800.
- Deng, W., Yu, H.B., de Hoog, C.L., Stoyanov, N., Li, Y., Foster, L.J., and Finlay, B.B. (2012). Quantitative proteomic analysis of type III secretome of enteropathogenic *Escherichia coli* reveals an expanded effector repertoire for attaching/effacing bacterial pathogens. *Mol. Cell. Proteomics* *11*, 692–709.
- DeVinney, R., Puente, J.L., Gauthier, A., Goosney, D., and Finlay, B.B. (2001). Enterohaemorrhagic and enteropathogenic *Escherichia coli* use a different Tir-based mechanism for pedestal formation. *Mol. Microbiol.* *41*, 1445–1458.

- Dong, N., Liu, L., and Shao, F. (2010). A bacterial effector targets host DH-PH domain RhoGEFs and antagonizes macrophage phagocytosis. *EMBO J.* 29, 1363–1376.
- Donnenberg, M.S., and Finlay, B.B. (2013). Combating enteropathogenic *Escherichia coli* (EPEC) infections: the way forward. *Trends Microbiol.* 21, 317–319.
- Donnenberg, M.S., Tacket, C.O., James, S.P., Losonsky, G., Nataro, J.P., Wasserman, S.S., Kaper, J.B., and Levine, M.M. (1993). Role of the *eaeA* gene in experimental enteropathogenic *Escherichia coli* infection. *J. Clin. Invest.* 92, 1412–1417.
- Edwards, R.A., Keller, L.H., and Schifferli, D.M. (1998). Improved allelic exchange vectors and their use to analyze 987P fimbria gene expression. *Gene* 207, 149–157.
- Esmaili, A., Nazir, S.F., Borthakur, A., Yu, D., Turner, J.R., Saksena, S., Singla, A., Hecht, G.A., Alrefai, W.A., and Gill, R.K. (2009). Enteropathogenic *Escherichia coli* infection inhibits intestinal serotonin transporter function and expression. *Gastroenterology* 137, 2074–2083.
- Faire, K., Waterman-Storer, C.M., Gruber, D., Masson, D., Salmon, E.D., and Bulinski, J.C. (1999). E-MAP-115 (ensconsin) associates dynamically with microtubules *in vivo* and is not a physiological modulator of microtubule dynamics. *J. Cell Sci.* 112 (Pt 23), 4243–4255.
- Farfán, M.J., Toro, C.S., Barry, E.M., and Nataro, J.P. (2011). *Shigella* enterotoxin-2 is a type III effector that participates in *Shigella*-induced interleukin 8 secretion by epithelial cells. *FEMS Immunol. Med. Microbiol.* 61, 332–339.
- Farfán, M.J. and Torres, A.G. (2012). Molecular mechanisms that mediate colonization of Shiga-toxin-producing *Escherichia coli* strains. *Infect. Immun.* 80, 903–913.
- Ferens, W.A., and Hovde, C.J. (2011). *Escherichia coli* O157:H7: animal reservoir and sources of human infection. *Foodborne Pathog. Dis.* 8, 465–487.
- Ferrières, L., Hémerly, G., Nham, T., Guérout, A.M., Mazel, D., Beloin, C., and Ghigo, J.M. (2010). Silent mischief: bacteriophage Mu insertions contaminate products of *Escherichia coli* random mutagenesis performed using suicidal transposon delivery plasmids mobilized by broad-host-range RP4 conjugative machinery. *J. Bacteriol.* 192, 6418–6427.
- Fitzhenry, R., Dahan, S., Torres, A.G., Chong, Y., Heuschkel, R., Murch, S.H., Thomson, M., Kaper, J.B., Frankel, G., and Phillips AD. (2006). Long polar fimbriae and tissue tropism in *Escherichia coli* O157:H7. *Microbes Infect.* 8, 1741–1749.
- Foster, L.J., De Hoog, C.L., and Mann, M. (2003). Unbiased quantitative proteomics of lipid rafts reveals high specificity for signaling factors. *Proc. Natl. Acad. Sci. U. S. A.* 100, 5813–5818.

- Frankel, G., Candy, D.C., Everest, P., and Dougan, G. (1994). Characterization of the C-terminal domains of intimin-like proteins of enteropathogenic and enterohemorrhagic *Escherichia coli*, *Citrobacter freundii*, and *Hafnia alvei*. *Infect. Immun.* 62, 1835–1842.
- Frankel, G., Phillips, A.D., Novakova, M., Field, H., Candy, D.C., Schauer, D.B., Douce, G., and Dougan, G. (1996). Intimin from enteropathogenic *Escherichia coli* restores murine virulence to a *Citrobacter rodentium eaeA* mutant: induction of an immunoglobulin A response to intimin and EspB. *Infect. Immun.* 64, 5315–5325.
- Frankel, G., Phillips, A.D., Rosenshine, I., Dougan, G., Kaper, J.B., and Knutton, S. (1998). Enteropathogenic and enterohaemorrhagic *Escherichia coli*: more subversive elements. *Mol. Microbiol.* 30, 911–921.
- Gallaud, E., Caous, R., Pascal, A., Bazile, F., Gagné, J.P., Huet, S., Poirier, G.G., Chrétien, D., Richard-Parpaillon, L., and Giet, R. (2014). Ensconsin/Map7 promotes microtubule growth and centrosome separation in *Drosophila* neural stem cells. *J. Cell Biol.* 204, 1111–1121.
- Gao, X., Wan, F., Mateo, K., Callegari, E., Wang, D., Deng, W., Puente, J., Li, F., Chaussee, M.S., Finlay, B.B., et al. (2009). Bacterial effector binding to ribosomal protein s3 subverts NF-kappaB function. *PLoS Pathog.* 5, e1000708.
- Gao, X., Wang, X., Pham, T.H., Feuerbacher, L.A., Lubos, M.L., Huang, M., Olsen, R., Mushegian, A., Slawson, C., and Hardwidge, P.R. (2013). NleB, a bacterial effector with glycosyltransferase activity, targets GAPDH function to inhibit NF-κB activation. *Cell Host Microbe* 13, 87–99.
- Gauthier, A., Puente, J.L., and Finlay, B.B. (2003). Secretin of the enteropathogenic *Escherichia coli* type III secretion system requires components of the type III apparatus for assembly and localization. *Infect. Immun.* 71, 3310–3319.
- Ghaem-Maghami, M., Simmons, C.P., Daniell, S., Pizza, M., Lewis, D., Frankel, G., and Dougan, G. (2001). Intimin-specific immune responses prevent bacterial colonization by the attaching-effacing pathogen *Citrobacter rodentium*. *Infect. Immun.* 69, 5597–5605.
- Gill, R.K., Saksena, S., Tyagi, S., Alrefai, W.A., Malakooti, J., Sarwar, Z., Turner, J.R., Ramaswamy, K., and Dudeja, P.K. (2005). Serotonin inhibits Na⁺/H⁺ exchange activity via 5-HT₄ receptors and activation of PKC alpha in human intestinal epithelial cells. *Gastroenterology* 128, 962–974.
- Gill, R.K., Borthakur, A., Hodges, K., Turner, J.R., Clayburgh, D.R., Saksena, S., Zaheer, A., Ramaswamy, K., Hecht, G., and Dudeja, P.K. (2007). Mechanism underlying inhibition of intestinal apical Cl/OH exchange following infection with enteropathogenic *E. coli*. *J. Clin. Invest.* 117, 428–437.
- Girón, J.A., Ho, A.S., and Schoolnik, G.K. (1991). An inducible bundle-forming pilus of enteropathogenic *Escherichia coli*. *Science* 254, 710–713.

- Goosney, D.L., Gruenheid, S., and Finlay, B.B. (2000). Gut feelings: enteropathogenic *E. coli* (EPEC) interactions with the host. *Annu. Rev. Cell Dev. Biol.* 16, 173–189.
- Gruenheid, S., DeVinney, R., Blatt, F., Goosney, D., Gelkop, S., Gish, G.D., Pawson, T., and Finlay, B.B. (2001). Enteropathogenic *E. coli* Tir binds Nck to initiate actin pedestal formation in host cells. *Nat. Cell Biol.* 3, 856–859.
- Gruenheid, S., Sekirov, I., Thomas, N.A., Deng, W., O'Donnell, P., Goode, D., Li, Y., Frey, E.A., Brown, N.F., Metalnikov, P., et al. (2004). Identification and characterization of NleA, a non-LEE-encoded type III translocated virulence factor of enterohaemorrhagic *Escherichia coli* O157:H7. *Mol. Microbiol.* 51, 1233–1249.
- Guttman, J.A., Li, Y., Wickham, M.E., Deng, W., Vogl, A.W., and Finlay, B.B. (2006). Attaching and effacing pathogen-induced tight junction disruption *in vivo*. *Cell. Microbiol.* 8, 634–645.
- Guttman, J.A., Samji, F.N., Li, Y., Deng, W., Lin, A., and Finlay, B.B. (2007). Aquaporins contribute to diarrhoea caused by attaching and effacing bacterial pathogens. *Cell. Microbiol.* 9, 131–141.
- Gyles, C.L. (2007). Shiga toxin-producing *Escherichia coli*: an overview. *J. Anim. Sci.* 85, E45–E62.
- Hardwidge, P.R., Deng, W., Vallance, B.A., Rodriguez-Escudero, I., Cid, V.J., Molina, M., and Finlay, B.B. (2005). Modulation of host cytoskeleton function by the enteropathogenic *Escherichia coli* and *Citrobacter rodentium* effector protein EspG. *Infect. Immun.* 73, 2586–2594.
- Hartland, E.L., Batchelor, M., Delahay, R.M., Hale, C., Matthews, S., Dougan, G., Knutton, S., Connerton, I., and Frankel, G. (1999). Binding of intimin from enteropathogenic *Escherichia coli* to Tir and to host cells. *Mol. Microbiol.* 32, 151–158.
- Hayashi, T., Makino, K., Ohnishi, M., Kurokawa, K., Ishii, K., Yokoyama, K., Han, C.G., Ohtsubo, E., Nakayama, K., Murata, T., et al. (2001). Complete genome sequence of enterohemorrhagic *Escherichia coli* O157:H7 and genomic comparison with a laboratory strain K-12. *DNA Res.* 8, 11–22.
- Hecht, G. (2001). Microbes and microbial toxins: paradigms for microbial-mucosal interactions. VII. Enteropathogenic *Escherichia coli*: physiological alterations from an extracellular position. *Am. J. Physiol. Gastrointest. Liver Physiol.* 281, G1–G7.
- Hemrajani, C., Berger, C.N., Robinson, K.S., Marchès, O., Mousnier, A., and Frankel, G. (2010). NleH effectors interact with Bax inhibitor-1 to block apoptosis during enteropathogenic *Escherichia coli* infection. *Proc. Natl. Acad. Sci. U. S. A.* 107, 3129–3134.
- Hernandes, R.T., Elias, W.P., Vieira, M.A.M., and Gomes, T.A.T. (2009). An overview of atypical enteropathogenic *Escherichia coli*. *FEMS Microbiol. Lett.* 297, 137–149.

- Hirokawa, N., and Noda, Y. (2008). Intracellular transport and kinesin superfamily proteins, KIFs: structure, function, and dynamics. *Physiol. Rev.* 88, 1089–1118.
- Hirokawa, N., Noda, Y., and Okada, Y. (1998). Kinesin and dynein superfamily proteins in organelle transport and cell division. *Curr. Opin. Cell Biol.* 10, 60–73.
- Hirokawa, N., Noda, Y., Tanaka, Y., and Niwa, S. (2009). Kinesin superfamily motor proteins and intracellular transport. *Nat. Rev. Mol. Cell Biol.* 10, 682–696.
- Hoiseth, S.K., and Stocker, B.A. (1981). Aromatic-dependent *Salmonella* Typhimurium are non-virulent and effective as live vaccines. *Nature* 291, 238–239.
- Iguchi, A., Thomson, N.R., Ogura, Y., Saunders, D., Ooka, T., Henderson, I.R., Harris, D., Asadulghani, M., Kurokawa, K., Dean, P., et al. (2009). Complete genome sequence and comparative genome analysis of enteropathogenic *Escherichia coli* O127:H6 strain E2348/69. *J. Bacteriol.* 191, 347–354.
- Iizumi, Y., Sagara, H., Kabe, Y., Azuma, M., Kume, K., Ogawa, M., Nagai, T., Gillespie, P.G., Sasakawa, C., and Handa, H. (2007). The enteropathogenic *E. coli* effector EspB facilitates microvillus effacing and antiphagocytosis by inhibiting myosin function. *Cell Host Microbe* 2, 383–392.
- Janmey, P.A. (1998). The cytoskeleton and cell signaling: component localization and mechanical coupling. *Physiol. Rev.* 78, 763–781.
- Jaqaman, K., Loerke, D., Mettlen, M., Kuwata, H., Grinstein, S., Schmid, S.L., and Danuser, G. (2008). Robust single-particle tracking in live-cell time-lapse sequences. *Nat. Methods* 5, 695–702.
- Johnson, W.M., and Lior, H. (1984). Toxins produced by *Campylobacter jejuni* and *Campylobacter coli*. *Lancet* 323, 229–230.
- Kalman, D., Weiner, O.D., Goosney, D.L., Sedat, J.W., Finlay, B.B., Abo, A., and Bishop, J.M. (1999). Enteropathogenic *E. coli* acts through WASP and Arp2/3 complex to form actin pedestals. *Nat. Cell Biol.* 1, 389–391.
- Kaniuk, N.A., Canadien, V., Bagshaw, R.D., Bakowski, M., Braun, V., Landekic, M., Mitra, S., Huang, J., Heo, W.D., Meyer, T., et al. (2011). *Salmonella* exploits Arl8B-directed kinesin activity to promote endosome tubulation and cell-to-cell transfer. *Cell. Microbiol.* 13, 1812–1823.
- Kaper, J.B., Nataro, J.P., and Mobley, H.L. (2004). Pathogenic *Escherichia coli*. *Nat. Rev. Microbiol.* 2, 123–140.
- Kelly, M., Hart, E., Mundy, R., Marchès, O., Wiles, S., Badea, L., Luck, S., Tauschek, M., Frankel, G., Robins-Browne, R.M., et al. (2006). Essential role of the type III secretion system effector NleB in colonization of mice by *Citrobacter rodentium*. *Infect. Immun.* 74, 2328–2337.

- Kenny, B. (2002). Mechanism of action of EPEC type III effector molecules. *Int. J. Med. Microbiol.* 291, 469–477.
- Kenny, B., DeVinney, R., Stein, M., Reinscheid, D.J., Frey, E.A., and Finlay, B.B. (1997). Enteropathogenic *E. coli* (EPEC) transfers its receptor for intimate adherence into mammalian cells. *Cell* 91, 511–520.
- Kim, J., Thanabalasuriar, A., Chaworth-Musters, T., Fromme, J.C., Frey, E.A., Lario, P.I., Metalnikov, P., Rizg, K., Thomas, N.A., Lee, S.F., et al. (2007). The bacterial virulence factor NleA inhibits cellular protein secretion by disrupting mammalian COPII function. *Cell Host Microbe* 2, 160–171.
- Klapproth, J.M.A., Sasaki, M., Sherman, M., Babbitt, B., Sonnenberg, M.S., Fernandes, P.J., Scaletsky, I.C.A., Kalman, D., Nusrat, A., and Williams, I.R. (2005). *Citrobacter rodentium* *lifA/efa1* is essential for colonic colonization and crypt cell hyperplasia *in vivo*. *Infect. Immun.* 73, 1441–1451.
- Komada, M., McLean, D.J., Griswold, M.D., Russell, L.D., and Soriano, P. (2000). E-MAP-115, encoding a microtubule-associated protein, is a retinoic acid-inducible gene required for spermatogenesis. *Genes Dev.* 14, 1332–1342.
- Konishi, Y., and Setou, M. (2009). Tubulin tyrosination navigates the kinesin-1 motor domain to axons. *Nat. Neurosci.* 12, 559–567.
- Kotloff, K.L., Nataro, J.P., Blackwelder, W.C., Nasrin, D., Farag, T.H., Panchalingam, S., Wu, Y., Sow, S.O., Sur, D., Breiman, R.F., et al. (2013). Burden and aetiology of diarrhoeal disease in infants and young children in developing countries (the Global Enteric Multicenter Study, GEMS): a prospective, case-control study. *Lancet* 382, 209–222.
- Kum, W.W.S., Lo, B.C., Deng, W., Ziltener, H.J., and Finlay, B.B. (2010). Impaired innate immune response and enhanced pathology during *Citrobacter rodentium* infection in mice lacking functional P-selectin. *Cell. Microbiol.* 12, 1250–1271.
- Lacher, D.W., Steinsland, H., Blank, T.E., Sonnenberg, M.S., and Whittam, T.S. (2007). Molecular evolution of typical enteropathogenic *Escherichia coli*: clonal analysis by multilocus sequence typing and virulence gene allelic profiling. *J. Bacteriol.* 189, 342–350.
- Landry, M.C., Sicotte, A., Champagne, C., and Lavoie, J.N. (2009). Regulation of cell death by recycling endosomes and golgi membrane dynamics via a pathway involving Src-family kinases, Cdc42 and Rab11a. *Mol. Biol. Cell* 20, 4091–4106.
- Law, R.J., Gur-Arie, L., Rosenshine, I., and Finlay, B.B. (2013). *In vitro* and *in vivo* model systems for studying enteropathogenic *Escherichia coli* infections. *Cold Spring Harb. Perspect. Med.* 3, a009977.
- Levine, M.M., and Edelman, R. (1984). Enteropathogenic *Escherichia coli* of classic serotypes associated with infant diarrhea: epidemiology and pathogenesis. *Epidemiol. Rev.* 6, 31–51.

Levine, M.M., Bergquist, E.J., Nalin, D.R., Waterman, D.H., Hornick, R.B., Young, C.R., and Sotman, S. (1978). *Escherichia coli* strains that cause diarrhoea but do not produce heat-labile or heat-stable enterotoxins and are non-invasive. *Lancet* 311, 1119–1122.

Levine, M.M., Ferreccio, C., Prado, V., Cayazzo, M., Abrego, P., Martinez, J., Maggi, L., Baldini, M.M., Martin, W., and Maneval, D. (1993). Epidemiologic studies of *Escherichia coli* diarrheal infections in a low socioeconomic level peri-urban community in Santiago, Chile. *Am. J. Epidemiol.* 138, 849–869.

Li, S., Zhang, L., Yao, Q., Li, L., Dong, N., Rong, J., Gao, W., Ding, X., Sun, L., Chen, X., et al. (2013). Pathogen blocks host death receptor signalling by arginine GlcNAcylation of death domains. *Nature* 501, 242–246.

Luperchio, S.A., and Schauer, D.B. (2001). Molecular pathogenesis of *Citrobacter rodentium* and transmissible murine colonic hyperplasia. *Microbes Infect.* 3, 333–340.

Ma, C., Wickham, M.E., Guttman, J.A., Deng, W., Walker, J., Madsen, K.L., Jacobson, K., Vogl, W.A., Finlay, B.B., and Vallance, B.A. (2006). *Citrobacter rodentium* infection causes both mitochondrial dysfunction and intestinal epithelial barrier disruption *in vivo*: role of mitochondrial associated protein (Map). *Cell. Microbiol.* 8, 1669–1686.

Maranhão, H.S., Medeiros, M.C.C., Scaletsky, I.C.A., Fagundes-Neto, U., and Morais, M.B. (2008). The epidemiological and clinical characteristics and nutritional development of infants with acute diarrhoea, in north-eastern Brazil. *Ann. Trop. Med. Parasitol.* 102, 357–365.

Marchès, O., Nougayrède, J.P., Boullier, S., Mainil, J., Charlier, G., Raymond, I., Pohl, P., Boury, M., De Rycke, J., Milon, A., et al. (2000). Role of *tir* and intimin in the virulence of rabbit enteropathogenic *Escherichia coli* serotype O103:H2. *Infect. Immun.* 68, 2171–2182.

Marchès, O., Batchelor, M., Shaw, R.K., Patel, A., Cummings, N., Nagai, T., Sasakawa, C., Carlsson, S.R., Lundmark, R., Cougoule, C., et al. (2006). EspF of enteropathogenic *Escherichia coli* binds sorting nexin 9. *J. Bacteriol.* 188, 3110–3115.

Marchès, O., Covarelli, V., Dahan, S., Cougoule, C., Bhatta, P., Frankel, G., and Caron, E. (2008). EspJ of enteropathogenic and enterohaemorrhagic *Escherichia coli* inhibits opsonophagocytosis. *Cell. Microbiol.* 10, 1104–1115.

Martinez, E., Schroeder, G.N., Berger, C.N., Lee, S.F., Robinson, K.S., Badea, L., Simpson, N., Hall, R.A., Hartland, E.L., Crepin, V.F., et al. (2010). Binding to Na⁽⁺⁾/H⁽⁺⁾ exchanger regulatory factor 2 (NHERF2) affects trafficking and function of the enteropathogenic *Escherichia coli* type III secretion system effectors Map, EspI and NleH. *Cell. Microbiol.* 12, 1718–1731.

Masson, D., and Kreis, T.E. (1993). Identification and molecular characterization of E-MAP-115, a novel microtubule-associated protein predominantly expressed in epithelial cells. *J. Cell Biol.* 123, 357–371.

- Matsuzawa, T., Kuwae, A., Yoshida, S., Sasakawa, C., and Abe, A. (2004). Enteropathogenic *Escherichia coli* activates the RhoA signaling pathway via the stimulation of GEF-H1. *EMBO J.* 23, 3570–3582.
- Matsuzawa, T., Kuwae, A., and Abe, A. (2005). Enteropathogenic *Escherichia coli* type III effectors EspG and EspG2 alter epithelial paracellular permeability. *Infect. Immun.* 73, 6283–6289.
- McDaniel, T.K., and Kaper, J.B. (1997). A cloned pathogenicity island from enteropathogenic *Escherichia coli* confers the attaching and effacing phenotype on *E. coli* K-12. *Mol. Microbiol.* 23, 399–407.
- McDaniel, T.K., Jarvis, K.G., Donnenberg, M.S., and Kaper, J.B. (1995). A genetic locus of enterocyte effacement conserved among diverse enterobacterial pathogens. *Proc. Natl. Acad. Sci. U. S. A.* 92, 1664–1668.
- McNamara, B.P., Koutsouris, A., O’Connell, C.B., Nougayrède, J.P., Donnenberg, M.S., and Hecht, G. (2001). Translocated EspF protein from enteropathogenic *Escherichia coli* disrupts host intestinal barrier function. *J. Clin. Invest.* 107, 621–629.
- Abu-Median, A.B., van Diemen, P.M., Dziva, F., Vlisidou, I., Wallis, T.S., and Stevens, M.P. (2006). Functional analysis of lymphostatin homologues in enterohaemorrhagic *Escherichia coli*. *FEMS Microbiol. Lett.* 258, 43–49.
- Metzger, T., Gache, V., Xu, M., Cadot, B., Folker, E.S., Richardson, B.E., Gomes, E.R., and Baylies, M.K. (2012). MAP and kinesin-dependent nuclear positioning is required for skeletal muscle function. *Nature* 484, 120–124.
- Miller, V.L., and Mekalanos, J.J. (1988). A novel suicide vector and its use in construction of insertion mutations: osmoregulation of outer membrane proteins and virulence determinants in *Vibrio cholerae* requires *toxR*. *J. Bacteriol.* 170, 2575–2583.
- Mills, E., Baruch, K., Charpentier, X., Kobi, S., and Rosenshine, I. (2008). Real-time analysis of effector translocation by the type III secretion system of enteropathogenic *Escherichia coli*. *Cell Host Microbe* 3, 104–113.
- Misyurina, O., Asper, D.J., Deng, W., Finlay, B.B., Rogan, D., and Potter, A.A. (2010). The role of Tir, EspA, and NleB in the colonization of cattle by Shiga toxin producing *Escherichia coli* O26:H11. *Can. J. Microbiol.* 56, 739–747.
- Miyahara, A., Nakanishi, N., Ooka, T., Hayashi, T., Sugimoto, N., and Tobe, T. (2009). Enterohemorrhagic *Escherichia coli* effector EspL2 induces actin microfilament aggregation through annexin 2 activation. *Cell. Microbiol.* 11, 337–350.
- Moon, H.W., Whipp, S.C., Argenzio, R.A., Levine, M.M., and Giannella, R.A. (1983). Attaching and effacing activities of rabbit and human enteropathogenic *Escherichia coli* in pig and rabbit intestines. *Infect. Immun.* 41, 1340–1351.

- Moura, R.A., Sircili, M.P., Leomil, L., Matté, M.H., Trabulsi, L.R., Elias, W.P., Irino, K., and Pestana de Castro, A.F. (2009). Clonal relationship among atypical enteropathogenic *Escherichia coli* strains isolated from different animal species and humans. *Appl. Environ. Microbiol.* 75, 7399–7408.
- Müller, D., Benz, I., Liebchen, A., Gallitz, I., Karch, H., and Schmidt, M.A. (2009). Comparative analysis of the locus of enterocyte effacement and its flanking regions. *Infect. Immun.* 77, 3501–3513.
- Mundy, R., Petrovska, L., Smollett, K., Simpson, N., Wilson, R.K., Yu, J., Tu, X., Rosenshine, I., Clare, S., Dougan, G., et al. (2004). Identification of a novel *Citrobacter rodentium* type III secreted protein, EspI, and roles of this and other secreted proteins in infection. *Infect. Immun.* 72, 2288–2302.
- Mundy, R., MacDonald, T.T., Dougan, G., Frankel, G., and Wiles, S. (2005). *Citrobacter rodentium* of mice and man. *Cell. Microbiol.* 7, 1697–1706.
- Nadler, C., Baruch, K., Kobi, S., Mills, E., Haviv, G., Farago, M., Alkalay, I., Bartfeld, S., Meyer, T.F., Ben-Neriah, Y., et al. (2010). The type III secretion effector NleE inhibits NF-kappaB activation. *PLoS Pathog.* 6, e1000743.
- Nataro, J.P., and Kaper, J.B. (1998). Diarrheagenic *Escherichia coli*. *Clin. Microbiol. Rev.* 11, 142–201.
- National Enteric Surveillance Program. 2010. National Enteric Surveillance Program (NESP) annual summary 2010. The National Microbiology Laboratory (NML) and Centre for Food-borne, Environmental and Zoonotic Infectious Diseases (CFEZID), Public Health Agency of Canada and Provincial Public Health Microbiology Laboratories, Winnipeg, Canada.
- Neter, E., Westphal, O., Luderitz, O., Gino, R.M., and Gorzynski, E.A. (1955). Demonstration of antibodies against enteropathogenic *Escherichia coli* in sera of children of various ages. *Pediatrics* 16, 801–808.
- Newman, J.V., Zabel, B.A., Jha, S.S., and Schauer, D.B. (1999). *Citrobacter rodentium* *espB* is necessary for signal transduction and for infection of laboratory mice. *Infect. Immun.* 67, 6019–6025.
- Newton, H.J., Pearson, J.S., Badea, L., Kelly, M., Lucas, M., Holloway, G., Wagstaff, K.M., Dunstone, M.A., Sloan, J., Whisstock, J.C., et al. (2010). The type III effectors NleE and NleB from enteropathogenic *E. coli* and OspZ from *Shigella* block nuclear translocation of NF-kappaB p65. *PLoS Pathog.* 6, e1000898.
- Nguyen, R.N., Taylor, L.S., Tauschek, M., and Robins-Browne, R.M. (2006). Atypical enteropathogenic *Escherichia coli* infection and prolonged diarrhea in children. *Emerg. Infect. Dis.* 12, 597–603.

- Nougayrède, J.P., and Donnenberg, M.S. (2004). Enteropathogenic *Escherichia coli* EspF is targeted to mitochondria and is required to initiate the mitochondrial death pathway. *Cell. Microbiol.* 6, 1097–1111.
- O'Brien, A.D., Newland, J.W., Miller, S.F., Holmes, R.K., Smith, H.W., and Formal, S.B. (1984). Shiga-like toxin-converting phages from *Escherichia coli* strains that cause hemorrhagic colitis or infantile diarrhea. *Science* 226, 694–696.
- Ochoa, T.J., and Contreras, C.A. (2011). Enteropathogenic *Escherichia coli* infection in children. *Curr. Opin. Infect. Dis.* 24, 478–483.
- Ochoa, T.J., Barletta, F., Contreras, C., and Mercado, E. (2008). New insights into the epidemiology of enteropathogenic *Escherichia coli* infection. *Trans. R. Soc. Trop. Med. Hyg.* 102, 852–856.
- Oelschlaeger, T.A., Guerry, P., and Kopecko, D.J. (1993). Unusual microtubule-dependent endocytosis mechanisms triggered by *Campylobacter jejuni* and *Citrobacter freundii*. *Proc. Natl. Acad. Sci. U. S. A.* 90, 6884–6888.
- Ogura, Y., Ooka, T., Iguchi, A., Toh, H., Asadulghani, M., Oshima, K., Kodama, T., Abe, H., Nakayama, K., Kurokawa, K., et al. (2009). Comparative genomics reveal the mechanism of the parallel evolution of O157 and non-O157 enterohemorrhagic *Escherichia coli*. *Proc. Natl. Acad. Sci. U. S. A.* 106, 17939–17944.
- Olsen, R.L., Echtenkamp, F., Cheranova, D., Deng, W., Finlay, B.B., and Hardwidge, P.R. (2013). The enterohemorrhagic *Escherichia coli* effector protein NleF binds mammalian Tmp21. *Vet. Microbiol.* 164, 164–170.
- Ong, S.E., Foster, L.J., and Mann, M. (2003). Mass spectrometric-based approaches in quantitative proteomics. *Methods* 29, 124–130.
- Pearson, J.S., Riedmaier, P., Marchès, O., Frankel, G., and Hartland, E.L. (2011). A type III effector protease NleC from enteropathogenic *Escherichia coli* targets NF- κ B for degradation. *Mol. Microbiol.* 80, 219–230.
- Pearson, J.S., Giogha, C., Ong, S.Y., Kennedy, C.L., Kelly, M., Robinson, K.S., Lung, T.W.F., Mansell, A., Riedmaier, P., Oates, C.V.L., et al. (2013). A type III effector antagonizes death receptor signalling during bacterial gut infection. *Nature* 501, 247–251.
- Penttilä, T.L., Parvinen, M., and Paranko, J. (2003). Microtubule-associated epithelial protein E-MAP-115 is localized in the spermatid manchette. *Int. J. Androl.* 26, 166–174.
- Perez, M., Santa-Maria, I., Gomez de Barreda, E., Zhu, X., Cuadros, R., Cabrero, J.R., Sanchez-Madrid, F., Dawson, H.N., Vitek, M.P., Perry, G., et al. (2009). Tau--an inhibitor of deacetylase HDAC6 function. *J. Neurochem.* 109, 1756–1766.

- Perna, N.T., Plunkett, G., Burland, V., Mau, B., Glasner, J.D., Rose, D.J., Mayhew, G.F., Evans, P.S., Gregor, J., Kirkpatrick, H.A., et al. (2001). Genome sequence of enterohaemorrhagic *Escherichia coli* O157:H7. *Nature* 409, 529–533.
- Petty, N.K., Bulgin, R., Crepin, V.F., Cerdano-Tárraga, A.M., Schroeder, G.N., Quail, M.A., Lennard, N., Corton, C., Barron, A., Clark, L., et al. (2010). The *Citrobacter rodentium* genome sequence reveals convergent evolution with human pathogenic *Escherichia coli*. *J. Bacteriol.* 192, 525–538.
- Pflughoeft, K.J., and Versalovic, J. (2012). Human microbiome in health and disease. *Annu. Rev. Pathol.* 7, 99–122.
- Raymond, B., Crepin, V.F., Collins, J.W., and Frankel, G. (2011). The WxxxE effector EspT triggers expression of immune mediators in an Erk/JNK and NF- κ B-dependent manner. *Cell. Microbiol.* 13, 1881–1893.
- Reid, S.D., Herbelin, C.J., Bumbaugh, A.C., Selander, R.K., and Whittam, T.S. (2000). Parallel evolution of virulence in pathogenic *Escherichia coli*. *Nature* 406, 64–67.
- Rivero, M.A., Passucci, J.A., Rodriguez, E.M., and Parma, A.E. (2010). Role and clinical course of verotoxigenic *Escherichia coli* infections in childhood acute diarrhoea in Argentina. *J. Med. Microbiol.* 59, 345–352.
- Robins-Browne, R.M. (1987). Traditional enteropathogenic *Escherichia coli* of infantile diarrhea. *Rev. Infect. Dis.* 9, 28–53.
- Robins-Browne, R.M., Tokhi, A.M., Adams, L.M., Bennett-Wood, V., Moisisidis, A.V., Krejany, E.O., and O’Gorman, L.E. (1994). Adherence characteristics of attaching and effacing strains of *Escherichia coli* from rabbits. *Infect. Immun.* 62, 1584–1592.
- Rogers, L.D., Kristensen, A.R., Boyle, E.C., Robinson, D.P., Ly, R.T., Finlay, B.B., and Foster, L.J. (2008). Identification of cognate host targets and specific ubiquitylation sites on the *Salmonella* SPI-1 effector SopB/SigD. *J. Proteomics* 71, 97–108.
- Rosales, A., Hofer, J., Zimmerhackl, L.B., Jungtraithmayr, T.C., Riedl, M., Giner, T., Strasak, A., Orth-Höller, D., Würzner, R., Karch, H., et al. (2012). Need for long-term follow-up in enterohemorrhagic *Escherichia coli*-associated hemolytic uremic syndrome due to late-emerging sequelae. *Clin. Infect. Dis.* 54, 1413–1421.
- Rosenshine, I., Ruschkowski, S., Stein, M., Reinscheid, D.J., Mills, S.D., and Finlay, B.B. (1996). A pathogenic bacterium triggers epithelial signals to form a functional bacterial receptor that mediates actin pseudopod formation. *EMBO J.* 15, 2613–2624.
- Ruchaud-Sparagano, M.H., Mühlen, S., Dean, P., and Kenny, B. (2011). The enteropathogenic *E. coli* (EPEC) Tir effector inhibits NF- κ B activity by targeting TNF α receptor-associated factors. *PLoS Pathog.* 7, e1002414.

- Sanger, J.M., Chang, R., Ashton, F., Kaper, J.B., and Sanger, J.W. (1996). Novel form of actin-based motility transports bacteria on the surfaces of infected cells. *Cell Motil. Cytoskeleton* *34*, 279–287.
- Scaletsky, I.C., Silva, M.L., and Trabulsi, L.R. (1984). Distinctive patterns of adherence of enteropathogenic *Escherichia coli* to HeLa cells. *Infect. Immun.* *45*, 534–536.
- Scaletsky, I.C.A., Souza, T.B., Aranda, K.R.S., and Okeke, I.N. (2010). Genetic elements associated with antimicrobial resistance in enteropathogenic *Escherichia coli* (EPEC) from Brazil. *BMC Microbiol.* *10*, 25.
- Scallan, E., Hoekstra, R.M., Angulo, F.J., Tauxe, R.V., Widdowson, M.A., Roy, S.L., Jones, J.L., and Griffin, P.M. (2011). Foodborne illness acquired in the United States--major pathogens. *Emerg. Infect. Dis.* *17*, 7–15.
- Schauer, D.B., and Falkow, S. (1993a). The *eae* gene of *Citrobacter freundii* biotype 4280 is necessary for colonization in transmissible murine colonic hyperplasia. *Infect. Immun.* *61*, 4654–4661.
- Schauer, D.B., and Falkow, S. (1993b). Attaching and effacing locus of a *Citrobacter freundii* biotype that causes transmissible murine colonic hyperplasia. *Infect. Immun.* *61*, 2486–2492.
- Schauer, D.B., Zabel, B.A., Pedraza, I.F., O'Hara, C.M., Steigerwalt, A.G., and Brenner, D.J. (1995). Genetic and biochemical characterization of *Citrobacter rodentium* sp. nov. *J. Clin. Microbiol.* *33*, 2064–2068.
- Schmidt, M.R., Maritzen, T., Kukhtina, V., Higman, V.A., Doglio, L., Barak, N.N., Strauss, H., Oschkinat, H., Dotti, C.G., and Haucke, V. (2009). Regulation of endosomal membrane traffic by a Gadkin/AP-1/kinesin KIF5 complex. *Proc. Natl. Acad. Sci. U. S. A.* *106*, 15344–15349.
- Schüller, S., Chong, Y., Lewin, J., Kenny, B., Frankel, G., and Phillips, A.D. (2007). Tir phosphorylation and Nck/N-WASP recruitment by enteropathogenic and enterohaemorrhagic *Escherichia coli* during *ex vivo* colonization of human intestinal mucosa is different to cell culture models. *Cell. Microbiol.* *9*, 1352–1364.
- Sekse, C., Sunde, M., Lindstedt, B.A., Hopp, P., Bruheim, T., Cudjoe, K.S., Kvitle, B., and Urdahl, A.M. (2011). Potentially human-pathogenic *Escherichia coli* O26 in Norwegian sheep flocks. *Appl. Environ. Microbiol.* *77*, 4949–4958.
- Selyunin, A.S., Reddick, L.E., Weigele, B.A., and Alto, N.M. (2014). Selective protection of an ARF1-GTP signaling axis by a bacterial scaffold induces bidirectional trafficking arrest. *Cell Rep.* *6*, 878–891.
- Sham, H.P., Shames, S.R., Croxen, M.A., Ma, C., Chan, J.M., Khan, M.A., Wickham, M.E., Deng, W., Finlay, B.B., and Vallance, B.A. (2011). Attaching and effacing bacterial effector NleC suppresses epithelial inflammatory responses by inhibiting NF- κ B and p38 mitogen-activated protein kinase activation. *Infect. Immun.* *79*, 3552–3562.

- Shames, S.R., Deng, W., Guttman, J.A., de Hoog, C.L., Li, Y., Hardwidge, P.R., Sham, H.P., Vallance, B.A., Foster, L.J., and Finlay, B.B. (2010). The pathogenic *E. coli* type III effector EspZ interacts with host CD98 and facilitates host cell prosurvival signalling. *Cell. Microbiol.* *12*, 1322–1339.
- Shames, S.R., Bhavsar, A.P., Croxen, M.A., Law, R.J., Mak, S.H.C., Deng, W., Li, Y., Bidshari, R., de Hoog, C.L., Foster, L.J., et al. (2011). The pathogenic *Escherichia coli* type III secreted protease NleC degrades the host acetyltransferase p300. *Cell. Microbiol.* *13*, 1542–1557.
- Shaner, N.C., Sanger, J.W., and Sanger, J.M. (2005). Actin and alpha-actinin dynamics in the adhesion and motility of EPEC and EHEC on host cells. *Cell Motil. Cytoskeleton* *60*, 104–120.
- Sharp, T.M., and Estes, M.K. (2010). An inside job: subversion of the host secretory pathway by intestinal pathogens. *Curr. Opin. Infect. Dis.* *23*, 464–469.
- Sharp, T.M., Guix, S., Katayama, K., Crawford, S.E., and Estes, M.K. (2010). Inhibition of cellular protein secretion by norwalk virus nonstructural protein p22 requires a mimic of an endoplasmic reticulum export signal. *PloS One* *5*, e13130.
- Shaw, R.K., Smollett, K., Cleary, J., Garmendia, J., Straatman-Iwanowska, A., Frankel, G., and Knutton, S. (2005). Enteropathogenic *Escherichia coli* type III effectors EspG and EspG2 disrupt the microtubule network of intestinal epithelial cells. *Infect. Immun.* *73*, 4385–4390.
- Simon, R., Priefer, U., and Puhler, A. (1983). A broad host range mobilization system for *in vivo* genetic engineering: transposon mutagenesis in gram negative bacteria. *Nat. Biotechnol.* *1*, 784–791.
- Smith, A.D., Botero, S., Shea-Donohue, T., and Urban, J.F. (2011). The pathogenicity of an enteric *Citrobacter rodentium* infection is enhanced by deficiencies in the antioxidants selenium and vitamin E. *Infect. Immun.* *79*, 1471–1478.
- Snedeker, K.G., Shaw, D.J., Locking, M.E., and Prescott, R.J. (2009). Primary and secondary cases in *Escherichia coli* O157 outbreaks: a statistical analysis. *BMC Infect. Dis.* *9*, 144.
- Stevens, J.M., Galyov, E.E., and Stevens, M.P. (2006). Actin-dependent movement of bacterial pathogens. *Nat. Rev. Microbiol.* *4*, 91–101.
- Sung, H.H., Telley, I.A., Papadaki, P., Ephrussi, A., Surrey, T., and Rørth, P. (2008). *Drosophila* ensconsin promotes productive recruitment of Kinesin-1 to microtubules. *Dev. Cell* *15*, 866–876.
- Swennes, A.G., Buckley, E.M., Parry, N.M.A., Madden, C.M., García, A., Morgan, P.B., Astrofsky, K.M., and Fox, J.G. (2012). Enzootic enteropathogenic *Escherichia coli* infection in laboratory rabbits. *J. Clin. Microbiol.* *50*, 2353–2358.
- Takemura, R., Okabe, S., Umeyama, T., Kanai, Y., Cowan, N.J., and Hirokawa, N. (1992). Increased microtubule stability and alpha tubulin acetylation in cells transfected with microtubule-associated proteins MAP1B, MAP2 or tau. *J. Cell Sci.* *103* (Pt 4), 953–964.

- Tardelli Gomes, T.A., and Gonzalez-Pedrajo, B. (2010). Enteropathogenic *Escherichia coli* (EPEC), pp. 66–126. In Torres A.G. (ed), Pathogenic *Escherichia coli* in Latin America. Bentham Science Publishers, Oak Park, IL.
- Tarr, P.I., Gordon, C.A., and Chandler, W.L. (2005). Shiga-toxin-producing *Escherichia coli* and haemolytic uraemic syndrome. *Lancet* 365, 1073–1086.
- Tauschek, M., Strugnell, R.A., and Robins-Browne, R.M. (2002). Characterization and evidence of mobilization of the LEE pathogenicity island of rabbit-specific strains of enteropathogenic *Escherichia coli*. *Mol. Microbiol.* 44, 1533–1550.
- Thanabalasuriar, A., Koutsouris, A., Weflen, A., Mimee, M., Hecht, G., and Gruenheid, S. (2010). The bacterial virulence factor NleA is required for the disruption of intestinal tight junctions by enteropathogenic *Escherichia coli*. *Cell. Microbiol.* 12, 31–41.
- Thanabalasuriar, A., Bergeron, J., Gillingham, A., Mimee, M., Thomassin, J.L., Strynadka, N., Kim, J., and Gruenheid, S. (2012). Sec24 interaction is essential for localization and virulence-associated function of the bacterial effector protein NleA. *Cell. Microbiol.* 14, 1206–1218.
- Thanabalasuriar, A., Kim, J., and Gruenheid, S. (2013). The inhibition of COPII trafficking is important for intestinal epithelial tight junction disruption during enteropathogenic *Escherichia coli* and *Citrobacter rodentium* infection. *Microbes Infect.* 15, 738–744.
- Tobe, T., Beatson, S.A., Taniguchi, H., Abe, H., Bailey, C.M., Fivian, A., Younis, R., Matthews, S., Marches, O., Frankel, G., et al. (2006). An extensive repertoire of type III secretion effectors in *Escherichia coli* O157 and the role of lambdoid phages in their dissemination. *Proc. Natl. Acad. Sci. U. S. A.* 103, 14941–14946.
- Tomson, F.L., Viswanathan, V.K., Kanack, K.J., Kanteti, R.P., Straub, K.V., Menet, M., Kaper, J.B., and Hecht, G. (2005). Enteropathogenic *Escherichia coli* EspG disrupts microtubules and in conjunction with Orf3 enhances perturbation of the tight junction barrier. *Mol. Microbiol.* 56, 447–464.
- Touchon, M., Hoede, C., Tenaillon, O., Barbe, V., Baeriswyl, S., Bidet, P., Bingen, E., Bonacorsi, S., Bouchier, C., Bouvet, O., et al. (2009). Organised genome dynamics in the *Escherichia coli* species results in highly diverse adaptive paths. *PLoS Genet.* 5, e1000344.
- Touzé, T., Hayward, R.D., Eswaran, J., Leong, J.M., and Koronakis, V. (2004). Self-association of EPEC intimin mediated by the beta-barrel-containing anchor domain: a role in clustering of the Tir receptor. *Mol. Microbiol.* 51, 73–87.
- Trabulsi, L.R., Keller, R., and Tardelli Gomes, T.A. (2002). Typical and atypical enteropathogenic *Escherichia coli*. *Emerg. Infect. Dis.* 8, 508–513.
- Tuttle, J., Gomez, T., Doyle, M.P., Wells, J.G., Zhao, T., Tauxe, R.V., and Griffin, P.M. (1999). Lessons from a large outbreak of *Escherichia coli* O157:H7 infections: insights into the

infectious dose and method of widespread contamination of hamburger patties. *Epidemiol. Infect.* *122*, 185–192.

Vallance, B.A., Deng, W., Jacobson, K., and Finlay, B.B. (2003). Host susceptibility to the attaching and effacing bacterial pathogen *Citrobacter rodentium*. *Infect. Immun.* *71*, 3443–3453.

Vallance, B.A., Khan, M.A., Deng, W., Gruenheid, S., and Finlay, B.B. (2004). Modeling enteropathogenic and enterohemorrhagic *E. coli* infections and disease. *Drug Discov. Today* *1*, 73–79.

Vanier, M.T., Deck, P., Stutzmann, J., Gendry, P., Arnold, C., Dirrig-Grosch, S., Keding, M., and Launay, J.F. (2003). Expression and distribution of distinct variants of E-MAP-115 during proliferation and differentiation of human intestinal epithelial cells. *Cell Motil. Cytoskeleton* *55*, 221–231.

Vieira, M.A.M., Salvador, F.A., Silva, R.M., Irino, K., Vaz, T.M.I., Rockstroh, A.C., Guth, B.E.C., and Gomes, T.A.T. (2010). Prevalence and characteristics of the O122 pathogenicity island in typical and atypical enteropathogenic *Escherichia coli* strains. *J. Clin. Microbiol.* *48*, 1452–1455.

Viswanathan, V.K., Koutsouris, A., Lukic, S., Pilkinton, M., Simonovic, I., Simonovic, M., and Hecht, G. (2004). Comparative analysis of EspF from enteropathogenic and enterohemorrhagic *Escherichia coli* in alteration of epithelial barrier function. *Infect. Immun.* *72*, 3218–3227.

Wales, A.D., Woodward, M.J., and Pearson, G.R. (2005). Attaching-effacing bacteria in animals. *J. Comp. Pathol.* *132*, 1–26.

Wan, F., Weaver, A., Gao, X., Bern, M., Hardwidge, P.R., and Lenardo, M.J. (2011). IKK β phosphorylation regulates RPS3 nuclear translocation and NF- κ B function during infection with *Escherichia coli* strain O157:H7. *Nat. Immunol.* *12*, 335–343.

Whittam, T.S., Wolfe, M.L., Wachsmuth, I.K., Orskov, F., Orskov, I., and Wilson, R.A. (1993). Clonal relationships among *Escherichia coli* strains that cause hemorrhagic colitis and infantile diarrhea. *Infect. Immun.* *61*, 1619–1629.

Wickham, M.E., Lupp, C., Mascarenhas, M., Vazquez, A., Coombes, B.K., Brown, N.F., Coburn, B.A., Deng, W., Puente, J.L., Karmali, M.A., et al. (2006). Bacterial genetic determinants of non-O157 STEC outbreaks and hemolytic-uremic syndrome after infection. *J. Infect. Dis.* *194*, 819–827.

Wickham, M.E., Lupp, C., Vázquez, A., Mascarenhas, M., Coburn, B., Coombes, B.K., Karmali, M.A., Puente, J.L., Deng, W., and Finlay, B.B. (2007). *Citrobacter rodentium* virulence in mice associates with bacterial load and the type III effector NleE. *Microbes Infect.* *9*, 400–407.

Wirth, T., Falush, D., Lan, R., Colles, F., Mensa, P., Wieler, L.H., Karch, H., Reeves, P.R., Maiden, M.C.J., Ochman, H., et al. (2006). Sex and virulence in *Escherichia coli*: an evolutionary perspective. *Mol. Microbiol.* *60*, 1136–1151.

- Wlodarska, M., Willing, B., Keeney, K.M., Menendez, A., Bergstrom, K.S., Gill, N., Russell, S.L., Vallance, B.A., and Finlay, B.B. (2011). Antibiotic treatment alters the colonic mucus layer and predisposes the host to exacerbated *Citrobacter rodentium*-induced colitis. *Infect. Immun.* **79**, 1536–1545.
- Wong, A.R.C., Raymond, B., Collins, J.W., Crepin, V.F., and Frankel, G. (2012a). The enteropathogenic *E. coli* effector EspH promotes actin pedestal formation and elongation via WASP-interacting protein (WIP). *Cell. Microbiol.* **14**, 1051–1070.
- Wong, A.R.C., Clements, A., Raymond, B., Crepin, V.F., and Frankel, G. (2012b). The interplay between the *Escherichia coli* Rho guanine nucleotide exchange factor effectors and the mammalian RhoGEF inhibitor EspH. *mBio* **3**, e00250–11.
- Xicohtencatl-Cortes, J., Monteiro-Neto, V., Ledesma, M.A., Jordan, D.M., Francetic, O., Kaper, J.B., Puente, J.L., and Girón, J.A. (2007). Intestinal adherence associated with type IV pili of enterohemorrhagic *Escherichia coli* O157:H7. *J. Clin. Invest.* **117**, 3519–3529.
- Xicohtencatl-Cortes, J., Monteiro-Neto, V., Saldaña, Z., Ledesma, M.A., Puente, J.L., and Girón, J.A. (2009). The type 4 pili of enterohemorrhagic *Escherichia coli* O157:H7 are multipurpose structures with pathogenic attributes. *J. Bacteriol.* **191**, 411–421.
- Yang, Z., Kovar, J., Kim, J., Nietfeldt, J., Smith, D.R., Moxley, R.A., Olson, M.E., Fey, P.D., and Benson, A.K. (2004). Identification of common subpopulations of non-sorbitol-fermenting, beta-glucuronidase-negative *Escherichia coli* O157:H7 from bovine production environments and human clinical samples. *Appl. Environ. Microbiol.* **70**, 6846–6854.
- Yen, H., Ooka, T., Iguchi, A., Hayashi, T., Sugimoto, N., and Tobe, T. (2010). NleC, a type III secretion protease, compromises NF- κ B activation by targeting p65/RelA. *PLoS Pathog.* **6**, e1001231.
- Yoshida, S., and Sasakawa, C. (2003). Exploiting host microtubule dynamics: a new aspect of bacterial invasion. *Trends Microbiol.* **11**, 139–143.
- Yoshida, S., Handa, Y., Suzuki, T., Ogawa, M., Suzuki, M., Tamai, A., Abe, A., Katayama, E., and Sasakawa, C. (2006). Microtubule-severing activity of *Shigella* is pivotal for intercellular spreading. *Science* **314**, 985–989.
- Zhang, L., Ding, X., Cui, J., Xu, H., Chen, J., Gong, Y.N., Hu, L., Zhou, Y., Ge, J., Lu, Q., et al. (2012). Cysteine methylation disrupts ubiquitin-chain sensing in NF- κ B activation. *Nature* **481**, 204–208.

Appendix A – Additional publications

Publications arising during graduate work but not directly related to the research presented in this dissertation:

van der Heijden, J., Scholz, R., Reynolds, L.A., Bosman, E.S., **Law, R.J.**, Foster, L.J., and Finlay, B.B. (2015). Oxidation of a cysteine residue in the *Salmonella* effector SteB regulates tubulin-mediated bacterial translocation to the juxtanuclear position. (*In Preparation*)

Croxen, M.A., **Law, R.J.**, Scholz, R., Keeney, K.M., Wlodarska, M., and Finlay, B.B. (2013). Recent advances in understanding enteric pathogenic *Escherichia coli*. Clinical Microbiology Reviews. **26**(4):822.

Law, R.J., Gur-Arie, L., Rosenshine, I., and Finlay, B.B. (2013). *In vitro* and *in vivo* model systems for studying enteropathogenic *Escherichia coli* infections. Cold Spring Harbor Perspectives in Medicine. **3**(3):a009977.

Shames, S.R., Bhavsar, A.P. Croxen, M.A., **Law, R.J.**, Mak, S.H.C., Deng, W., Bidshari, R., de Hoog, C.L., Foster, L.J., and Finlay B.B. (2011). The pathogenic *Escherichia coli* type III secreted protease NleC degrades the host acetyltransferase p300. Cellular Microbiology. **13**(10):1542-1557.

Appendix B – Particle tracking of TfR-mCherry containing vesicles in EPEC-infected Ptk2 cells (stringent track linking parameters)

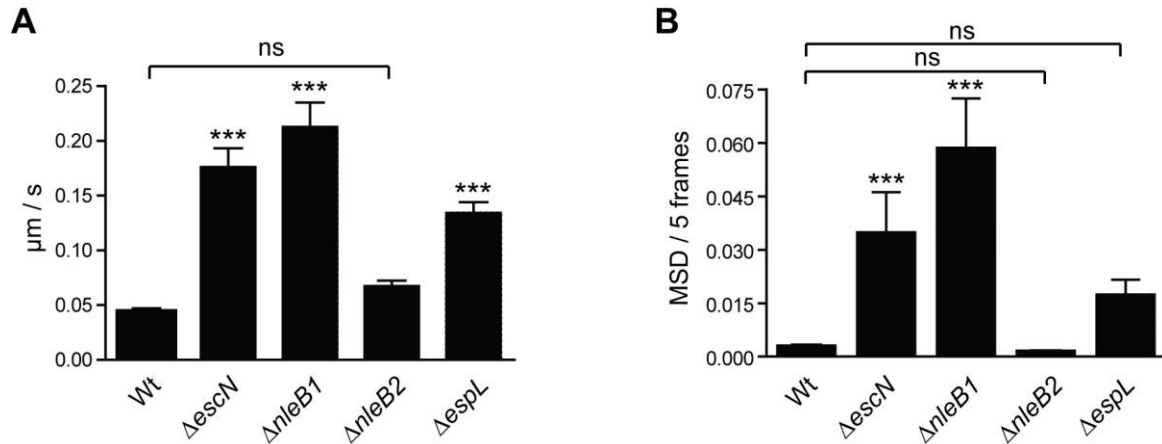


Figure B.1 EPEC disrupts TfR-mCherry trafficking in an NleB1/EspL-dependent manner. Movement of TfR-mCherry vesicles during EPEC infection. Ptk2 cells transfected with pTfR-mCherry were infected with EPEC and fluorescent TfR containing vesicles were imaged using time lapse microscopy. U-track multiple particle tracking software was used to track fluorescent vesicle movement. (A) Mean particle speed with 95% CI. (B) Mean MSD/5 frames with 95% CI. Particle speeds and MSDs were calculated for all tracks with ≥ 10 visible segments from at least 3 cells per infection condition using stringent track linking parameters. Asterisks indicate a significant difference from wild type using one-way ANOVA with Tukey's multiple comparison's test ($P < 0.001$). ns: not significant.

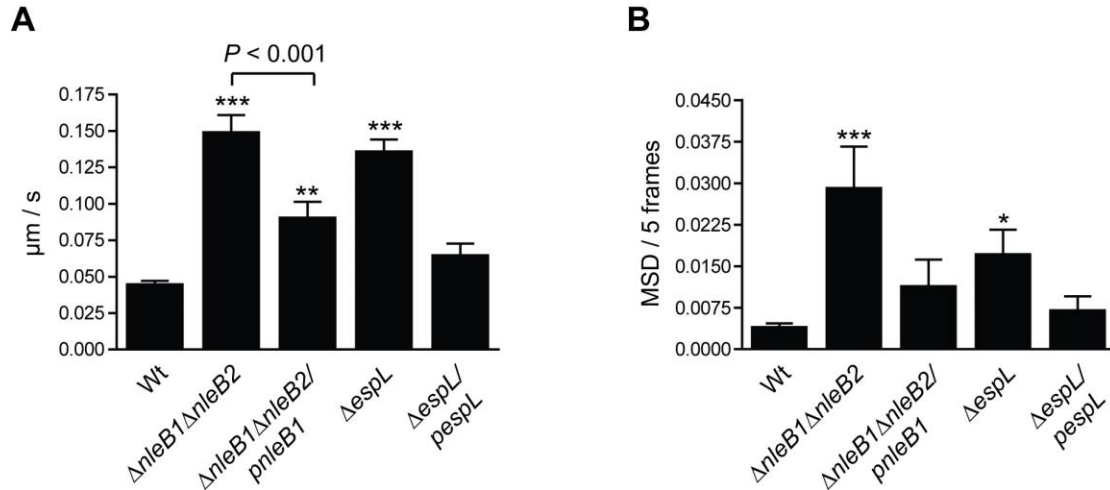


Figure B.2 Complementation of *nleB1/espL* restores trafficking inhibition.

Movement of TfR-mCherry vesicles during infection with EPEC effector mutants or *nleB/espL* complemented strains. Ptk2 cells transfected with pTfR-mCherry were infected with EPEC and fluorescent TfR-mCherry containing vesicles were tracked using u-track multiple particle tracking software. (A) Mean particle speed with 95% CI. (B) Mean MSD/5 frames with 95% CI. Particle speeds and MSDs were calculated for all tracks with ≥ 10 visible segments from at least 3 cells per infection condition using stringent track linking parameters. Asterisks indicate significant differences from wild type using one-way ANOVA with Tukey's multiple comparisons test ($P < 0.001$; $P < 0.01$; $P < 0.05$).

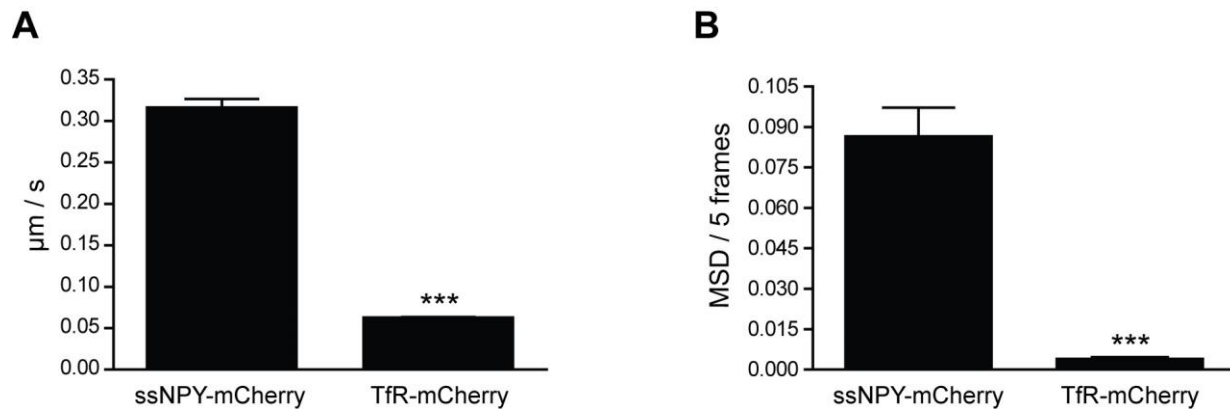


Figure B.3 EPEC specifically disrupts kinesin-1-based vesicle movement.

Ptk2 cells infected with wild type EPEC show reduced movement of TfR-mCherry in comparison to the general vesicle marker, ssNPY-mCherry. (A) Mean particle speed with 95%

CI of tracked TfR-mCherry containing vesicles during EPEC infection. (B) Mean MSD/5 frames with 95% CI of pooled tracks showing disrupted TfR-mCherry movement compared to ssNPY-mCherry during EPEC infection. Particle speeds and MSDs were calculated for all particle trajectories with ≥ 10 visible track segments using stringent track linking parameters. Asterisks indicate significant differences using an unpaired *t*-test ($P < 0.0001$).

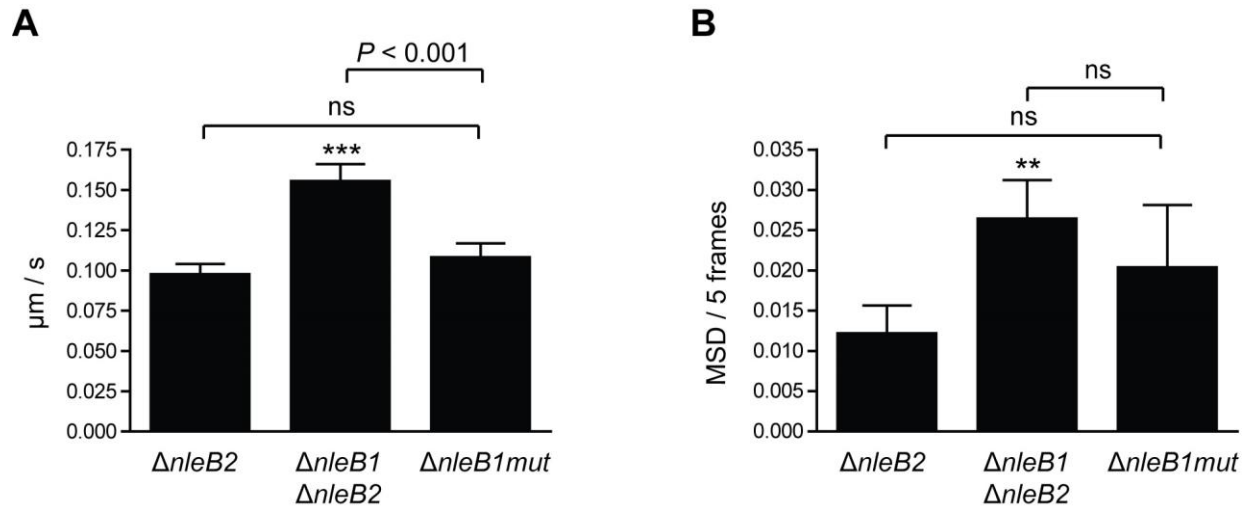


Figure B.4 NleB1 GlcNAcylation activity does not affect TfR-mCherry trafficking.

Ptk2 cells infected with an NleB1 catalytic mutant strain show intermediate reduction in TfR-mCherry movement in comparison to controls. Ptk2 cells transfected with pTfR-mCherry were infected with EPEC and fluorescent TfR containing vesicles were tracked using u-track multiple particle tracking software. (A) Mean particle speed with 95% CI. (B) Mean MSD/5 frames with 95% CI. Particle speeds and MSDs were calculated for all tracks with ≥ 10 visible segments from at least 3 cells per infection condition using stringent track linking parameters. Asterisks indicate significant differences from $\Delta nleB2$ using one-way ANOVA with Tukey's multiple comparisons test ($P < 0.001$; $P < 0.01$). ns: not significant.